2007

# The Characterization of Cationic Pseudostationary Phases for Electrokinetic Chromatography

Vincent Patrick Schnee
*The University of Montana*

# The Characterization of Cationic

# Pseudostationary Phases for Electrokinetic Chromatography

By

Vincent Patrick Schnee

B.S. Xavier University, Cincinnati, Ohio, USA, 2003

Dissertation

Presented in partial fulfillment of the requirements
for the degree of

Doctor of Philosophy
in Chemistry

The University of Montana
Missoula, MT

Autumn 2007

Approved by:

Dr. David A. Strobel, Dean
Graduate School

Dr. Christopher P. Palmer, Chair
Chemistry

Dr. Michael D. DeGrandpre
Chemistry

Dr. Edward Rosenberg
Chemistry

Dr. Donald E. Kiely
Chemistry

Dr. Fernando Cardozo-Pelaez
Biomedical Pharmaceutical Science

Schnee, Vincent, Ph.D., Autumn 2007 Chemistry

The Characterization of Cationic Pseudostationary Phases for Electrokinetic Chromatography

Chairperson: Christopher P. Palmer

Micellar electrokinetic chromatography (MEKC) and linear solvation energy relationships (LSER) have been used to characterize the solute distribution between water and self-assemblies formed from cationic surfactants containing systematic variations in structure.

One series of surfactants consisted of *N*-Alkyl-*N*-methylpyrrolidinium Ionic Liquid type headgroups. This is the first report of an ionic liquid surfactant used as the pseudostationary phase in MEKC. The solvent characteristics of these ionic liquid type surfactants did not vary in any systematic manner with increasing tail length but were found to be significantly different compared to the well-studied hexadecyl-trimethyl-ammonium; Bromide (CTAB). The new surfactants interact more strongly with polar compounds and less strongly with compounds having nonbonding or π-electrons, and are more cohesive.

Two series of surfactants with systematic variations in head group structure were synthesized, subjected to LSER analysis, and evaluated for the separation of representative analytes. One series consists of linear alkyl substitutions on the ammonium center while the other incorporates the ammonium into alkyl ring structures of varying size. Trends were observed in the cohesivity and polarity of the linear surfactant series, both increasing with the size of the headgroup. No trends in the LSER parameters were observed in the cyclic series, but the LSER results show that the surfactants with cyclic head groups provide a significantly different solvation environment from the linear series. The performance of these two series of surfactants was evaluated for the separation of three representative sets of analytes. Representative phenolic analytes were comprised of methoxyphenols, which are of interest due to their prevalence in wood smoke. The representative amine containing solutes consisted of compounds often found in forensic urine analysis, and represent structures typical of pharmaceuticals. Six pharmaceutical corticosteroids, which are used in replacement therapy of adrenocortical insufficiency and nonspecific treatment of inflammatory and allergic conditions, were studied as representative hydrophobic analytes.

The fist example of a phosphonium surfactant as a pseudostationary phase for MEKC is introduced. Its performance and selectivity are compared to that of an analogous ammonium surfactant. The change from an ammonium to a phosphonium charge center caused differences in the cohesivity and acid/base interactions of the pseudostationary phase.

Finally, two cationic carbohydrate based surfactants were used as a MEKC pseudostationary phase for the first time. The newly characterized glucocationic phases provided differences in interactions as seen in the LSER results.

**Acknowledgements**

I would like to thank Chris Palmer for his guidance, support, and patience in dealing with a difficult student.

I would also like to thank the members of my committee for their thoughtful input.

I would like to thank Gary Baker for providing me with the N-Alkyl-N-methylpyyrrolidinium surfactants and Pierluigi Quagliotto for supplying the glucocationic surfactants

I would also like to acknowledge the other students that have worked in the lab with me, Jesse, Pat, and Megan

**Table of Contents**

## List of Tables

## List of Figures

## List of Equations

## List of Abbreviations and Mathematical Symbols

| | |
|---|---|
| AGENT | Allyl glycidyl ether N-methyltaurine siloxane |
| AGESS | Dodecane allyl gycidyl ether sulfite-modified siloxane |
| ALE | Sodium N-lauroyl-N-methyl-beta-alaninate |
| AMPS | 2-acrylamido-2-methyl-1-propanesulfonic acid |
| AMPS | 2-acrylamide-2methyl-1-propanesulfonic acid |
| AOT | Bis(2-ethylhexl)sodium sulfosuccinate |
| Brij 35 | Polyoxyethylene(23) dodecyl ether |
| $C_{12}$MPYB | 1-dodecyl-1-methylpyrrolidinium; bromide |
| $C_{14}$MPYB | 1-tetradecyl-1-methylpyrrolidinium; bromide |
| $C_{16}$MACB | 1-Hexadecyl-1-methyl-azocane; bromide |
| $C_{16}$MAPB | 1-Hexadecyl-1-methyl-azepanium; bromide |
| $C_{16}$MPDB | 1-Hexadecyl-1-methyl-piperidinium; bromide |
| $C_{16}$MPYB | 1-Hexadecyl-1-methylpyrrolidinium |
| $C_{16}$TBAB | Hexadecyltributylammonium; bromide |
| $C_{16}$TBPB | Hexadecyltributylphosphonium; bromide |
| $C_{16}$TEAB | Hexadecyltriethylammonium; bromide |
| $C_{16}$TPAB | Hexadecyltripropylammonium; bromide |
| Chol | Cholesterol |
| CTAB, ($C_{16}$TMAB) | Hexadecyltrimethylammonium bromide |
| Cu(DS)2 | Copper dodecyl sulfate |
| CMC | Critical micelle concentration |
| DAGENT | Dodecane allyl glycidyl ether N-methyl taurine siloxane |
| DHAB | Dihexadecyldimethylammonium bromide |
| DHP | Dihexadecylphosphate |
| DPPC | Dipalmitoylphosphatidyl choline |
| DPPG | Dipalmitoylphosphatidyl glycerol |
| DTAC | Dodecyltrimethylammonium choride |
| E | Electric field strength |
| EKC | Electrokinetic chromatography |
| Elvacite 2669 | Poly(methyl methacrylate-ethyl acrylate-methacrylic acid) |
| EOF | Electroosmotic flow |
| G | Gibbs free energy |
| HBA | Hydrogen bond acidity |
| HBB | Hydrogen bond basicity |
| k | Retention factor |
| KDC | Potassium depxycholate |
| KGDC | 3-beta-glucopyranosyl-5-beta-cholan-12-alpha-hydroy-24-olc acid |
| LDS | Lithium dodecyl sulfate |
| LMT | Sodium N-lauroyl-N-methyltaurate |
| LPFOS | Lithium perfluorooctane |
| LSER | Linear solvation energy relatioinships |
| MECC | Micellar electrokinetic capillary chromatography |
| MEKC | Micellar electrokinetic chromatography |

| | |
|---|---|
| Mg(DS)2 | Magnesium dodecyl sulfate |
| OAGENT | Octane AGENT |
| P | Equilibrium partition coefficient |
| PAAU | Poly(sodium 11-acrylamidondecanoate) |
| PCA | Principal component analysis |
| poly-(SDeS) | Poly(sodium 9-decenyl sulfate |
| poly-(SNoS) | Poly(sodium 8- nonenyl sulfate |
| poly-(SOcS) | Poly(sodium 7-octenyl sulfate) |
| poly-(SUS) | Poly(sodium 10-undecenyl sulfate) |
| PSP | Pseudostationary phase |
| PSUA | Poly(sodium 10-undecylenate) |
| r | Radius |
| R | Gas Constant |
| SAGENT | Seryl AGENT |
| SDCV | Sodium dodecyl carbonyl valine |
| SDecS | Sodium decyl sulfate |
| SLN | Sodium N-lauroylsarcosinate |
| SLSA | Sodium dodecyl sulfoacetate |
| SOS | Sodium octyl sulfate |
| SPN | Sodium N-parmitoyl sarcosinate |
| T | Temperature |
| tmob | Time the solute spends in the mobile phase |
| tpsp | Time the solute spends associated with the pseudostationary phase |
| TTAB | Tetradecyltrimethylammonium bromide |
| $v_{eo}$ | Velocity of the electroosmotic flow |
| $v_{ep}$ | Electrophoretic velocity of a charged species in an electric field |
| $v_{epsp}$ | Electrophoretic velocity of the pseudostationary phase |
| $V_{mob}$ | Volume of the mobile phase |
| $v_{psp}$ | Veolicity of the pseudostationary phase |
| $V_{psp}$ | Volume of the pseudostationary phase |
| $v_s$ | Velocity of a solute zone |
| $\zeta$ | Zeta potential |
| $\eta$ | Viscosity |
| $\mu_{eo}$ | Electroosmotic mobility |
| $\mu_{ep}$ | Electrophoretic mobility |
| $\mu_{ep}$ | Electrophoretic mobility |
| $\mu_{sol}$ | Apparent mobility of the solute |

# Chapter 1
# Electrokinetic Chromatography and Theory

## 1.1 Introduction

Chromatography was first introduced in 1900 by Russian botanist Mikhail Tsvet to separate plant pigments. Chromatography is a chemical separation technique in which the separation is achieved through differential partitioning of analytes between a mobile phase and a stationary phase. In the 107 year evolution of chromatography, methods such as gas chromatography and high performance liquid chromatography have become routine analytical methods in most of chemical laboratories around the world [1-3].

Recent developments in the area of chromatographic separations include miniaturization of conventional approaches [4-6], the development of novel support materials for liquid chromatography [7], and the development of novel techniques such as electrokinetic chromatography (EKC) [8].

Electrokinetic chromatography was introduced by Terabe et al. in 1984 [9,10]. Since that time, the technique has seen significant development and application. The primary advantages that have promoted the development and acceptance of the technique are its speed, efficiency, compatibility with miniaturized formats including chip based microfluidic devices, and ease of use.

Electrokinetic chromatography (EKC) is defined by IUPAC as "A separation technique based on a combination of electrophoresis and interaction of the analytes with additives (e.g., surfactants), which form a dispersed phase moving at a different velocity. In order to achieve separation either the analytes or this secondary phase should be

charged." [11] This definition emphasizes that separation in EKC is dependent on both electromigration and chemical equilibrium.

The electromigration component consists of electrophoresis and electroosmosis. Electrophoresis is a selective transport mechanism that allows separation of charged species by their charge and size. Electroosmotic flow is the bulk flow mechanism in EKC techniques.

The second aspect in EKC is the chemical equilibrium of solutes between a separation electrolyte and a second, charged phase dispersed uniformly throughout the separation electrolyte called the separation carrier or pseudostationary phase. The pseudostationary phase might consist of microdroplets, liposomes, vesicles, dissolved polymers, or micelles. In the case that the pseudostationary phase is a micelle the technique is called micellar electrokinetic chromatography (MEKC) or micellar electrokinetic capillary chromatography (MECC), which will be the focus of this dissertation.

A micelle is a self forming aggregate formed by surfactants above their critical micelle concentration (CMC). The driving force for the formation of a micelle is the favorable free energy change accompanying the segregation of the hydrocarbon tails of the surfactant from the water by packing them into a central core surrounded by their polar headgroups. This is opposed by the electrostatic repulsive interactions between the headgroups. The formation of a micelle is represented by Equation 1.1 [12].

$$\Delta G^\circ_f = \Delta G^\circ_{hc} + \Delta G^\circ_H \qquad (1.1)$$

The free energy of formation ($\Delta G^\circ_f$) is equal to the contribution of the hydrophobic moiety ($\Delta G^\circ_{hc}$) and the contribution of the hydrophilic headgroup ($\Delta G^\circ_H$).

## 1.2 Theory

The observed velocity of a solute zone in MEKC is the weighted average of the velocity of the solute when dissolved in the separation electrolyte and its velocity when associated with the pseudostationary phase ($v_{psp}$). For a neutral solute, the velocity when dissolved in the separation electrolyte is equal to the velocity of the electroosmotic flow ($v_{eo}$). Differential partitioning between these two phases is what allows EKC techniques to separate neutral solutes and to change the selectivity for separations of charged solutes. In EKC $v_{psp}$ is less than $v_{eo}$ but is not equal to zero. This is in contrast to traditional chromatography, wherein the stationary phase has zero velocity ($v_{psp} = 0$) and the velocity of the mobile phase is greater than zero.

The instrument used in EKC is the same as in capillary electrophoresis (CE) and a schematic of such an instrument is show in Figure 1.1.

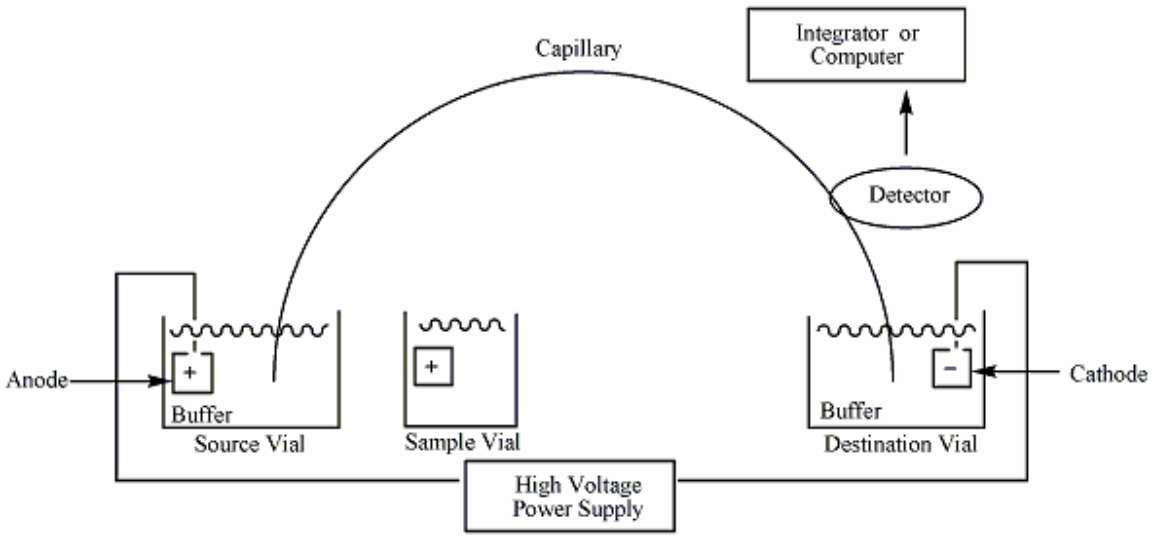


**Figure 1.1:** Schematic of a capillary electrophoresis instrument.

The instrument consists of two buffer vials in which opposite ends of a fused silica capillary are submerged. Electrodes from a high voltage power supply are placed in vials

filled with the separation electrolyte. Injections are made by inserting one end of the capillary in the sample vial and applying pressure or voltage. Detection for the work presented in this dissertation is by UV-Vis absorbance, but detectors for CE and EKC can consist of fluorescence, laser induced fluorescence, electrochemical, conductivity, thermal lens detection, and mass spectrometry.

The power supply creates an electric field along the length of the capillary supported by the aqueous buffer medium. In the presence of this electric field charged species migrate at a steady-state velocity determined by the balance between motivating electrostatic forces and retarding friction forces of the buffer medium. This steady-state velocity is termed the electrophoretic velocity ($v_{ep}$) and its magnitude is defined by equation 1.2

$$v_{ep} = \frac{qE}{6\pi\eta r} = \mu_{ep}E \qquad (1.2)$$

where $q$ is the charge of the species, $E$ is the electric field strength, $\eta$ is the viscosity of the surrounding medium, and $r$ is the radius of the species. The term $\mu_{ep}$ is the electrophoretic mobility of the charged species in that specific medium.

The second important electromigration phenomenon is electroosmostic flow which serves as the bulk flow in CE and EKC. Electroosmosis or electroosmotic flow (EOF) is due to the way ions are distributed near the surface of the capillary. The surface of a bare fused silica capillary is negatively charged in most pH ranges. This surface charge attracts a cloud of oppositely charged ions into adjacent layers of liquid, forming a double layer. When an electric field is applied along the length of the capillary (parallel to the surface plane), electrostatic forces cause the ions in the double layer to migrate. The net effect of this migration is that the bulk solution in the capillary is carried or

"pumped" through the capillary under the influence of the electric field. The velocity of the electroosmotic flow is given by equation 1.3

$$v_{eo} = \frac{\varepsilon \zeta E}{4\pi\eta} = \mu_{eo} E \qquad (1.3)$$

where $\zeta$ is the zeta potential at the surface of the charged capillary and $\mu_{eo}$ is the electroosmotic mobility. The equation for electroosmotic velocity is limited to the conditions of the capillary inner diameter being much larger than the thickness of the electric double layers. It is also important to note that, unlike pressure-induced laminar flow, there is no radial dependence for electroosmotic flow. Thus, electroosmotic flow does not contribute to zone broadening.

The observed velocity of a solute zone ($v_s$) under purely electrophoretic conditions corresponds to the sum of the effective electrophoretic velocity ($v_{ep}$) and the electroosmotic velocity ($v_{eo}$) given in equation 1.4.

$$v_s = v_{ep} + v_{eo} \qquad (1.4)$$

This can also be written as the apparent mobility of the solute ($\mu_{sol}$) being the sum of the electrophoretic ($\mu_{ep}$) and electroosmotic ($\mu_{eo}$) mobilities ($\mu_{sol} = \mu_{ep} + \mu_{eo}$).

The addition of a pseudostationary phase can change the migration velocity of a solute by adding chemical partitioning as another element of the separation as solutes partition between the pseudostationary phase and the bulk mobile phase. The separation electrolyte depicted in Figure 1.2 where the solute S is partitioning between a micellar phase and the surrounding buffer medium. The association of the solute with the micellar phase is dependent on the solutes' equilibrium partition coefficient ($P$).

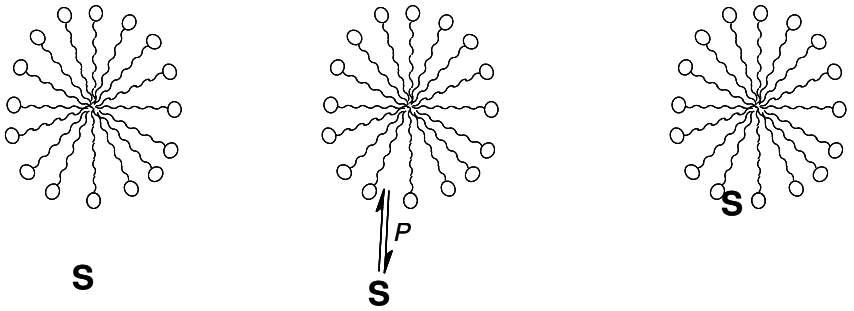


. **Figure 1.2:**

Pseudostationary phases are not immobilized but are dissolved or dispersed into the separation electrolyte. Charged Pseudostationary phases have non-zero electrophoretic mobility and observed velocity.

The observed velocity of a solute zone becomes a time weighted average of the velocity of the separation electrolyte ($v_{eo}$) and the velocity of the pseudostationary phase ($v_{psp}$) given by equation 1.5

$$v_s = \frac{t_{mob}}{t_{mob} + t_{psp}} v_{eo} + \frac{t_{psp}}{t_{mob} + t_{psp}} v_{psp} = \frac{1}{k+1} v_{eo} + \frac{k}{k+1} v_{psp} \qquad (1.5)$$

where $t_{mob}$ is the time the solute spends in the separation electrolyte, $t_{psp}$ is the time the solute spends associated with the pseudostationary phase, $v_{psp}$ is the observed velocity of the pseudostationary phase ($v_{psp} = v_{epsp} + v_{eo}$) where $v_{epsp}$ is the electrophoretic velocity of the pseudostationary phase ($v_{epsp} = \varepsilon\zeta E/6\pi\eta = \mu_{psp}E$) and $k$ is the retention factor defined by the ratio of $t_{psp}$ to $t_{mob}$.

The retention factor ($k$) can also be defined by the ratio of the equilibrium amount of solute associated with the pseudostationary phase to the amount in the mobile phase at any given time. This is related to volume of the pseudostationary phase ($V_{psp}$) over the volume of the separation electrolyte ($V_{mob}$) multiplied by the equilibrium partition coefficient ($P$) Equation 1.6.

$$k = \frac{V_{psp}}{V_{mob}} P \qquad (1.6)$$

The retention factor is an important parameter for the identification of analytes in CE and EKC separations due to the fact that it is not affected by variations in EOF which cause irreproduciblities in solute migration times. The natural logartithm of the retention factor is additionally proportional to free energy by $\Delta G^\circ = -RTlnP$ and Eq 1.6. Retention factors can be calculated from experimental migration times using the standard equation given by Equation 1.7 [9,10], which can be derived by substituting distance-over- time values for velocities and rearranging Equation 1.5.

$$k = \frac{t_r - t_0}{t_0(1 - \frac{t_r}{t_{mc}})} \qquad (1.7)$$

The variables in Equation 1.7 are $t_0$, the time for a completely unretained solute or a marker of EOF; $t_r$, the migration time of a solute; and $t_{mc}$, the migration time of a solute always associated with the micelle or effectively the migration time of a micelle. Rearrangement of Equation 1.7 was needed to calculate retention factors for the work presented in this dissertation, due to the difficulty in measuring $t_{mc}$ in each run. The rearrangement is as follows in Equations 1.8- 1.11.

$$k = \frac{1 - \frac{t_0}{t_r}}{\frac{t_0}{t_r}(1 - \frac{t_r}{t_{mc}})} \qquad (1.8)$$

$$k = \frac{\frac{1}{t_0} - \frac{1}{t_r}}{\frac{1}{t_r} - \frac{1}{t_{mc}}} \qquad (1.9)$$

Substitution of the apparent mobility, for the solute $\mu_{sol} = lL/Vt_r$ , the electroosmotic mobility $\mu_{eo} = lL/Vt_0$ and the apparent mobility of the pseudostationary phase $\mu_{effmc} = \mu_{eo} + \mu_{mc} = lL/Vt_{mc}$ yields equations 1.10 and 1.11. The term $lL$ is separation length of the capillary multiplied by the total length of the capillary, and $V$ is the applied voltage.

$$k = \frac{\mu_{eo} - \mu_{sol}}{\mu_{sol} - \mu_{effmc}} \qquad (1.10)$$

$$k = \frac{\mu_{eo} - \mu_{sol}}{\mu_{sol} - (\mu_{eo} + \mu_{mc})} \qquad (1.11)$$

Equation 1.11 was used to calculate all of the retention factors presented in this work.

The goal of any separation process is resolving the components in a mixture. Resolution ($R_s$) is a measure of the overlap of two solute zones. Resolution can be defined as the difference in distance traveled by two solute zones ($X_1$, $X_2$) divided by their average zone width ($w$), ($R_s = (X_2-X_1)/w$). The resolution in EKC depends on retention and separation efficiency according to the master resolution equation represented in Equation 1.12

$$R_s = \frac{\sqrt{N}}{4}\left(\frac{\alpha - 1}{\alpha}\right)\left(\frac{k_2}{k_2 + 1}\right)\left(\frac{1 - \frac{t_0}{t_{mc}}}{1 + (\frac{t_0}{t_{mc}})k_1}\right) \qquad (1.12)$$

Resolution is dependent on the efficiency of the separation in the plate number (N), which is proportional to the variance in the migration time of the solute zone caused by various zone broadening mechanisms. The selectivity (α), which is the ratio of retention factors ($\alpha = k_2/k_1$), the retention factor and the migration range ($t_{mc}/t_0$) are also important factors in determining the resolution. The migration range term in equation 1.12 is unique to MEKC relative to conventional chromatography and reflects limitations caused

by the so-called migration window or migration range. In MEKC neutral solutes can only elute between $t_0$, the time it would take a completely unretained solute to elute, and $t_{mc}$, the time it would take a solute completely retained in the micelle to elute. The importance of the migration window term in the resolution equation is illustrated in Figure 1.3, which is a plot of the last two terms of the resolution equation (eq. 1.13) against average $k$ ($k_{ave}$).

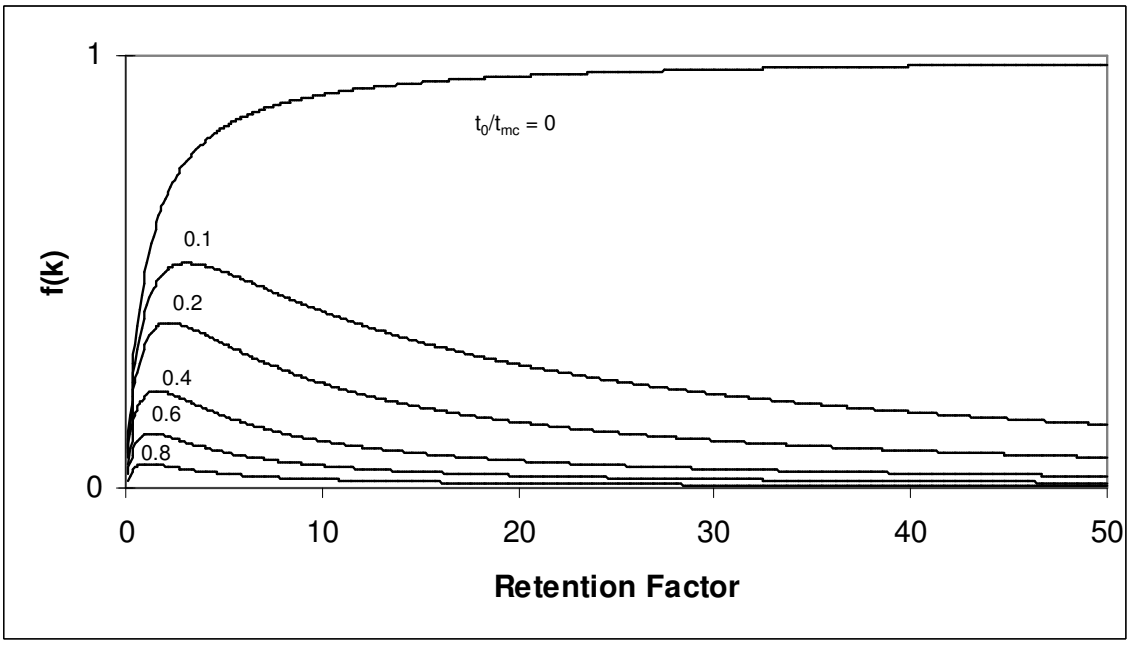


**Figure 1.3:** The dependence of *f(k)* on the retention factor in MEKC using Equation 1.13 for several ratios of $t_0/t_{mc}$.

This plot shows that the contribution of retention factor to resolution is at its greatest when the migration window is at its largest ($t_0/t_{mc} = 0$; $t_{mc} \rightarrow \infty$). It also shows that MEKC ($t_0/t_{mc} > 0$) is at a disadvantage relative to conventional chromatography where the stationary phase does not move and effectively $t_0/t_{mc}=0$.

$$f(k_{ave}) = \left(\frac{k_{ave}}{k_{ave}+1}\right)\left(\frac{1-\frac{t_0}{t_{mc}}}{1+\frac{t_0}{t_{mc}}k_{ave}}\right) \quad (1.13)$$

The plot also illustrates that, unlike conventional chromatography in which the primary distraction of high retention factors is long analysis times, high retention factors adversely affect resolution in MEKC. It has been found that the optimum value of retention factor is equal to $\sqrt{(t_{mc}/t_0)}$ [13,14].

The limited migration window also affects the total number of analytes that can theoretically be resolved. The peak capacity ($n$, Equation 1.14) is dependent on the ratio of the migration time of the last solute zone ($t_2$) and migration time of the first solute zone ($t_1$).

$$n = 1 + \frac{\sqrt{N}}{4}\ln\left(\frac{t_2}{t_1}\right) \quad (1.14)$$

In MEKC, $t_1$ corresponds to a completely unretained solute traveling at the same velocity as the EOF, and $t_2$ corresponds to a completely retained solute traveling at the same velocity as the micelle. The migration window in MEKC adds a fundamental limitation to the number of resolvable solutes.

Despite the limitations of MEKC compared to other forms of chromatography it is still a more powerful method for the analysis of many samples. The efficiencies ($N$) generated by MEKC are typically >200,000 on well optimized runs. This is much higher than other liquid phase methods and is close to the plate number generated by gas chromatography. MEKC also provides more abundant and easier methods of optimizing separation selectivity. The selectivity in MEKC can be easily changed by modifying the run buffer with complexing agents, chiral additives, co-solvents, and/or changing the

pseudostationary phase. EKC is at an advantage over GC where the selectivity is principally determined by the stationary phase in the column and is not a practical variable for method optimization. Additionally, the speed, cost, and efficiency of EKC methods provide an advantage over LC.

Due to the ease in changing selectivity by modifying the pseudostationary phase it is important to have a catalog of well characterized pseudostationary phases. Additionally, understanding the properties that control selectivity in a pseudostationary phase is important so that novel pseudostationary phases can be developed which provide diverse selectivity while maintaining low $t_0/t_{mc}$ values and high efficiencies.

# Chapter 2
# Understanding Retention and Selectivity in EKC

As noted in Chapter 1, optimization of resolution in MEKC separations can be achieved by the adjustment of three factors; efficiency which is controlled by the applied voltage, retention which can be controlled by the concentration of pseudostationary phase, and selectivity. Selectivity is controlled by the buffer conditions and the choice of pseudostationary phase. The ability to easily change pseudostationary phases and thus selectivity is a significant advantage of EKC. This advantage can only be realized, however, by the introduction and characterization of novel pseudostationary phases with unique selectivity. As new phases are introduced, it is important to be able to characterize the solute-solvent interactions that they provide [15]. The method for characterizing pseudostationary phase in this dissertation is the linear solvation energy relationship model.

## 2.1 Characterization of Selectivity Using the LSER Model

The linear solvation energy relationship model (LSER) or the solvation parameter model describes five free energy based chemical interactions between a solute and solvent. This model is similar to the Kamlet-Taft solvatochromic model [16-18] but in Abraham's model all of the solute descriptors are free energy related properties [19-22]. The solvation parameter model is based the formation of a solvation cavity for the solute and additional chemical interactions between the solute and the solvent. First a cavity of suitable size to accommodate the solute is formed in the solvent while the solvent molecules maintain their same orientation. The change in free energy is the sum of the

forces holding the solvent molecules together and is also dependent on the size of the cavity required for the solute. Second the solute is inserted into the cavity and the solvent molecules reorganized around the solute creating various solute-solvent interactions. For neutral compounds these are dispersion, induction, orientation, and hydrogen-bonding. The sum of the energy of cavity formation and the energies of the interactions is the total solvation energy.

In MEKC transfer occurs between two condensed phases composed of the separation electrolyte and the micelle. The free energy of transfer between the two phases is equivalent to the difference in the solvation energies in the separation electrolyte and the pseudostationary phase. The contribution of each interaction in the transfer is represented by the sum of the product terms made of solute descriptors and phase descriptors. A solute has the ability to participate in each intermolecular interaction and the contribution of each interaction to the free energy of transfer is the product of solute-solvent properties given by equation 2.1.

$$logSP = c + vV + eE + sS + aA + bB \qquad (2.1)$$

SP is a solute property related to free energy and in all the work presented in this dissertation logarithm of retention factor (*logk*)was used. The other terms in Eq 2.1 are made up of solute descriptors (V, E, S, A, B) and system constants (v, e, s, a, b). The solute descriptor *V* represents McGowan's characteristic volume; it is calculated by the summation rules for any compound whose structure is known [20,23]. The value is in units of $cm^3mol^{-1}/100$ and is the sum of all atomic volumes minus 6.56 $cm^3mol^{-1}$ for each bond. The polarizability of the solute is represented by E, the excess molar refraction, and accounts for the solute interactions though n- and π-electrons. The excess molar

refraction is defined as the solute's molar refraction less the molar refraction of an imaginary *n*-alkane with the same characteristic volume [19,24,25]. E can be calculated from the refractive index of the solute by $E = 10V[(\eta^2-1)/(\eta^2+2)] - 2.832V + 0.526$ and is in units of $cm^3mol^{-1}/10$. The solute's hydrogen bonding ability is accounted for by A the hydrogen bond donating ability, and B the hydrogen bond accepting ability. These descriptors are determined in conjunction with other solute descriptors using liquid-liquid distribution and chromatographic measurements [20, 26]. The A and B terms in the solvation parameter model do not refer to proton transfer acidity expressed by the pKa scale. The dipolarity/polarizability of the solute is described by the S term. It is determined in combination with the hydrogen bond descriptors from liquid-liquid distribution constants and chromatographic measurements [19, 20]. Solute descriptors have been determined for over 4000 compounds and are listed extensively in the literature. Additionally, these terms are additive and can be estimated from a solute's functional group fragments. A software program Absolv has been developed to predict the molecular descriptor from a set of 81 atom and functional group fragments and is capable of reproducing experimentally derived results with correlation coefficients ranging form 0.95 to 0.99 [27].

The system constants are obtained by multiple linear regression analysis and are not just regression constants but contain important chemical information about the system. The phase descriptors reflect the difference in solute interactions between the separation electrolyte and the pseudostationary phase. The differences in interactions with n- and π-electrons is represented by e. The dipole-type interactions are represented by s, the ability for the pseudostationary phase to accept a hydrogen bond is represented

by a, where as b represents the pseudostationary ability to donate a hydrogen bond. The difference in cavity formation and residual dispersion between the separation electrolyte and the pseudostationary phase is accounted for by v, also described as the relative cohesivity of the pseudostationary phase.

To obtain meaningful results from the LSER model a few requirements must be accounted for. First the SP in Eq 2.1, which is log($k$) in the work presented here, must cover a reasonable numerical range with uniform distribution throughout. Clustering of low or high log($k$) values will result in large prediction error and erroneous or imprecise system constants [28]. Additionally, careful consideration must be used when choosing the solutes. A sufficient number and variety of solutes must be used to define all interactions and establish statistical validity of the model [29]. A minimum of seven solutes is sufficient to solve Eq 2.1 by multiple linear regression techniques. The general minimum requirements are considered to be three varied values for each solute descriptor and the intercept, but since individual solutes express several interactions simultaneously the number of solutes required drops from 18 to 9 [8]. As in this work it is common to obtain an exhaustive fit with the use of 20-40 solutes. Careful selection of the solutes is also necessary to avoid cross correlation between the solute descriptors [29]. An unintentional correlation between descriptor values results in the multiple linear regression algorithm to be unable to distinguish between the correlated descriptors. While correlation between some solute descriptors like s and e is inevitable due to the similarity in the chemical interactions they describe, cross correlation is only a significant problem when $r \geq 0.8$. Furthermore, solutes that are significantly ionized at the working pH should not be used for an LSER analysis.

## 2.2 LSER of EKC Systems

There have now been multiple published studies that utilize the LSER approach to characterize the retention and selectivity of pseudostationary phases for EKC. The phase descriptors for 55 EKC systems, including anionic surfactants, double chain surfactants, amide containing surfactants, perfluornated surfactants, bile salts, cationic surfactants, microemulsion/SDS, liposomes, and polymeric phases are listed in Table 2.1.

**Table 2.1**: Characterization results of EKC systems

| | Systems | LSER Phase descriptors | | | | | | Ref. |
|---|---|---|---|---|---|---|---|---|
| | | c | e | s | a | b | v | |
| 1 | SDS | -1.68 | 0.56 | -0.6 | -0.27 | -1.67 | 2.72 | [30] |
| 2 | SDecS | -2.43 | 0.32 | -0.24 | 0 | -1.6 | 2.69 | [31] |
| 3 | SOS | -1.97 | 0.45 | -0.31 | -0.12 | -1.87 | 2.85 | [31] |
| 4 | SDSu | -1.92 | 0.33 | -0.42 | -0.02 | -1.78 | 2.84 | [32] |
| 5 | SDCar | -1.95 | 0.15 | -0.39 | 0.23 | -1.77 | 2.96 | [32] |
| 6 | SDP | -1.92 | 0.24 | -0.55 | 0.15 | -2 | 3.01 | [32] |
| 7 | SDCV | -1.65 | 0.42 | -0.61 | 0.11 | -2.38 | 2.94 | [32] |
| 8 | SLSA | -1.82 | 0.41 | -0.37 | 0.1 | -2.39 | 2.96 | [32] |
| 9 | THADS | -1.43 | 0.57 | -0.66 | -0.33 | -1.56 | 2.56 | [29] |
| 10 | LDS | -1.58 | 0.59 | -0.6 | -0.32 | -1.57 | 2.61 | [30] |
| 11 | Mg(DS)2 | -1.55 | 0.27 | -0.42 | -0.27 | -1.88 | 3.02 | [33] |
| 12 | Cu(DS)2 | -1.51 | 0.35 | -0.51 | -0.26 | -1.92 | 3.05 | [33] |
| 13 | LMT | -1.9 | 0.51 | -0.35 | 0.39 | -2.37 | 2.88 | [34] |
| 14 | ALE | -1.89 | 0.44 | -0.37 | 0.49 | -2.41 | 2.92 | [34] |
| 15 | SLN | -1.99 | 0.44 | -0.39 | 0.45 | -2.32 | 2.92 | [34] |
| 16 | SPN | -1.72 | 0.42 | -0.45 | 0.48 | -2.58 | 3.11 | [35] |
| 17 | AOT | -1.82 | 0.34 | -0.43 | 0.02 | -3.02 | 3.09 | [36] |
| 18 | LPFOS | -1.41 | -0.11 | -0.24 | -0.88 | -0.46 | 1.97 | [30] |
| 19 | SC | -1.41 | 0.69 | -0.69 | 0.12 | -1.94 | 2.27 | [30] |
| 20 | DOC | -1.83 | 0.93 | -0.87 | 0.07 | -1.79 | 2.42 | [30] |
| 21 | KDC | -1.97 | -0.53 | -0.92 | 0 | -2.5 | 3.1 | [37] |
| 22 | STC | -2.1 | 0.6 | -0.34 | 0 | -2.06 | 2.43 | [29] |
| 23 | STDC | -1.99 | 0.67 | -0.45 | 0 | -2.17 | 2.62 | [29] |
| 24 | KGDC | -1.83 | -0.6 | -1.03 | 0 | -1.99 | 2.78 | [37] |
| 25 | CTAB | -1.83 | 1.11 | -0.76 | 0.82 | -2.44 | 2.71 | [30] |
| 26 | TTAB | -1.85 | 0.9 | -0.62 | 0.77 | -2.41 | 2.63 | [30] |
| 27 | DTAC | | 0.75 | -0.43 | 0.87 | -2.67 | 2.82 | [38] |
| 28 | DHAB | -2.96 | 1.46 | -0.59 | 1.34 | -4.38 | 4.01 | [39] |
| 29 | EMULSION (SDS, butan- 1-ol) | -1.13 | 0.28 | -0.69 | -0.06 | -2.81 | 3.05 | [21] |

| | | | | | | | | |
|---|---|---|---|---|---|---|---|---|
| 30 | DPPG:DPPC:Chol | -2.3 | 0.54 | -0.65 | 0.32 | -3.12 | 3.01 | [40] |
| 31 | DPPG:DPPC | -2.21 | 0.45 | -0.44 | 0.71 | -3.23 | 3.13 | [40] |
| 32 | DHP | -2.68 | 0.42 | -0.65 | 0.47 | -3.27 | 3.59 | [41] |
| 33 | DHP+Chol | -2.28 | 0.53 | -0.77 | 0.43 | -3.29 | 3.35 | [41] |
| 34 | PAAU | -1.86 | 0.26 | -0.16 | -0.27 | -1.05 | 2.11 | [42] |
| 35 | PSUA | -2.28 | 0.18 | 0.45 | -0.15 | -1.18 | 1.64 | [42] |
| 36 | poly-(SocS) | 2.68 | 0.22 | 0.26 | -0.14 | -1.15 | 2.25 | [43] |
| 37 | poly-(SnoS) | -3.02 | 0.48 | 0.08 | -0.15 | -1.5 | 2.91 | [43] |
| 38 | poly-(SDeS) | -2.93 | 0.52 | -0.04 | -0.14 | -1.64 | 2.95 | [43] |
| 39 | poly-(SUS) | -3.01 | 0.69 | -0.19 | -0.1 | -1.77 | 3.18 | [43] |
| 40 | AGENT | -2.81 | 0.76 | -0.07 | 0.45 | -1.93 | 2.07 | [44] |
| 41 | OAGENT | -1.65 | 0.71 | -1.08 | 0.11 | -2.29 | 2.06 | [44] |
| 42 | DAGENT | -1.98 | 0.59 | -0.78 | 0.23 | -2.42 | 2.39 | [44] |
| 43 | SAGENT | -1.75 | 0.63 | -1.14 | 0.33 | -2.64 | 2.51 | [44] |
| 44 | AGESS | -2.4 | 0.46 | -0.43 | 0.27 | -2.46 | 2.72 | [45] |
| 45 | Elvacite 2669 | -1.67 | 0.36 | -0.19 | 0.07 | -1.88 | 2.05 | [46] |
| 46 | poly(AMPS-sodium octyl methacrylate 21) (pOMAT-21-Na) | -2.66 | 0.47 | -0.6 | -0.41 | -3.75 | 3.56 | [47] |
| 47 | poly(AMPS-sodiumlurylmethacrylate-15) (pLMAt-15-Na) | -2.84 | 0.44 | -0.67 | -0.27 | -3.7 | 3.65 | [47] |
| 48 | poly(AMPS-sodium steryl methacrylate-16) (pSMAt-16-Na) | -2.73 | 0.65 | -0.85 | -0.5 | -3.83 | 3.78 | [47] |
| 49 | poly(AMPS-sodium lauryl acrylate-13) (pAT-13-Na) | -2.96 | 0.39 | -0.4 | -0.02 | -3.52 | 3.58 | [47] |
| 50 | poly(AMPS-sodium luryl methacrylamide-19) (pLMAm-19-Na) | -2.69 | 0.37 | -0.32 | 0.25 | -2.45 | 2.88 | [47] |
| 51 | poly(AMPS-sodium lauryl methacrylamide-28) (pSAm-28-Na) | -2.57 | 0.42 | -0.53 | -0.19 | -3.05 | 3.39 | [47] |
| 52 | poly(AMPS-sodium dihydrocholesteryl acrylate-2) (pDHCHAt-2-Na) | -3.11 | 0.61 | -0.6 | -0.04 | -2.58 | 2.91 | [48] |
| 53 | poly(AMPS-triethyl-amine dihydrocholes-teryl acrylate-33) (pDHCHAt-33-TEA) | -2.68 | 0.65 | -0.46 | 0.24 | -3.21 | 3.4 | [48] |
| 54 | poly(AMPS-triethyl-amine lauryl acrylate-9.2) (pLAt-9.2-TEA) | -3.15 | 0.5 | -0.4 | 0.23 | -3.19 | 3.15 | [48] |
| 55 | poly(AMPS-sodium | -2.86 | 0.33 | -0.44 | 0.43 | -3.22 | 3.36 | [48] |

| | |
|---|---|
| | tert-octyl acrylamide-49) (ptOAm-49-Na) |

These are 55 representative systems out of over 200 that have been characterized with the LSER model. Anionic surfactants have been most frequently characterized by the LSER model to date.

The many reports described above include several systematic studies utilizing LSER to investigate the effects of surfactant structure on pseudostationary phase retention and selectivity. Trone and Khaledi used the LSER model to characterize MEKC selectivity based on different structural factors including tail length [49], counter ion [33], and headgroup [32]. They reported that the length of the hydrophobic tail had little effect on the selectivity the system [49], and this was also confirmed by Vitha and Carr [31]. The choice in counter ion was also found to provide little change in selectivity [33]. The selectivity changes that were induced by the counter ion were dependent on the ion's valence, and they report that a divalent counter ion when compared to a monovalent counter ion reduces the electrostatic repulsion between the surfactant headgroups and affects the packing of the monomers which in turn reduces the amount of water at the water-micelle interface. A reduction of water in the interfacial layer leads to a decrease in polar/polarizable and hydrogen bonding interactions between the solute and the micelle. The most significant factor they found to effect selectivity was the headgroup of the surfactant (Table 2.1 systems 1, 4-8) [32]. The control of selectivity by the headgroup is believed to be a result of the water that resides near the micelle surface. From the previous works it is considered that the headgroup is the most important structural factor in determining selectivity in MEKC [30,32-34,49].

Excluding the work presented herein there have been only four cationic surfactants characterized by the LSER model (Table 2.1, systems 25-28). The structures of these four surfactants are shown in Figure 2.1.

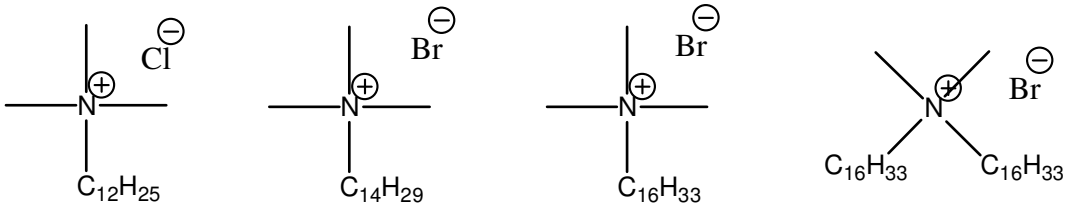


DTAC TTAB HTAB DHAB

**Figure 2.1:** Structures of DTAC, dodecyltrimethylammonium chloride; TTAB, tetradecyltrimethyammonium bromide; CTAB, hexadecyltrimethylammonium bromide; DHAB, dihexadecyldimethylammonium bromide.

All of the surfactants in Figure 2.1 are ammonium based surfactants with a tail in length of 12-16 carbons. The additional substituents on the headgroup are all methyl; accept for DHAB which has two 16 carbon chains and two methyl groups. The results from Trone and Khaledi's studies into how structure affects selectivity suggest that the three single chained surfactants will provide similar selectivity because they differ only in tail length and counter ion but have the same trimethyl headgroup.

The similarities and differences between surfactant systems can be seen more clearly when the five variable matrix of the LSER phase descriptors is expressed in two dimensions by a principle component analysis (PCA). A PCA of the 55 systems in Table 2.1 was preformed in 2006 by Fuguet *et. al*. after the values in Table 2.1 under went the data pretreatment of being divided by ω ($\omega = \sqrt{e^2 + s^2 + a^2 + b^2 + v^2}$). The results of this PCA are presented in Figures 2.3 and 2.4. The results graphically depict where in "selectivity space" each system is located in relation to the others [50].

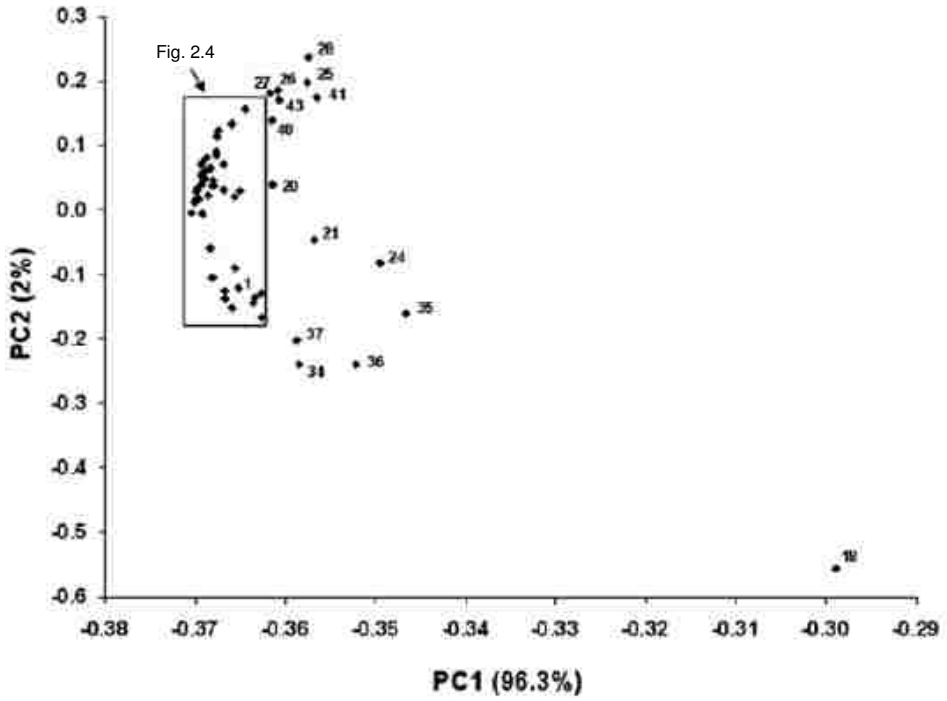


**Figure 2.3:** Plot of the two main PCs from the normalized phase descriptor values in Table 2.1. Reproduce from Ref [50] with permission from Wiley-VCH

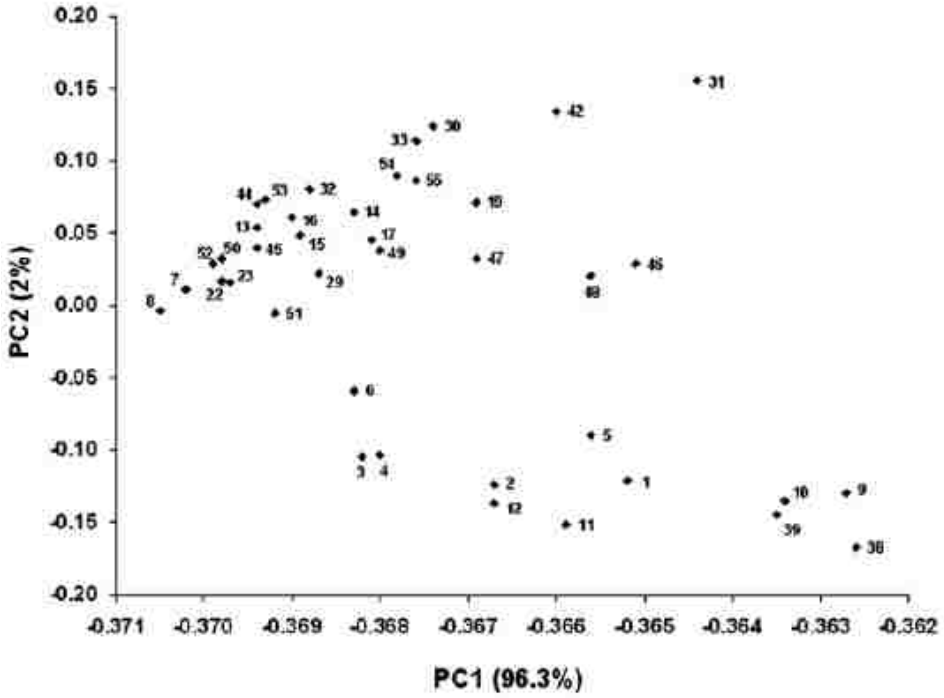


**Figure 2.4:** Detail of the two main PCs from the normalized phase descriptor values in Table 2.1. . Reproduce from Ref [50] with permission from Wiley-VCH

The PCA shows that the cationic surfactants (systems 25-28) occupy a unique selectivity space away from the majority of other characterized systems. The cationic surfactants occupy a space of an average value in PC1, excluding the perfluorinated surfactant lithium perfluoroocatane (LPFOS, system 18). The cohesivity of the phase (v) is the major contributor to PC1, with v being the dominant factor in controlling separation and having the largest phase descriptor values. The main contributors to PC2 are the hydrogen bonding terms a and b. The cationic surfactants on average have more negative b values and more positive a values than the other surfactants. This may be the cause for them occupying higher PC2 values than the other characterized systems.

The solvation parameter model is useful for characterizing the selectivity afforded by a pseudostationary phase. The model allows pseudostationary phases that have similar and unique selectivity to be identified. This is beneficial in method optimization so that a proper pseudostationary phase can be selected, or a pseudostationary phase that has opposing selectivity can be substituted. The phase descriptors also aid in rational design for novel phases that may be need for unique applications. Advantageous, properties of the solvation parameter model include its ease of use, the robustness of it being able to be applied to different forms of chromatography (EKC, LC, GC), and the insight it gives into the physical processes that control retention. Despite all the valuable aspects of the solvation parameter model it is limited in its ability for predicting experimental results and the results for the solvation parameter model can be easily over interpreted.

## Chapter 3
## Included Work

The primary focus of the research in this dissertation is to introduce and characterize new cationic surfactants for EKC. Cationic surfactants are of interest because they occupy a unique selectivity space away from the other characterized MEKC systems. Cationic surfactants are amendable to synthetic manipulation to provide novel surfactant structures. They also provide a unique opportunity to systematically examine how structure affects selectivity.

In the following chapters of this dissertation I examine the structure-selectivity relationship of cationic surfactants. In Chapter 4 the asymmetrical headgroup *N*-alkyl-*N*-methylpyrrolidinium gives rise to the first example of an ionic liquid based surfactant used as the sole pseudostationary phase in EKC [51]. In Chapter 5 the structure-selectivity relationship of pseudostationary phases is examined by changing the size headgroup. Additions of one methylene unit (-$CH_2$-) are added to surfactant headgroups consisting of three linear alkyl substituents and one series of surfactants where the ammonium is incorporated into a ring structure of increasing size. Chapter 6 measures the effects of increasing headgroup size with some representative applications. The applications include acidic methoxyphenols that are chemical markers of wood smoke, analytes representative of basic pharmaceuticals, and of a group of hydrophobic pharmaceutical corticosteroids. In Chapter 7 the role of the charge center is examined and is the first example of a phosphonium surfactant to be characterized and applied in an

EKC system. In Chapter 8 two glucocationic surfactants are investigated to determine the effect of differing functionality adjacent to the headgroup.

This work greatly contributes to the field of EKC with only a few (3) cationic surfactants having been characterized in the literature. This dissertation includes 16 new pseudostationary phase, 81% of all cationic surfactants characterized for MEKC.

Furthermore, cationic surfactants occupy a selectivity space that is different from other EKC phases which make them likely candidates for the separation of mixtures that can't be separated by an anionic surfactant or to give orthogonal selectively in a multidimensional separation system.

# Chapter 4
# Electrokinetic Chromatographic Characterization of Novel Pseudo-Phases Based on N-Alkyl-N-methylpyrrolidinium Ionic Liquid type Surfactants

## 4.1 Introduction

Micellar electrokinetic chromatography (MEKC) is a particularly powerful extension of CE for the separation of mixtures of uncharged and/or charged compounds in which the former are separated according to their distribution between the aqueous phase and a micellar pseudostationary phase. The selectivity of MEKC separations is primarily determined by the choice of micelle-forming surfactant. Multiple studies have been performed characterizing the selectivity of micellar [30-33, 49], polymeric [52-56], vesicular [39, 57], and liposome [40, 58, 59] pseudostationary phases. Despite the large number of characterized phases reported previous to this work, there had been relatively few reports concerning cationic pseudostationary phases and no work characterizing an ionic liquid as a pseudostationary phase. In order to gain insight on how an ionic-liquid surfactant would affect MEKC selectivity, as well as to study the effects of pendant alkyl chain length, I studied four *N*-alkyl-*N*-methylpyrrolidinium bromide ($C_n$MPYB, $n \geq 10$) surfactants (Figure 4.1), which resemble the popular room temperature ionic liquid (RTIL) $[C_4MPY]^+[X]^-$ [60, 61], and compared the selectivity and solvation milieu to the classical cationic surfactant cetyltrimethylammonium bromide ($C_{16}$TMAB).

RTILs have many unique properties and potential applications in analytical chemistry. The combination of thermal stability, inflammability, nonvolatility, broad temperature range of the liquid state and options for simple iterative design place RTILs as excellent solvents for developing and expanding a plethora of chemical analyses. Surprisingly,

only recently have RTILs begun to gain momentum in use as solvent, co-solvent, additive, and matrix components in analytical chemistry [60, 62].

Currently, the most frequent analytical utility of RTILs has been within the separation sciences, particularly as stationary phases in gas–liquid chromatography (GLC) [63-65] or mobile phase additives or run buffer modifiers in capillary separations where they have found merit in improving band broadening, resolution, peak efficiency, separation time, tailing/symmetry, as well as in suppressing the deleterious effects of free silanols [66-71]. Given the broad range of solvation-type interactions available to RTILs, GLC has been particularly useful in mapping out the nature, efficiency, and selectivity of solute retentive behavior by RTILs [75].

Recently, several investigations have found that RTILs may also be used to improve CE or EKC as well. For example, Stalcup and co-workers reproducibly (RSD ≈ 2%) resolved several catechin constituents isolated from grape seed extracts using six aqueous 1-alkyl-3-methylimidazolium ($[C_nMIM]^+$, $n$ = 2, 4 with several anions) RTIL solutions as running electrolytes [71]. Warner and co-workers used $[C_nMIM]^+$ RTILs as buffer modifiers in combination with poly(sodium *N*-undecylenic sulfate) and poly(sodium oleyl-L-leucylvalinate) polymeric pseudo-stationary phases for the separation of two achiral mixtures (alkyl aryl ketones and chlorophenols) and a single chiral mixture (binaphthyl derivatives), respectively [69]. Additionally, Shamsi and Rizvi were the first to use solely a chiral ionic liquid surfactant and its polymeric analog to resolve the enantiomers of (±)-α-bromophenylacetic acid and (±)-2-(2-chlorophenoxy)propanic acid [76]. Furthermore, Tian et al [77] found that the addition of $[C_4MIM]^+[BF_4]^-$ to sodium

dodecyl sulfate (SDS) in buffer led to the complete resolution of otherwise intractable lignan herbal medicine extracts from *S. chinensis* and *S. henryi* seeds.

Given their widespread industrial and technological applications, surfactants with novel features are of considerable current interest. Recently, the potential of long hydrocarbon chain RTILs and RTIL analogs to act as ion exchangers, surfactants, and phase transfer agents has been recognized [78, 79]. An interesting aspect of RTILs is that even their shorter-chained versions, such as $[C_nMIM]^+$ with n=4 and 8 may possess inherent amphiphilicity [80, 81]. For example, Göktürk et al. [81] have shown that the RTIL $[C_4MIM]^+$[*n*-octyl sulfate]$^-$ supports micelle formation in aqueous solution. Baker *et al.* investigated the aqueous aggregation behavior of long-chained $C_nMPYB$ ($n \geq 10$) surfactants which resemble the popular RTIL $[C_4MPY]^+[X]^-$[60, 61]. It is important to note that, upon ion exchange with $Li^+[(CF_3SO_2)_2N]^-$, $C_{10}MPYB$ indeed generates a true RTIL.

In order to determine the utility of the ionic liquid type surfactants as a pseudostationary phase in EKC, to better understand how pseudostationary phase structure affects selectivity, and to expand the range of analytical utility of RTILs, I characterized C*n*MPYB surfactants with the solvation parameter model discussed in Chapter 2. This work was reported in *Electrophoresis* in 2006 as the first example of the use of RTILs as the sole separation carrier in EKC [51]. Additionally, these were the first cationic surfactants characterized using EKC that did not contain a trimethyl ammonium headgroup.

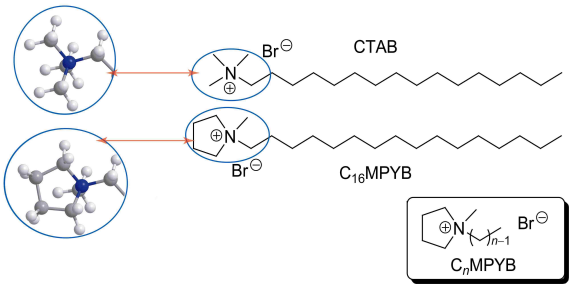


**Figure 4.1.** Chemical structures of cetyltrimethylammonium bromide (CTAB) and its $C_n$MPYB analog *N*-cetyl-*N*-methylpyrrolidinium bromide ($C_{16}$MPYB). Energy-minimized ball and stick models of the headgroups are provided for comparison with the N heteroatoms shown in black.

Of course, with the aim of using such surfactants in future MEKC separations, it is possible that these solvation parameter correlations could be used to predict the partitioning behavior using the molecular descriptors available for a broad variety of prospective solutes not directly studied.

### 4.2 Results and Discussion

Under the separation conditions, the $[C_n MPY]^+$ ions provided a dynamic coating on the fused-silica capillary surface, changing the sign of the zeta potential and engendering anodic EOF [39]. In this way, micelles move counterflow with respect to the EOF, allowing separation of neutrals principally governed by partition to and association with a $C_n$MPYB or $C_{16}$TMAB-based pseudostationary phase electrophoretically migrating toward the cathode. Moreover, $[C_n MPY]^+$ imparts to the fused-silica capillary wall a permanent charge not subject to pH-induced variations in ionization so long as the ionic attraction between anionic silanols and the cationic surfactant is not perturbed. These results are reminiscent of those obtained by Stalcup and co-workers using short-chain $[C_2MIM]^+$ and $[C_4MIM]^+$ RTILs [71]. However, in our case the long-chain

$[C_nMPY]^+$ surfactants are capable of forming supported bilayers or hemimicelles on the bare silica surface [82].

The general characteristics of $C_{16}$TMAB and $C_n$MPYB-based pseudo-phases are listed in Table 4.1.

**Table 4.1.** Electrophoretic Mobilities and Chromatographic Properties of RTIL and CTAB Surfactant Micelles[a,b]

| Surfactant | $\mu_{ep} \times 10^4$ ($cm^2\ V^{-1}\ s^{-1}$) | $\alpha_{(CH2)}$ | $\mu_{eo} \times 10^4$ ($cm^2\ V^{-1}\ s^{-1}$) | $t_{mc}/t_0$ | Phase Ratio[c] | Theroetical Plates (N=9) | CMC (mM)[d] |
|---|---|---|---|---|---|---|---|
| $C_{12}$MPYB | 2.73 (0.02) | 2.17 (0.02) | -3.71 (0.05) N=120 | 2.70 (0.04) | 78 | 250 000 (14 000) | 13.6 (0.24) |
| $C_{14}$MPYB | 2.68 (0.01) | 2.33 (0.01) | -4.59 (0.04) N=96 | 2.41 (0.03) | 120 | 320 000 (5 300) | 3.30 (0.15) |
| $C_{16}$MPYB | 2.21 (0.02) | 2.45 (0.01) | -3.75 (0.05) N=96 | 2.38 (0.01) | 169 | 280 000 (14 000) | 0.83 (0.06) |
| $C_{18}$MPYB | 2.44 (0.01) | 2.49 (0.01) | -4.16 (0.03) N=123 | 2.15 (0.03) | 227 | 210 000 (18 000) | 0.25 (0.03) |
| CTAB | 2.53 (0.01) | 2.34 (0.01) | -5.043 (0.002) N=44 | 2.081 (0.002) | 64 | 174 000 (2 000) | 0.92[e] |

[a] The errors reported in parentheses are the standard errors, $\pm\sigma/\sqrt{N}$. N=3 unless otherwise noted. [b] Conditions given in text. [c] $V_{aq}/V_{mic}$, calculated using $(1-V_m(C_{srf}-CMC))/ V_m(C_{srf}-CMC)$, where $V_m$ is the approximate molecular volume of the surfactant estimated from atomic van der Waals increments using the Bondi method; see ref. 45. [d] Data from ref 13. [e] Fendler, J. H. *Membrane Mimetic Chemistry;* Wiley Interscience: New York, 1982; p 9.

The electrophoretic mobilities of the micelles do vary significantly between the materials, and generally become lower with increases in the alkyl chain length. Electroosmotic mobilities are affected by the type of surfactant used because of differences in adsorption at the capillary wall. There is no trend in the electroosmotic mobility with alkyl chain length, but the magnitude of the electroosmotic mobility is greater when $C_{16}$TMAB is used. The lower electroosmotic mobilities, combined with similar electrophoretic mobilities, result in a wider migration range ($t_{mc}/t_0$) for the $C_n$MPYB surfactants. Methylene selectivity, $\alpha_{(CH2)}$, a measure of the hydrophobicity of

the micelles, increases with alkyl chain length, as expected. Furthermore, the separation efficiencies employing $C_n$MPYB micelles are excellent compared to results obtained with $C_{16}$TMAB and other conventional micelles. For instance, separations using $C_{16}$MPYB generated efficiencies near 300,000 plates (N), a 65% increase relative to $C_{16}$TMAB. It is not clear why the efficiency is better with the $C_n$MPYB micelles.

Experimentally measured retention factors of a set of 31 to 34 (*x*) test solutes were regressed against tabulated Abraham's solute descriptors for $C_{16}$TMAB and $C_n$MPYB (*n* = 12, 14, 16, and 18) surfactant systems. (Use of a consistent set of 27 solutes for all surfactants did not have a significant effect on the LSFER values reported). This test pool of solutes, listed in the experimental section, covered a wide range of solute types, including nitrogen heterocyclic bases and phenols, and was selected to be of adequate size and with properties sufficiently varied to define properly all interactions represented in solvation parameter model. The importance of this point as well as careful avoidance of cross-correlation between the descriptors and use of "generic" experimental conditions has been definitively argued by Poole *et al*. [29]. The greatest correlation coefficient ($r^2$) for the solute descriptors parameters used in this study is 0.54 between S and E, and the average of the absolute values of the cross-correlation coefficients is 0.3. A representative MEKC separation of four neutral benzene-type hydrophobic solutes using the $C_{16}$MPYB aqueous micelle system is provided in Figure 4.2.

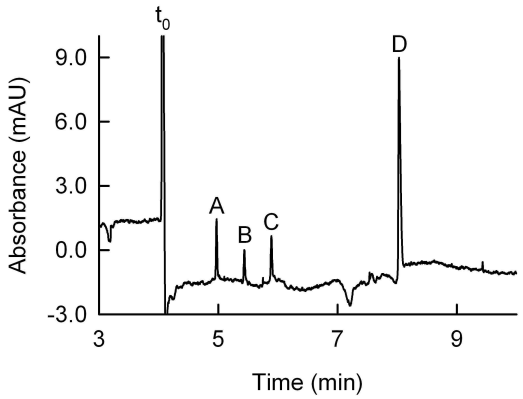


**Figure 4.2.** Representative MEKC electropherogram of a benzonitrile (peak A), nitrobenzene (peak B), phenol (peak C), and benzene (peak D) mixture using 15 mM $C_{16}$MPYB. Conditions are as follows: 30 mM TRIS buffer, pH 7.00, 25 °C; 60 mbar s injection; applied voltage, 20 kV; anodic detection at 214 nm. Acetone was used as the EOF marker.

This is a typical or representative result at 214 nm; baselines were more stable at 254 nm. The correlation coefficients for fits to eq 1 ranged from $r^2 = 0.87$ for $C_{14}$MPYB ($x = 33$) to 0.90 for $C_{16}$MPYB ($x = 33$) and $C_{18}$MPYB ($x = 34$) and 0.97 for $C_{12}$MPYB ($x = 31$). Although the fits to solvation parameter model were in some cases somewhat poorer for the $C_n$MPYB surfactants compared with typical surfactant systems such as $C_{16}$TMAB ($r^2 \approx 0.95$), the results are still statistically meaningful. The slight differences in the number of solutes included in each fit are due to the elimination of one or more solutes that were not well resolved from $t_0$, gave poor peak shape, or were or were severe outliers from the model.

Solvation parameter results for MLRA performed on the set of probe molecule solute descriptors and their retention factors using $C_n$MPYB and $C_{16}$TMAB-based pseudo-phases are summarized in Figure 4.3.

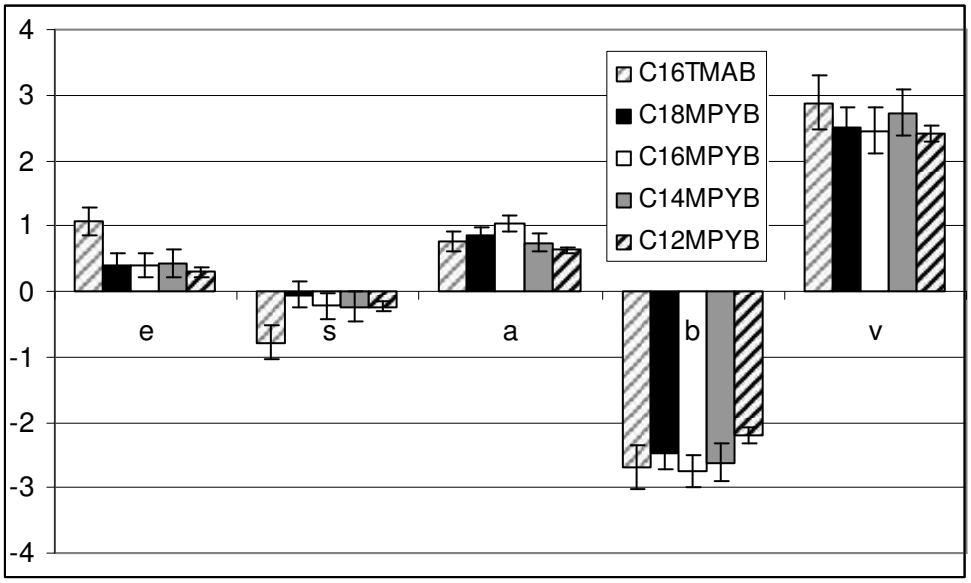


**Figure 4.3.** Summary of LSER results for MEKC separations using CTAB and the four $C_n$MPYB surfactants.

The values of each coefficient (*e*, *s*, *a*, *b*, *v*) of the correlation reflect the system properties for the corresponding solute properties and are measures of the difference in solvent properties between the micelle and the buffer, as discussed in Chapter 2. The *c* constant being irrelevant in this respect, it is not included.

The results for 40 mM $C_{16}$TMAB compare favorably to those reported previously by Rosés, Abraham, and co-workers for 20 mM $C_{16}$TMAB[30]. In fact, the recovered coefficients in the current study and the one from the Rosés group differ by 6.0% on average and are not significantly different at better than 95% confidence. The slight differences reported in the literature in some cases may come from selection of a different set of analyzed compounds as well as the uncertainty in obtaining each coefficient, generally ≈2–10%.

Our data clearly show that the headgroup chemistry has a greater impact on the chemical selectivity than does the aliphatic chain length over the $n$ = 12–18 range. The

fact that the headgroup has an influence on selectivity is perhaps not altogether surprising [83, 84]. The degree to which this seemingly minor structural change transforms the behavior of the resulting micellar pseudo-phase is somewhat surprising, however. In particular, the polarity and polarizability characteristics of the RTIL surfactants are significantly different from those of $C_{16}$TMAB, a fact made particularly evident from head-to-head comparisons between the same chain-length analogs $C_{16}$MPYB and $C_{16}$TMAB. Individually, these surfactants do not show significant differences in acid base interactions or cohesivity, but in aggregate the results do suggest that the $C_n$MPYB surfactants are more cohesive than $C_{16}$TMAB. Overall, the $C_n$MPYB surfactants appear to be more cohesive, are better able to interact with polar compounds, and are less able to interact with n- and π-electrons relative to $C_{16}$TMAB. In light of these results, it is important to introduce the fact that the degree of micellar dissociation $\beta = 1 - q$, where $q$ is the fraction of "bound" charge, extracted from the conductance data is little affected by headgroup substitution; i.e., $\beta = 0.759$ and 0.742 for $C_{16}$MPYB and $C_{16}$TMAB, respectively. Given their statistically equivalent counter-ion binding and similarity in CMC (0.83 and 0.92 mM) [60], striking differences in MEKC behavior would not be expected.

Our results suggest that, in regard to the relative weight of the individual interactions represented in the solvation parameter model, the most important are the terms containing $V$ and $B$. As $v$ is a measure of dispersive interactions and the relative ease of forming a cavity for the solute, the large magnitude and positive sign of the coefficient at $V$ indicates that the energy needed to form a cavity for the solute molecule

works in favor of solute retention; i.e., all micelle phases studied are adequate for separating solutes according to their size.

Our results also suggest that the $C_n$MPYB surfactants may generate a relatively cohesive solvent environment compared to most surfactant phases, a fact reflected in the relative magnitude of *v*. As benchmarks, *v* values for cationic micellar phases based on the alkyltrimethylammonium bromides usually fall in the 2.6 to 3.0 range [30,39] while cationic vesicular phases, such as those formed from the two-tailed surfactant dihexadecyldimethylammonium bromide (DHAB), are even less cohesive (more "hydrocarbon-like") with *v* values as high as 4.0 [39]. Consistent with the latter value is the fact that, in the case of DHAB, bromide counter-ions remain tightly bound to the vesicle surface ($\beta < 0.01$). Anionic micelles, on the other hand, possess *v* values from 2.0 for lithium perfluorooctanesulfonate (LPFOS) [30] and 2.3 for the bile salt detergent sodium cholate [30, 85] to 2.7–3.0 for SDS, depending on conditions and counter-ion valency [30, 33, 39, 49]. The $C_n$MPYB series, despite being a linear surfactant and not being fluorinated, yields values of *v* ranging from 2.4 to 2.7 and a composite value of $2.52 \pm 0.30$, without any clear trend with chain length. While these values do overlap with those for other cationic linear surfactants, they are generally lower and in aggregate suggest greater cohesivity. One tentative possibility is that the pyrrolidinium headgroup displays additional van der Waals attractions leading to more "cross-linked" headgroup association, similar to but much weaker than the case of cationic headgroups being ionically bridged pairwise by a divalent anion.

Regarding the *s* coefficient, the value for $C_{16}$TMAB was –0.78 indicating a phase that is less dipolar than water and completely in line with the reported value of –0.76

[30]. Reported values of *s* generally vary little with the class of surfactant and span the moderate range from –0.24 for LPFOS to about –0.87 for sodium deoxycholate [30]. In contrast, *s* is not significantly different from zero for the $C_n$MPYB surfactants. Considering the imprecision in these values, we can conclude that the RTIL-based surfactants are able to interact with polar compounds with an affinity that generally does not differ appreciably from water. Again, this is unique to micellar systems. Although in one case an *s* of 0.46 was reported for LPFOS [33], this value was later called into question and the discrepancy attributed to use of an inadequate training set of solutes or, possibly, purification difficulties stemming from the tensioactive nature of the LPFOS surfactant [30]. It is important to make the distinction that our results do not necessarily suggest that $C_n$MPYB-based micelles are more polar than other micelles, but that they do have a greater ability to interact with polar species relative to virtually all known micelle systems. Previously it was concluded, based on the pyrene $I_1/I_3$ index as a measure of the local solvent dipolarity [86, 87], that the environment surrounding pyrene solubilized within $C_{18}$MPYB micelles was toluene-like [60]. If less remarkable, the acid-base attributes of the $C_n$MPYB-based micelles also merit brief discussion. The RTIL surfactants display hydrogen-bond basicity similar to $C_{16}$TMAB and, as is ubiquitous among cationic surfactants [30, 33, 39, 49], they show a higher affinity for acidic compounds than does water. Furthermore, direct comparison of the *a* coefficients determined for the $C_{16}$MPYB and $C_{16}$TMAB systems reveals that the former exhibits a moderately higher hydrogen-bond acceptor strength; $a = 1.04 \pm 0.12$ vs. $0.77 \pm 0.16$. The negative *b* coefficients for $C_n$MPYB ($–2.74 \pm 0.25$ for $C_{16}$MPYB; *b* shows no clear trend with chain length), which is very similar to the *b* coefficient determined for $C_{16}$TMAB (–

2.68 ± 0.33) and more negative than previously reported values for SDS (–1.67, –1.85)[33, 49], indicate that the hydrogen-bond acidity of $C_n$MPYB micelles is lower than water and similar to other cationic micellar phases. It can be deduced that this difference in hydrogen-bond donor strength relates to the attachment, penetration, content, and orientation of water at the interphase micellar regions (Stern and palisade layers). In turn, this hydration relates to interchain packing and headgroup repulsion, both of which are apparently not subject to substantial perturbation as a result of the changes in headgroup structure between the $C_n$MPYB surfactants and $C_{16}$TMAB.

The *e* coefficient gives the tendency of the pseudo-phase to interact with solutes through polarizability-type interactions, mostly via electron pairs. For other micellar systems studied to date, the value for *e* varied from about 0.25 to 1.10, with cationic micelles appearing at the upper end of this range [30, 33, 39, 49]. In the case of $C_n$MPYB, however, the composite *e* value is 0.38 ± 0.17. The fact that the polarizability for LPFOS is not significantly different from water [85] has been explained in terms of the high electronegativity of fluorine atoms [30]. However, the reason for the differences observed between $C_{16}$TMAB and $C_n$MPYB is more difficult to explain. For instance, given that the degree of micellar dissociation, $\beta$, is the same for $C_{16}$MPYB and $C_{16}$TMAB, within experimental error, the disparity in *e* coefficients cannot be ascribed to the surface effect of bromide counter ions [32].

Overall, the Abraham coefficients are not particularly influenced by the hydrocarbon chain length. This observation compares well with prior studies. For instance, Trone et al.[49] observed very moderate changes in MEKC selectivity for sodium *N*-alkylsarcosinates as the hydrocarbon tail was elongated from $n = 11$ to 15, but

saw even more minor differences between sodium alkyl sulfates (SAS) for $n$ = 12 (SDS) versus $n$ = 14 [49]. Similarly, Vitha and Carr found similar selectivity across a homologous series of SAS surfactants with intermediate-length hydrocarbon tails ($n$ = 8, 10, 12) [31]. Although chemical selectivity optimization in MEKC can be achieved through use of complexation agents, chiral additives (cyclodextrins), co-solvents, or by otherwise modifying the run buffer conditions (temperature, pH, ionic strength, urea), proper selection of the surfactant remains the most critical consideration [28, 29].

**4.3 Concluding Remarks**

The individual solute–solvent interactions of aqueous micellar assemblies of $C_n$MPYB were evaluated based on Abraham solvation parameter model correlations using an MEKC approach. The RTIL cation-derived surfactants examined in this study provided highly efficient MEKC separations and, as with conventional surfactants, the magnitudes of the solvation parameter coefficients showed that lipophilicity ($v$) and hydrogen-bond acidity ($b$) still play the most important roles in MEKC retention. Using $C_{16}$TMAB as a point of reference, however, $C_n$MPYB micellar pseudo-phases provide unique solvent characteristics and are: (i) less "hydrophobic", i.e., better able to interact with polar compounds; (ii) more cohesive; and (iii) less polarizable. No trends were found with alkyl tail length, showing the primary influence exerted by the nature of the headgroup on the chemical selectivity.

These findings may lead to improved separations in challenging samples, expanding the versatility of MEKC and other analytical methods. Additionally, one can tailor the structure of RTIL-based surfactants in order to solve different separation problems requiring varied chromatographic selectivity. We also believe these results

bode well for the continued expansion of RTILs into chemical analysis, in general. Further, their utility is expected to translate to other fields such as materials engineering and biotechnology. For example, the relatively high cohesivity of $C_n$MPYB micelle systems justifies a moderate optimism in regard to their possible application as cationic detergents for the isolation, extraction, and/or solubilization of membrane receptors and proteins. Although full toxicological studies are still pending, these surfactants and subsequent RTIL analogs may one day find use as emulsifiers and dispersion agents in a range of areas from cosmetics to (possibly) biomedical use.

**4.4 Materials and Methods**

Separations were conducted in 30 mM tris(hydroxymethyl)aminomethane (Aldrich, St. Louis, MO) buffer adjusted to pH 7.00 ± 0.05 using dilute phosphoric acid (Fisher Scientific). $C_{16}$TMAB was obtained from Acros (Geel, Belgium) and the $C_n$MPYB surfactants with $n$ = 12, 14, 16, and 18 were synthesized according to procedures described previously [60]. The $C_n$MPYB surfactants were dissolved in this buffer system at the following concentrations, well exceeding the critical micelle concentrations (CMC) determined earlier: [60] $n$ = 12 (50 mM), 14 (25 mM), 16 (15 mM), and 18 (10 mM). Micelles form spontaneously, survive freeze-thaw cycles, and appear stable over the course of several weeks under ambient storage. $C_{16}$TMAB was dissolved in the same buffer at a concentration of 40 mM. All aqueous solutions were passed through 0.45 μm nylon syringe filters prior to EKC separations. Analytes were obtained in the highest purity available from Sigma-Aldrich or Acros Organics and were not further purified.

For each surfactant, a fused silica capillary with dimensions 50 μm i.d. and 360 μm o.d. was obtained from Polymicro Technologies (Phoenix, AZ). The capillaries had total lengths of 48.5 to 50.4 cm, and effective lengths of 40–42 cm. The capillaries were first conditioned with a 30 min flush of doubly-distilled, deionized water and a 30 min flush with 0.10 M NaOH (Aldrich) followed by a 30 min flush with buffer.

All separations were carried out on an Agilent 3DCE system using Chemstation software. Between injections, the capillaries were flushed for 2 min with 0.10 M NaOH followed by 2 minutes with the surfactant buffer. The analyte solutions containing one to four solutes at 100–200 ppm in separation buffer were introduced by pressure at 50 mbar for 3 sec), and a separation potential of –20 kV was applied. All studies were conducted with a capillary temperature of 25 ºC, and the diode array detector signal was monitored at 214, 223 and 254 nm, each at a bandwidth of 20 nm. Solutes were identified by matching spectra with a library generated using solutions containing single solutes, or by spiking of the sample with particular solutes.

Acetone has been shown to be a suitable EOF marker when used with cationic surfactants [65] and was used in every separation to mark the EOF. The migration time of acetone was used to calculate $\mu_{eo}$. The apparent mobility of the solute ($\mu_{sol}$) was calculated from its retention time. The electrophoretic mobility of the micelle ($\mu_{mc}$) was determined using an iterative method presented by Bushey and Jorgenson [88]in which the migration behavior of a series of six alkyl phenyl ketone homologs: acetophenone, propiophenone, butyrophenone, valerophenone, hexanophenone, and heptanophenone was used to determine the retention time of the micelle. The increasing chain length in the homologues series represents and incremental addition to the free energy associated

with forming a micelle-solute complex. With the logarithm of retention factor being proportional to free energy a plot of log($k$) vs. carbon number converges on to a maximum retention factor value which is the value of a completely retained solute and the actual migration time of the micelle. A BASIC program written in-house was used to calculate $t_{mc}$ and the calculation proceeded until the deviation in $t_{mc}$ from the previous iteration was less then 0.10%. Methylene selectivities were calculated from the first four alkyl phenyl ketone homologs beginning with acetophenone.

Theoretical plate numbers were calculated for three representative solutes (benzonitrile, nitrobenzene, phenol) using the Agilent Chemstation software. LSFER analyses were conducted utilizing the solutes listed in Appendix A. Some solutes were eliminated for some surfactants because they were not well resolved from $t_0$, they gave poor peak shape, or they were significant outliers.

# Chapter 5
# The Effect of Headgroup on Cationic Surfactant selectivity in Micellar Electrokinetic Chromatography

## 5.1 Introduction

With the results in Chapter 4 showing that minor changes in pseudostationary phase structure affect the solvation characteristics of a pseudostationary phase, I chose to further investigate the structure-selectivity relationship for cationic micellar pseudostationary phases. Investigations into the structural effects that control selectivity are important because the selectivity of an MEKC system is primarily determined by the choice of pseudostationary phase (PSP). Although chemical selectivity optimization in MEKC can be achieved through the use of complexing agents, chiral additives, co-solvents, or by otherwise modifying the run buffer conditions, proper selection of the surfactant remains the most critical consideration [28,29].

As noted in Chapter 4, multiple studies have been performed to individually characterize the selectivity of a variety of EKC PSPs, including micelles [32,33,49], polymers [52-56,89], vesicles [39,57], liposomes [40,58,59]. Among micelles of anionic surfactants, the structure of the ionic headgroup has been shown to be the dominant factor in controlling EKC selectivity [32]. A collective comparison of EKC PSPs shows that cationic surfactants provide significantly different selectivity than other PSPs [50]. However, relatively few cationic surfactants have been studied compared to anionic surfactants.

The results presented in Chapter 4 have shown that micelles of two cationic surfactants with a relatively minor structural difference at the headgroup generate

significantly different EKC separation selectivity [51]. Cationic surfactants offer a unique synthetic flexibility that allows systematic changes in the headgroup of the surfactant. In an effort to further explore the selectivity afforded by cationic surfactants, as well as to investigate how headgroup structure affects selectivity, I synthesized and characterized the selectivity of two series of cationic surfactants with varied headgroup structure. The structures of the surfactants are presented in Figure 5.1, and the structural similarities and differences are detailed in section 5.2 below.

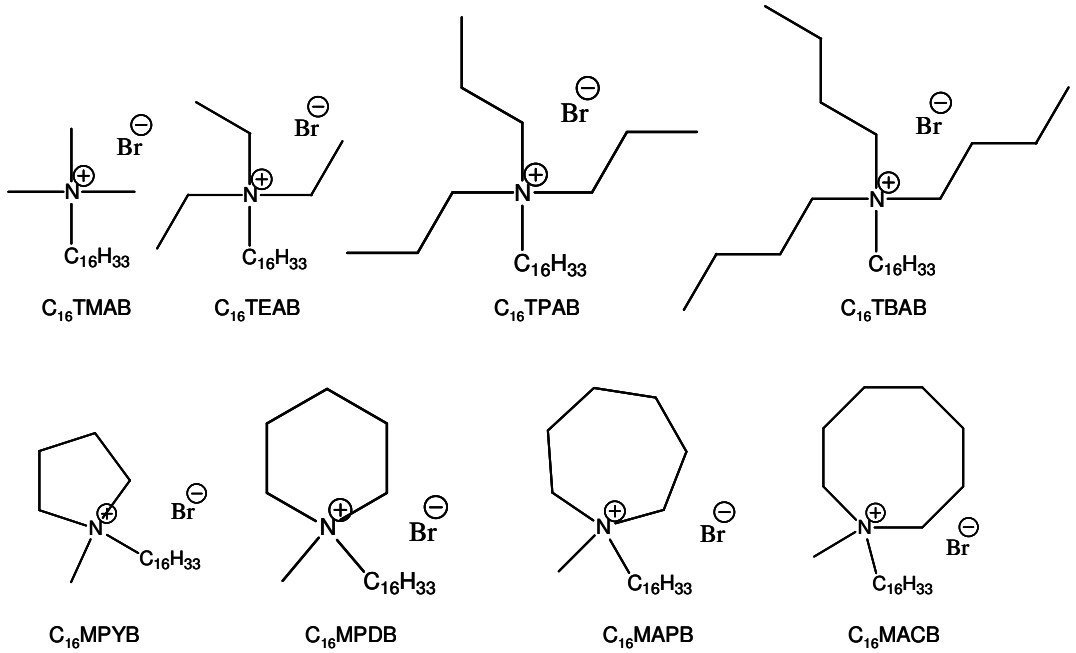


**Figure 5.1:** Structures of the Cationic Surfactants studied. Trimethyl-hexadecyl-ammonium; bromide ($C_{16}$TMAB), Triethyl-hexadecyl-ammonium; bromide ($C_{16}$TEAB), Tripropyl-hexadecyl-ammonium; bromide ($C_{16}$TPAB), Tributyl-hexadecyl-ammonium; bromide ($C_{16}$TBAB), 1-Headecyl-1-methylpyrrolidinium ($C_{16}$MPYB), 1-Hexadecyl-1-methyl-piperidinium; bromide ($C_{16}$MPDB), 1-Hexadecyl-1-methyl-azepanium; bromide ($C_{16}$MAPB), 1-Hexadecyl-1-methyl-azocane; bromide ($C_{16}$MACB)

To characterize the solvation environments provided by each surfactant I have used the solvation parameter model proposed by Abraham *et al* [19-21,90] and discussed in Chapter 2. This approach provides information on the relative strengths of five

different chemical interactions between the micelles and solutes. Due to the prevalent use of cationic trimethyl-hexadecyl ammonium bromide ($C_{16}$TMAB) micelles in EKC, particular attention is paid to the differences in selectivity between the newly introduced surfactants and $C_{16}$TMAB.

**5.2 Results and Discussion**

The influence of headgroup structure on the chemistry and EKC selectivity of micellar PSPs of cationic surfactants was investigated using two series of surfactants. All of the surfactants had a 16-carbon linear hydrocarbon tail, a quaternary ammonium headgroup, and a bromide counter ion. Those surfactants that are not available commercially were synthesized. The structure of all of the surfactants was confirmed spectroscopically and by elemental analysis. The critical micelle concentration (CMC) and micelle properties of the surfactants were determined, and the surfactants were characterized by the solvation parameter model using EKC.

The headgroup for the first series of surfactants consisted of a quaternary ammonium center with three additional linear hydrocarbon chains of varying length bonded to the central nitrogen atom (Figure 5.1). The synthesis of these linear headgroup surfactants is a common synthesis for quaternary ammonium surfactants that proceeded with moderate efficiency, with the synthetic yields decreasing with the increase in head-group size (86% for $C_{16}$TEAB, 78% for $C_{16}$TPAB and 71% for $C_{16}$TBAB). These surfactants have been synthesized and studied previously, particularly with respect to the effect of headgroup structure on micellization and phase behavior [91].

The second series of surfactants has the ammonium center incorporated into hydrocarbon rings of increasing size. This cyclic headgroup series required a two step synthesis because the tertiary amine headgroup structures are not commercially available. Synthesis of the tertiary amine ring structures was achieved by a reductive amination procedure [92] with sodium cyanoborohydride and formaldehyde. The resulting tertiary amines were then alkylated with 1-bromohexadecane to yield the quaternary ammonium surfactant. The yields for the seven and eight member ring headgroup were 63% and 64% respectively.

NMR and elemental analysis was used to confirm the structure of all of the surfactants. The NMR of the eight member ring $C_{16}$MACB showed the hydrogens off the alpha carbon to be non-equivalent. This is probably due to a coordination of the ammonium and bromide ions perturbing the large eight member ring, although variable temperature NMR experiments were unable to confirm this effect. Two dimensional NMR experiments confirmed the structure of this surfactant. Elemental analysis of the all the surfactants yielded good results within 93-105% of the calculated values.

The CMCs of the surfactants were measured using the conductivity method, and these results are summarized in Table 5.2. The CMCs of the two series follow a trend of the larger headgroup facilitating a lower CMC. The linear headgroup set has CMCs from 0.91 to 0.36 mM and the cyclic series from 0.83 to 0.67 mM. Increases in the size and hydrophobicity of the headgroups result in energetically unfavorable interactions in the aqueous buffer as well as stronger interactions at the micelle surface. These interactions can more effectively offset the repulsive interactions of the charged headgroups. Either or both of these effects would result in a lower CMC.

The results of the solvatochromic and aggregation number experiments are also summarized in Table 5.2. The solvatochromic probe pyrene was used to measure the polarity of the solvation environment provided by the micellar phases. The average pyrene I/III ratio for all the surfactants was 0.79 (±0.03) which is comparable to a chloroform type environment [93], and no clear trend is observed in the pyrene I/III ratios with headgroup size. This most likely indicates that pyrene is solvated in the core of the micelles, away from the headgroups, where the polarity is relatively low and the headgroup structure has relatively little effect. The aggregation numbers (average number of surfactant molecules in the micelle) were also measured using fluorescence quenching experiments. Aggregation numbers generally decrease as the size and hydrophobicity of the headgroup increase. The change in aggregation number is much greater for the linear headgroup series than for cyclic headgroup series. The micelles of the more hydrophobic surfactants are smaller, indicating that the stronger hydrophobic interactions between the individual molecules are able to stabilize these smaller aggregates.

**Table 5.1.** Characteristic parameters of the surfactant micelles [a]

| Surfactant | Pyrene I/III | *A* | CMC (mM) at 25°C | Kraft Temperature (°C) |
|---|---|---|---|---|
| $C_{16}$TMAB | 0.83 | 69 (6) | 0.91<br>0.91[b] | <25 |
| $C_{16}$TEAB | 0.76 | 60 (7) | 0.81<br>0.73[b] | <25 |
| $C_{16}$TPAB | 0.80 | 53 (6) | 0.48<br>0.46[b] | <25 |
| $C_{16}$TBAB | 0.77 | 30 (2) | 0.36<br>0.27[b] | <25 |
| $C_{16}$MPYB | 0.81 | 69 (5) | 0.83[c] | <25 |
| $C_{16}$MPDB | 0.77 | 53 (6) | 0.76 | <25 |

| | | | | |
|---|---|---|---|---|
| $C_{16}$MAPB | 0.79 | 54 (5) | 0.67 | <25 |
| $C_{16}$MACB | -[e] | -[e] | 0.63[d] | 29 (3) |

a) Conditions given in text
b) CMC value from ref [91]
c) CMC value from ref [60]
d) $C_{16}$MACB CMC was measured at 35°C
e) The $C_{16}$MACB surfactant is not soluble at experimental conditions

Under our EKC conditions, the cationic surfactants provided a dynamic coating on the fused-silica capillary surface, changing the sign of the zeta potential and engendering anodic electroosmotic flow (EOF). The cationic micelles have electrophoretic mobility counter to the EOF in the direction of the cathode, allowing separation of neutrals governed by partition to and association with a micellar PSP migrating counter to the EOF. The mean electroosmotic mobilities ($\mu_{eo}$) provided by each surfactant are presented in Table 5.2 and, in the absence of significant differences in viscosity, are a measure of the amount of surfactant that is adsorbed to the capillary wall. The linear headgroup series shows a trend toward lower electroosmotic mobility as the size of the headgroup increases, indicating that the more bulky headgroups reduce the extent of adsorption to the capillary wall, presumably due to steric effects. The cyclic headgroup series does not show the same trend in EOF with the increase in headgroup size.

The effective electrophoretic mobilities of the micelles ($\mu_{mc}$) presented in Table 5.2 were determined by an iterative method using the migration behavior of a series of six alky phenyl ketone homologs. The $\mu_{mc}$ of the linear headgroup series of micellar phases show trends relating to the size of the headgroup, with smaller headgroups having a larger $u_{mc}$ compared to the larger headgroups. This is likely related to the trend in

aggregation number and indicates that the micelles with larger aggregation numbers have a higher ratio of charge to size. Again, no significant trend in $\mu_{mc}$ is observed for the cyclic headgroup series, which all have $\mu_{mc}$ similar to $C_{16}$TEAB.

The variation in $\mu_{eo}$ and $\mu_{mc}$ results in significant differences in the migration range, as defined by $t_{mc}/t_0$. The migration range is a significant factor in EKC separations, because it affects the resolution attainable for solutes with a given selectivity and separation efficiency [14]. All of the new surfactants provided a significantly wider migration range than the commercially-available and commonly-employed $C_{16}$TMAB, with $C_{16}$TEAB, $C_{16}$TBAB and $C_{16}$MPDB giving the largest values. While this should result in better attainable resolution with these surfactants, the result is primarily due to reduced $\mu_{eo}$, meaning that any improvement in resolution would come at the expense of longer analysis times.

**Table 5.2**
Electrophoretic mobilities and chromatographic properties of surfactant micelles [a)b)]

| Surfactant | $\mu_{mc}$ x $10^4$ ($cm^2V^{-1}s^{-1}$) | $\mu_{eo}$ x $10^4$ ($cm^2V^{-1}s^{-1}$) | $t_{mc}/t_0$ | $\alpha_{(CH2)}$ | Theoretical plates |
|---|---|---|---|---|---|
| $C_{16}$TMAB | 2.35 (0.02) | -4.76 (0.10) | 1.97 (.002) | 2.49 (0.01) | 174000 (2000) |
| $C_{16}$TEAB | 2.29 (0.01) | -4.04 (0.18) | 2.90 (0.4) | 2.60 (0.02) | 183000 (2000) |
| $C_{16}$TPAB | 2.28 (0.02) | -3.39 (0.27) | 2.45 (0.1) | 2.57 (0.01) | 150000 (4000) |
| $C_{16}$TBAB | 2.27(0.07) | -3.05 (0.19) | 2.84 (0.12) | 2.66 (0.03) | 143000 (5000) |
| $C_{16}$MPYB | 2.21 (0.02) | -3.75 (0.17) | 2.38 (0.03) | 2.45 (0.03) | 280000 (14000) |
| $C_{16}$MPDB | 2.55 (0.03) | -4.14 (0.26) | 2.72 (0.03) | 2.18 (0.03) | 91000 (7000) |
| $C_{16}$MAPB | 2.32 (0.05) | -3.98 (0.14) | 2.50 (0.07) | 2.44 (0.13) | 106000 (4000) |
| $C_{16}$MACB[c] | 2.64 (0.03) | -4.02 (0.47) | 2.41 (0.03) | 2.64 (0.08) | 212000 (3000) |

a) The errors reported in parentheses are the standard errors.
b) Conditions given in text.

c) All measure measurements take at 35° C

The influence of the surfactant headgroup on solute-micelle interactions was also investigated using the LSER model. The retention behavior of 40 test solutes was measured in each surfactant system and the LSER model was applied to the results. This test pool of solutes covered a wide range of solute types, including nitrogen heterocyclic bases and phenols, and was selected to be of adequate size and with properties sufficiently varied to define properly all interactions represented in the solvation parameter model. The importance of this point as well as careful avoidance of cross-correlation between the descriptors and use of "generic" experimental conditions has been argued by Poole et. al. [29]. The greatest correlation coefficient ($r^2$) for the LSER parameters for the solutes used in this study is 0.29 between R and S, and the average of the values of the cross-correlation coefficients is 0.097. The correlation coefficients ($r^2$) for the least squares fit to equation 1 ranged from 0.88 to 0.97. The resulting coefficients from the solvation parameter model are presented in Figure 5.2 and Table 5.3.

The solvation parameter results for $C_{16}$TMAB reported here differ from previously reported values [30, 51]. Differences are most likely due the differences in buffer chemistry and concentration. The values for $C_{16}$TMAB reported in Figure 5.2 and Table 5.3 were obtained under the same conditions as the other seven surfactants and thus they are more appropriate for the current comparison.

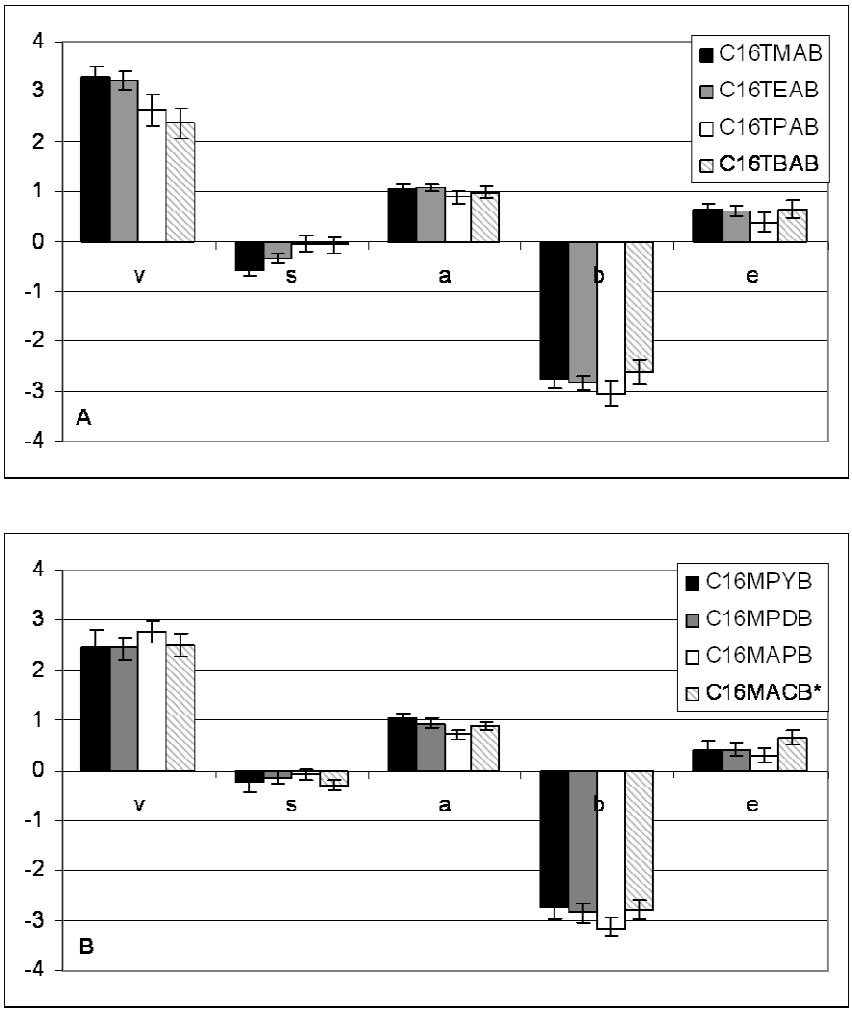


**Figure 5.2:** LSER parameter results. A: Linear headgroup surfactants, B: Cyclic headgroup surfactants.

Figure 5.2A presents the results for the linear headgroup series. A trend seen in this series of surfactants is a decrease in the v value with increasing size of the headgroup. This indicates that the pseudostationary phase is becoming more cohesive, providing less favorable change in energy as an analyte partitions into the phase from the cohesive aqueous environment, as the headgroup size increases. The added cohesiveness might be attributed to the increase in the hydrophobic interactions at the headgroup accompanying the increase of three methylene units for each surfactant in the series. Whether or not this

is the cause, the result is interesting because the McGowan characteristic volume is generally one of the dominant factors controlling retention and thus selectivity in EKC. The importance of cohesiveness is seen in the separation of larger more hydrophobic compounds such as steroids, where more cohesive phases are more successful in resolving these compounds [83, 94]. Additionally, reduction of the v value increases the relative importance of other factors that control separation selectivity, such as acid/base and dipolar interactions. To the author's knowledge, only two surfactants characterized by the LSER model are more cohesive than $C_{16}$TBAB: The fluorinated surfactant lithium perflourooctanesulfonic acid (LPFOS) and the bile salt sodium cholate [30]. The resistance to cavity formation for these micelles rivals that of many polymeric PSPs [52].

**Table 5.3:** Solvation parameter results

| Surfactant | v | s | a | b | e | $R^2$ |
|---|---|---|---|---|---|---|
| $C_{16}$TMAB | 3.28 (0.22) | -0.58 (0.11) | 1.06 (0.09) | -2.77 (0.18) | 0.65 (0.13) | 0.96 |
| $C_{16}$TEAB | 3.23 (0.18) | -0.33 (0.09) | 1.06 (0.07) | -2.83 (0.14) | 0.63 (0.11) | 0.97 |
| $C_{16}$TPAB | 2.62 (0.31) | -0.04 (0.89) | 0.89 (0.12) | -3.04 (0.26) | 0.39 (0.19) | 0.89 |
| $C_{16}$TBAB | 2.37 (0.30) | -0.06 (0.16) | 0.98 (0.12) | -2.61 (0.25) | 0.64 (0.18) | 0.90 |
| $C_{16}$MPYB[a] | 2.45 (0.34) | -0.23 (0.21) | 1.04 (0.12) | -2.75 (0.25) | 0.40 (0.19) | 0.88 |
| $C_{16}$MPDB | 2.43 (0.23) | -0.15 (0.12) | 0.95 (0.09) | -2.85 (0.19) | 0.42 (0.14) | 0.93 |
| $C_{16}$MAPB | 2.77 (0.22) | -0.09 (0.12) | 0.72 (0.09) | -3.14 (0.18) | 0.30 (0.13) | 0.94 |
| $C_{16}$MACB | 2.49 (0.23) | -0.30 (0.12) | 0.90 (0.09) | -2.79 (0.19) | 0.65 (0.14) | 0.94 |

a) values from ref [51]

The other term that shows a trend with headgroup in Figure 5.2A is the s term. Interactions between the micelles and polar compounds become less energetically unfavorable (s becomes less negative) as the size of the headgroup increases. The values for s are particularly high for the $C_{16}$TPAB and $C_{16}$TBAB surfactants, for which the values are not significantly different from zero. This indicates that the polarity of the solute does not affect its retention or strength of interaction with these two micelles and that the dipole interactions afforded by the micelle are not significantly different from those afforded by water. It should be noted that this is not correlated with the polarity as measured by the pyrene I/III ratios, which are a measure of the polarity of the environment where pyrene is solvated in the micelles. The less negative s values are, rather, an indication that the micelles have a greater free energy of interaction with polar species. Again, to the author's knowledge, these are the strongest dipolar interactions ever reported for micellar phases. Previously reported values of s generally vary little between various surfactants, with the only two other surfactants having comparable s values being sodium decyl sulfate (SDecS)[31] and LPFOS [30] which both have an s value of -0.24. Polymeric PSPs have been reported with similar s values including poly(sodium 9-decenyl sulfate) (poly-(SDeS)) [43] and allyl glycidyl ether *N*-methyltaurine siloxane (AGENT) [44] which have values of -0.04 and -0.07 respectively. The results suggest that the interactions with polar compounds may be related to the cohesivity of the micelles, in that polar compounds are not able to enter and be solvated within the hydrophobic core of the micelles, but are solvated at the more polar interface between the micelle and the aqueous buffer. These trends are represented in Figure 5.3, a

plot of the length of the akyl chain length around the headgroup of the surfactant versus the solvation parameter results for cohesivity (v) and polarity/polarizability (s).

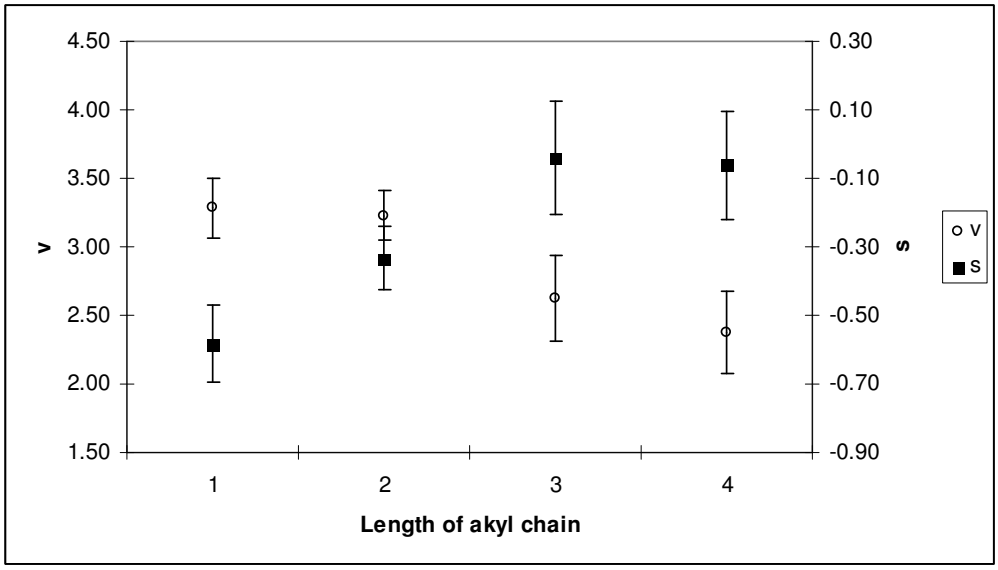


**Figure 5.3:** A plot representing the trend between the length of headgroup akyl chain length and chosevity and dipole-dipole interactions.

Changes in the linear headgroup size have no statistically significant effect on the acid-base properties of the pseudo-phase represented by the a and b terms in the solvation parameter model, and no trends are observed among these two values. The values for a and b are both slightly greater in magnitude than those reported for other cationic surfactants [30,38,39,50] with the average for surfactants we are reporting being a= 0.95 and b = -2.84. It has been suggested that differences in hydrogen-bond donor strength relates to the attachment, penetration, content, and orientation of water at the interphase micellar regions (Stern and palisade layers) [28,95-97]. It is somewhat surprising that the chemistry of the water in this region, which is related to interchain packing and headgroup repulsion, is apparently not altered significantly by iterative addition of methylene groups to the headgroup. This seems to be unique to ammonium based

cationic surfactants. A similar study performed by Khaledi and coworkers examining anionic surfactants found that changes in the headgroup resulted in significant changes in the acid/base properties of the pseudo-phase [32].

The e term of the solvation parameter model is a measure of the tendency of the PSP to interact with non-bonding and π-electrons. Considering the imprecision in these values, the linear headgroup series of surfactants reveals no significant trend. The aggregate mean value for e is 0.58 ± 0.13. Previously reported e values for surfactants range from 0.25 to 1.10, with cationic micelles appearing at the upper end of this range [50].

Our group had previously reported results for $C_{16}$MPYB, one of the surfactants in the cyclic headgroup series, and found that it provided significantly different chemical selectivity from $C_{16}$TMAB [51]. The current results confirm that significant differences in selectivity exist between linear headgroup and analogous cyclic headgroup p structures. However, no consistent overall trends are observed in the LSER results as the size of the ring is altered. The parameters s, a and b do show trends as the ring size is increased from five to seven atoms, but these trends are reversed when an additional methylene unit is added to make an eight member ring. Given that the LSER studies for $C_{16}$MACB were of necessity conducted at a different temperature, the uncertainties in the results, and the limited number of surfactants studied, it is impossible to conclude whether that trend or pattern is real. $C_{16}$MAPD, with the seven member ring, shows somewhat different selectivity overall relative to the other surfactants. The relatively large magnitudes of v and b for this surfactant, combined with the relatively small magnitudes of s, a and e, lead to the conclusion that solute size and basicity will have a

more dominant effect on retention and selectivity for this surfactant than for the other three. When compared to the most often used cationic surfactant, $C_{16}$TMAB, the cyclic headgroup surfactants are more cohesive, with a composite average v value of 2.54 ± 0.16 for the cyclic headgroups relative to 3.28 ± 0.22 for $C_{16}$TMAB. The cyclic headgroups also interact more strongly with polar solutes, with a composite average s value of -0.19 ± 0.09 versus $C_{16}$TMAB of -0.58 ± 0.11. The rest of the LSER coefficients, a, b and e, are essentially the same as those for the other cationic surfactants studied.

**5.3 Concluding Remarks**

Eight cationic surfactants have been characterized with respect to their micellization behavior and selectivity and performance as pseudostationary phases for electrokinetic chromatography. The results suggest that significant increases in the size and hydrophobicity of the cationic headgroup result in more stable, compact and cohesive micelles.

The micellization behavior of the surfactants is affected by the structure of headgroup, particularly for headgroups consisting of linear hydrocarbon chains of increasing length attached to an ammonium center. Among this series, the CMC and aggregation numbers of the surfactants decreased with increasing headgroup size and hydrophobicity. The formation of micelles is known to be a balance between the hydrophobic attractive forces of the tail and the ionic repulsive forces of the headgroup. Both the CMC and aggregation number results seem to indicate that the more hydrophobic headgroups are more effective at overcoming the ionic repulsive forces, [91] although decreases in aggregation number may also be due to steric effects. Steric

factors are likely responsible for the finding that the magnitude of the electroosmotic flow decreases as the size of the headgroup increases. The trends are not observed to the same magnitude in the series of surfactants with cyclic headgroups, most likely because the increased size of the ring structure does not have the same effect on the hydrophobicity or overall size of the headgroup.

LSER studies show that the solvation environment of the micelles is influenced by the structure of the surfactant headgroup. The solvation properties of the linear headgroup series vary in a systematic fashion, with the micelles becoming more cohesive and having greater ability to interact with polar compounds as the size and hydrophobic character of the headgroup increases. The surfactants with the largest, most hydrophobic headgroups provided a very cohesive environment and strongest interactions with polar compounds of any surfactants reported to date. Polar compounds are not as easily solvated within the interior of these more cohesive structures, or are sterically restricted from entering the micelle, and are thus solvated in a more polar environment at the exterior of the micellar structure. Somewhat surprisingly, alterations in the structure of the headgroup did not affect the strength of acid/base interactions, indicating that it had little effect on the chemistry of water in the palisade layer.

Effective increases in size and hydrophobicity are best achieved by increases in the length of alkyl chains bound to the ammonium center. Replacing the linear chains with ring structures does alter the retention behavior and selectivity, but variation in the size of the ring does not affect steric factors or hydrophobic interactions to the same extent, and thus does not result in significant trends in the micellization behavior or the nature and strength of interactions with solutes.

## 5.4 Reagents and Materials

Separations were conducted in 30 mM Tris (Hydroxymethyl) aminomethane (Aldrich, St. Louis, MO) buffer adjusted to pH 7 ± 0.05 using dilute phosphoric acid (Fisher Scientific). The surfactants were dissolved at a concentration of 15mM, which exceeds their critical micelle concentrations (CMC) as determined here in. All aqueous solutions were passed through 0.45 μm nylon syringe filters prior to MEKC separations. Analytes were obtained in the highest purity available form Sigma-Aldrich or Acros Organics and were not further purified. The synthetic reagents 1-bromohexadecane (Sigma-Aldrich), triethylamine (Fisher) tripropylamine (Sigma-Aldrich), tributylamine (Fluka), 1-methylpiperidine (Fluka), heptamethyleneimine (Sigma-Aldrich), hexamethyleneimine (Fluka), sodium cyanoborohydride (Sigma-Aldrich) and formaldehyde (Mallinckrodt) were used as received with no further purification

### 5.4.1 Synthesis of Linear Surfactants

$C_{16}$TMAB was obtained from Acros (Geel, Belgium) and was purified by precipitation from absolute ethanol and diethyl ether. The other linear surfactants were prepared by the same general procedure for quaternary amines. *Triethyl-hexadecyl-ammonium; bromide. ($C_{16}$TEAB); Tripropyl-hexadecyl-ammonium; bromide. ($C_{16}$TPAB); Tributyl-hexadecyl-ammonium; bromide ($C_{16}$TBAB)* Stoichiometric amounts of triethylamine (1.66g, 0.016 mol), tripropylamine (2.35g, 0.016 mol) , or tributylamine (3.04g, 0.016 mol) and 1-bromohexadecane (5.0 g, 0.016 mol) were refluxed at 65 °C in acetone for 24 h. The solvent was removed under vacuum leaving a yellow residue. The residue was dissolved minimal amounts of acetone (1.5 mL) and hexane (15 mL) was added until the surfactant precipitated. The surfactant was then filtered and redissolved in acetone and precipitated

with hexane three more times. The surfactant was then dried under high vacuum yielding analytical pure product; $C_{16}$TEAB 86% yield, $C_{16}$TPAB 78% yield; $C_{16}$TBAB 71% yield

**5.4.2 Synthesis of Cyclic Surfactants**

The synthesis of the 1-hexadecyl-1-methylpyrrolidinium; bromide ($C_{16}$MPYB) surfactant was described previously [60] and the synthesis of the other surfactants is described here in. *1-Hexadecyl-1-methyl-piperidinium; bromide ($C_{16}$MPDB)* Stoichiometric amounts of 1-methylpiperidine (1.624g, 0.016 mol) and 1-bromohexadecane (5g, 0.016 mol) were dissolved in 20 mL of ether and stirred for 24h. The white precipitate was filtered and purified by precipitation three times from absolute ethanol and diethyl ether. The resulting white solid was dried under high vacuum to yield analytically pure product at 93% yield.

*1-Hexadecyl-1-methyl-azepanium bromide ($C_{16}$MAPB), 1-Hexadecyl-1-methyl-azocane bromide ($C_{16}$MACB)* The rings with tertiary methylated amines were first synthesized from the rings with secondary amines, followed by synthesis of the quaternary ammonium surfactant. To a stirred solution of 1eq. of a cyclic secondary amine (1.8 g, 0.01637 mol hexamethyleneimine; 1.6 g 0.01637 mol heptamethyleneimine) 8 eq. of 37% aqueous formaldehyde (0.131 mol) in acetonirile (50 mL) and 5 eq of sodium cyanoborohydride (5.15 g, 0.082 mol) was added. An exothermic reaction ensued and the reaction mixture clouded over. The mixture was stirred for 20 min, after which glacial acetic acid was added dropwise until the solution tested neutral on wet pH paper. Stirring was continued for 45 min with acid being added occasionally to maintain the pH near neutrality. 2M KOH was added until the solution tested basic on wet pH paper, and the reaction mixture was then extracted three times

with portions of ether. The combined ether extracts were back extracted three times with portions of 2M HCl. The combined HCl extracts were made basic with solid KOH, and the resulting basic solution was extracted with three portions of ether. The ether extracts were combined and the solvent was evaporated leaving a viscous yellow liquid. Stoichiometric amounts of *N*-methyl-cyclic tertiary amine and 1-bromohexadecane were added to ether and stirred for 36 h, and the resulting precipitate was filtered and purified by precipitation from absolute ethanol and diethyl ether to yield analytically pure products. Yields: 1-Hexadecyl-1-methyl-azepanium bromide 63%, 1-Hexadecyl-1-methyl-azocane bromide 64%.

### 5.4.3 $^1$H NMR Spectroscopy

NMR data was collected with a Varian Unity 400 MHz spectrometer. $C_{16}$TEAB 64% yield. $^1$H NMR (400 MHz, $CDCl_3$) δ, 0.85(t, 3H), 1.22(m, 24H), 1.38(m, 11H), 1.67(m, 2H), 3.35(m, 2H), 3.50(m, 6H). $C_{16}$TPAB 58% yield. $^1$H-NMR (400 MHz, $CDCl_3$) δ, 0.88(t, 3H), 1.05(m, 11H), 1.31(m, 24H), 1.68(m, 2H), 1.79(m, 6H), 3.39(m, 8H). $C_{16}$TBAB 56% yield. $^1$H-NMR (400 MHz, $CDCl_3$) δ, 0.88(t, 3H), 0.99(m, 9H), 1.25(m, 24H), 1.45(m, 8H), 1.67(m, 8H), 3.39(m, 8H). $C_{16}$MPDB 86% yield. $^1$H-NMR (400 MHz, $CDCl_3$) δ, 0.84(t, 3H), 1.30(m, 26H), 1.72(m, 2H), 1.94(m, 6H), 3.37(s, 3H), 3.66(m, 4H), 3.82(m, 2H). $C_{16}$MAPB 51% yield . $^1$H-NMR (400 MHz, $CDCl_3$) δ, 0.88(t, 3H), 1.34(m, 18H), 1.39(m, 4H), 1.75(m, 8H), 1.92(m, 4H), 3.38(s, 3H), 3.59(m, 4H), 3.62(m, 2H). $C_{16}$MACB $^1$H-NMR (400 MHz, $CDCl_3$) δ, 0.88(t, 3H), 1.25(m, 24H), 1.38(m, 2H), 1.62(m, 2H), 1.70(m, 2H), 1.78(s, 4H), 1.97(m, 4H), 3.34(s, 3H), 3.48(m, 2H), 3.58(m,2H), 3.78(m,2H).

### 5.4.4 Elemental Analysis

For elemental analysis samples of the surfactants were sent to Schwarzkoff microanalytical laboratory (Woodside NY). $C_{16}$TEAB calcd. for $C_{22}H_{48}BrN$ C,65.00; H,11.90: N,3.45; Found: C,63.95; H,12.63; N,3.46. $C_{16}$TPAB calcd. for $C_{25}H_{54}BrN$ C,66.93; H,12.13: N,3.12; Found: C,66.11; H,12.94; N,2.96. $C_{16}$TBAB calcd. for $C_{28}H_{60}BrN$ C,68.54; H,12.32: N,2.85; Found: C,67.82; H,13.13; N,2.97. $C_{16}$MPDB calcd. for $C_{25}H_{46}BrN$ C,65.32; H,11.46: N,3.46; Found: C,65.22; H,11.46; N,3.46. $C_{16}$MAPB calcd. for $C_{22}H_{46}BrN$ C,66.00; H,11.56: N,3.35; Found: C,65.03; H,12.35; N,3.59. $C_{16}$MACB calcd. for $C_{24}H_{50}BrN$ C,65.32; H,11.46: N,3.46; Found: C,65.22; H,12.13; N,3.46.

### 5.4.5 Determination of the Critical Micelle Concentrations

The CMC was determined using an Agilent 3DCE system using ChemStation software. For all surfactants except for the $C_{16}$MACB surfactant a fused silica capillary of 33cm was placed in the instrument and the capillary temperature was maintained at 25 $^0$C. $C_{16}$MACB has a Kraft temperature slightly above room temperature so measurements were taken at 35$^0$C. The capillary was filled with surfactant solutions between 0 and 1.5 mM. A potential of 20kV was applied for each surfactant concentration, and a plot was made of current vs. surfactant concentration. The CMC was determined from the inflection point, which was estimated by taking the point of intersection of two linear fits to the data before and after the inflection point.

### 5.4.6 Fluorescence Measurements

Fluorescence measurements were obtained on a Jobin Yvon Fluorolog 3-22 at room temperature. A characterization of the solvation environment provided by the

micellar aggregate was determined by the solvatochromic probe pyrene. The hydrophobic compound pyrene is strongly associated with the core of the micelle, and the fluorescence emission of pyrene is dependent on the polarity of its solvation environment. Pyrene has five characteristic vibronic bands; an increase in band I at 372nm is accompanied by a decrease in the intensity of the band III at 383nm with increasing polarity of the environment. The polarities of surfactants were determined by recording the emission spectra of a pyrene-surfactant solution. The ratio of the intensity of band I to band III ($I_1/I_3$) for each surfactant-pyrene system was compared to previous pyrene I/III ratios to determine the polarity of solvation environment for each surfactant [93, 98].

Fluorescence measurements were also used to determine one of the most fundamental structural parameters of micellar aggregates: The aggregation number ($A$). The aggregation number of the surfactants was determined by a fluorescence quenching method [89, 99] using Eq (5.1):

$$\ln \frac{I_0}{I} = \frac{A[Q]}{[S_{tot}] - CMC} \qquad (5.1)$$

where $I_0$ and $I$ are the florescence intensities of the pyrene-surfactant mixture without and with quencher, respectively, $[Q]$ is the quencher concentration, $[S_{tot}]$ is the total surfactant concentration and CMC is the critical micelle concentration of the surfactant used. The excitation and emission wavelengths were set at 335 nm and 393 nm, respectively. Pyrene and cetylpyridinum; chloride (CPyrCl) were used as florescent probe and quencher, respectively. Aliquots of a 5 x$10^{-2}$ M surfactant, 1 x $10^{-6}$ pyrene and 1 x $10^{-3}$ M quencher were added sequentially to a solution consisting of 5 x$10^{-2}$ M surfactant and 1 x $10^{-6}$ pyrene 50μL. The solution was mixed gently after each addition before the

fluorescence measurement. The decreased in emission of the probe was recorded after each aliquot addition and the logarithm of the intensity ratio ($I_0/I$) was plotted vs. the quencher concentration. The aggregation number, A, was obtained from the slope of the plot $ln(I_0/I)$ vs. [$Q$] (where $A = slope \times \{[S_{tot}] - CMC\}$).

### 5.4.7 MEKC Separations

All the separations were carried out on an Agilent 3DCE system using ChemStation software. Fused-silica capillary from Polymicro Technologies (Phoenix, AZ) with dimensions 50 μm id and 360 μm od was used for all studies. Fresh capillaries with total lengths from 49.4 to 50.4 cm and effective lengths from 41.5-42.2 cm were prepared for each surfactant. The capillaries were first conditioned with a 30 min flush with 0.10 M NaOH (Aldrich) followed by a 30 min flush with buffer. Between injections, the capillaries were flushed for 2 min with 0.10 M NaOH then 2min with the surfactant buffer. Analyte solutions containing from one to six solutes at 100-200 ppm in separation buffer were introduced by 150 mbar· s injection, and a separation potential of -20kV was applied. A list of the measured solutes and their solvation parameter descriptors is in Appendix A. All studies were conducted with a capillary temperature of 25 $^0$C, except $C_{16}$MACB which was tested at 35 $^0$C, the diode array detector signal was monitored at 200, 223, and 254 nm, each at a bandwidth of 20 nm. Injected solutions contained from one to six well resolved solutes. Solutes were identified by matching spectra with a library generated using solutions containing single solutes, or by spiking of the sample with particular solutes.

Acetone has been shown to be a suitable EOF marker when used with cationic surfactants [65] and was used in every separation to mark the EOF. The migration time of

acetone was used to calculate $\mu_{eo}$. The apparent mobility of the solute ($\mu_{sol}$) was calculated from its retention time. The electrophoretic mobility of the micelle ($\mu_{mc}$) was determined using an iterative method presented by Bushey and Jorgenson [88] in which the migration behavior of a series of six alkyl phenyl ketone homologs: acetophenone, propiophenone, butyrophenone, valerophenone, hexanophenone, and heptanophenone was used to determine the retention time of the micelle. The increasing chain length in the homologues series represents and incremental addition to the free energy associated with forming a micelle-solute complex. With the logarithm of retention factor being proportional to free energy a plot of log($k$) vs. carbon number converges on to a maximum retention factor value which is the value of a completely retained solute and the actual migration time of the micelle. The excel application solver was used for the calculations maximizing the $R^2$ of the plot log($k$) vs. carbon number with all of the $R^2$ values being greater than 0.99.

# Chapter 6
# Representative Applications to Phenols, Amines, and Hydrophobic Analytes

## 6.1 Introduction

Due to advantageous features of capillary electrophoresis (CE) and CE based methods like high separation efficiency, rapid analysis times, and small sample volumes, these methods have become a viable alternative to LC for the separation mixtures of charged and neutral analytes. Among the various CE methods, electrokinetic chromatography (EKC) is particularly useful for the separation of uncharged analytes [8].

The selectivity of EKC separations is primarily determined by the pseudostationary phase that is used. Extensive efforts have been made in developing different pseudostationary phases including surfactants [100, 101] and polymers [52] for the separation of complex mixtures consisting of all types of analytes. Anionic surfactants have been the most widely used for these applications with only limited examples using cationic surfactants. The prevalent use of anionic surfactants is due to that they often provide larger migration windows and also that a multitude of anionic surfactants are commercially available. Applications utilizing cationic surfactants, on the other hand, have been less frequent due to migration window limitations [101] and a lack of diversity in commercially available surfactants. An advantage of cationic surfactants, however, is the synthetic flexibility in which the headgroup can be formed. This can be seen in recent reports of chiral separations using cationic surfactants [76, 102]. Other recent interest in cationic surfactants has been for the separation and determination of aminophenols and phenylenediamines, [103] as additives in CZE [104], and for the analysis of nucleotides in cells [105].

I discussed earlier in chapters 4 and 5 the synthesis of two series of cationic surfactants with systematically varied headgroup structure and the characterization of their retention and selectivity in EKC using the linear solvation energy relationships (LSER) model. My results showed that slight structural changes to the headgroups of cationic surfactants produce significant changes in retention and selectivity. In this chapter I applied the series of alky-ammonium headgroup surfactants and one with a cyclic headgroup to the separation of three different classes of analytes. The cationic surfactants studied herein were selected to include the series of increasing headgroup size with linear alkyl substituents on the ammonium center and one with the ammonium center incorporated into a ring structure. They were also selected because the LSER results show that the chromatographic selectivity should change significantly with these different headgroups, and because they showed excellent performance during LSER studies. The surfactants are evaluated for the separations of methoxyphenols that are chemical markers of wood smoke, amine analytes representative of basic pharmaceuticals, and of a group of hydrophobic pharmaceutical corticosteroids. The performance of these surfactants was evaluated with respect to changes in selectivity and by relating the observed selectivity changes to the previously determined solvation parameter results where possible.

**6.2 Results and Discussion**

To evaluate the selectivity differences of these cationic surfactants based on their headgroup chemistry, equivalent "generic" or mild buffer conditions were used as not to have a great impact on the migration or separation selectivity. The surfactant

concentrations, however, were optimized individually for each surfactant in order to achieve the best possible resolution of all of the analytes.

It is important to note the unusually long run times and large migration windows for the $C_{16}$TPAB and $C_{16}$TBAB surfactant as seen in Figures 6.1, 6.3, and 6.5. This is primarily caused by a slower electroosmotic flow with the $C_{16}$TPAB and $C_{16}$TBAB relative to the other surfactants, as discussed previously.

### 6.2.1 Separation of Methoxyphenol Solutes

Baseline resolution of all five methoxyphenols could not be achieved with two of the surfactants tested. With $C_{16}$TMAB and $C_{16}$TEAB we were unable to resolve all of the five analytes at any surfactant concentration. The migration order of three of the five solutes, guaiacol, acetovanillone, and syringaldehyde, varied between the surfactants, as seen in Figure 6.1. The calculated selectivities between the methoxyphenols using the surfactants are presented in Figure 6.2. Significant differences in chemical selectivity are observed between the various surfactants, with the most dramatic changes resulting in reversal of the migration order of some of the methoxyphenols solutes.

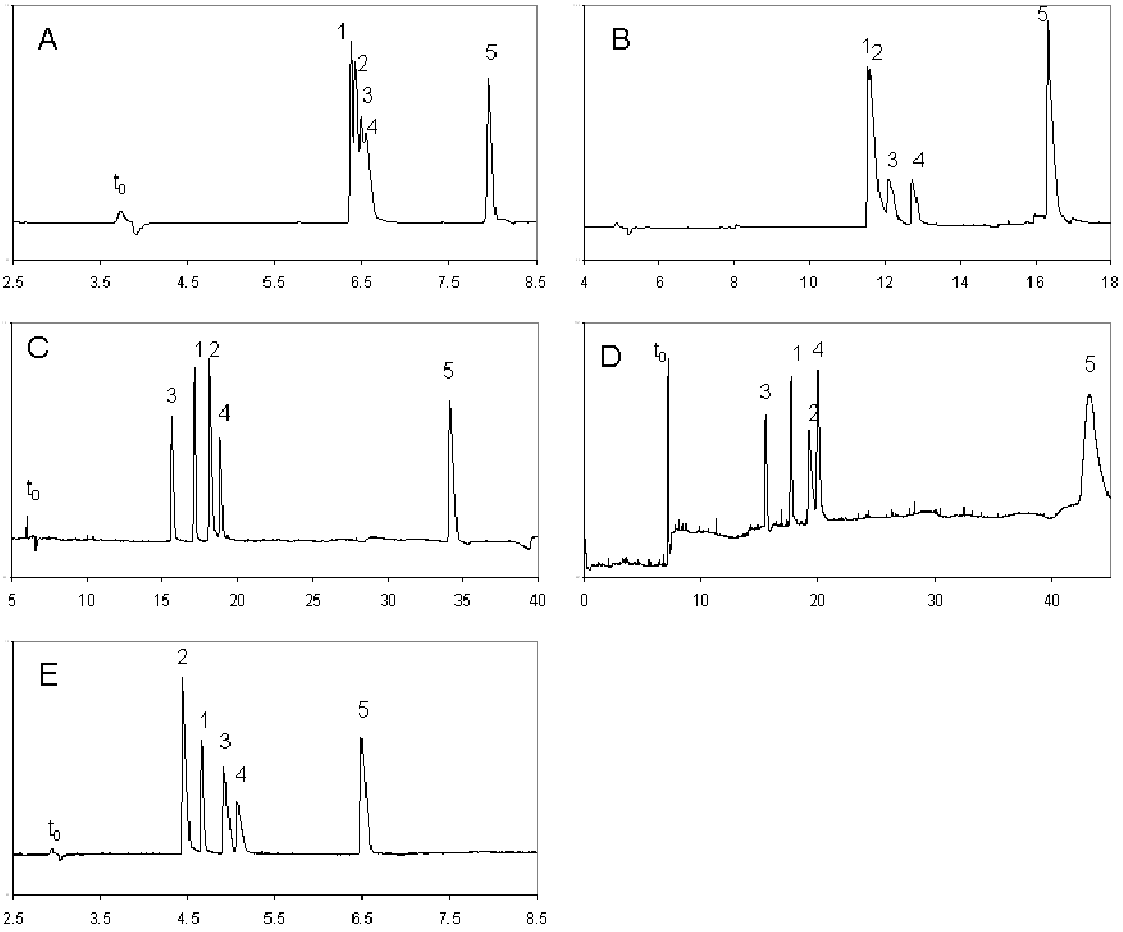


**Figure 6.1:** Electropherograms of methyoxyphenol analytes detection at 223nm. A: $C_{16}$TMAB 45mM. B: $C_{16}$TEAB 45mM. C: $C_{16}$TPAB 45mM. D: $C_{16}$TBAB 45mM. E: C16MPDB 45 mM. 1: Acetovanillone, 2: Guaiacol, 3: Syringaldehyde, 4: Vanillin, 5: 4-ethyl-2-methyoxyphenol.

The relative retention of syringaldehyde tends to decrease, while that of guaiacol tends to increase, as the size of the headgroup is increased. These changes in selectivity are not unexpected given the significant differences and trends observed in some of the LSER parameters in Table 5.3. The newly characterized surfactants $C_{16}$TPAB, $C_{16}$TBAB and $C_{16}$MPDB offer advantages over the most commonly used cationic surfactant, $C_{16}$TMAB, in their ability to resolve these phenolic analytes as well as in the different

selectivity they provide. It should be noted that although the selectivity is often lower, the resolution of these analytes is improved due to the wide migration range afforded by these surfactants. Additionally, a common limitation to all of the cationic surfactants used in this study for the analysis of phenolic solutes is poor peak shapes and relatively low separation efficiency. This is thought to be due to interactions at the capillary surface, which is cationic under our experimental conditions, causing the peaks to tail. Presumably this effect would be magnified at higher pH where the phenolic analytes are completely deprotonated, and could be minimized by the addition of a competing anion to the background electrolyte.

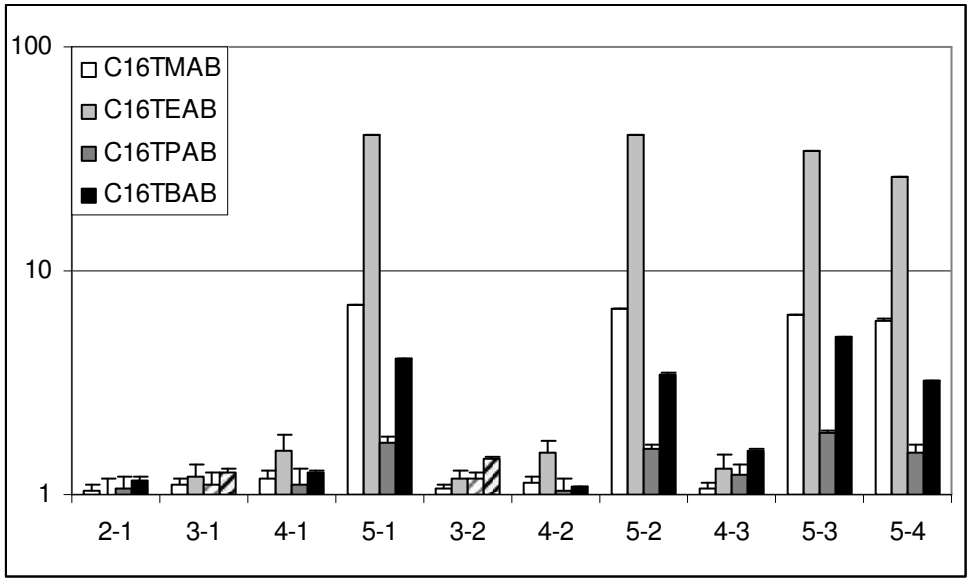


**Figure 6.2:** The selectivity (α) values of peak pairs for the methyoxyphenol analytes with the $C_{16}$TMAB, $C_{16}$TEAB, $C_{16}$TPAB, $C_{16}$TBAB, and $C_{16}$MPDB surfactants. Hashed bars represent a switch in migration order relative to $C_{16}$TMAB. The solutes are 1: Syringaldehyde, 2:Acetovanillone, 3: Guaiacol, 4: Vanillian, and 5: 4-ethyl-2-methyoxyphenol.

### 6.2.2 Separation of Amine Containing Solutes

Resolution of all six representative amine containing soultes was achieved with all surfactants studied except $C_{16}$TEAB, as seen in Figure 6.3. The surfactants did provide significant selectivity differences, as illustrated in Figures 6.3 and 6.4. Trends are observed in the relative migration and selectivity of guaifenesin and acetaminophen as well as quinine and caffeine as the headgroup size is increased.

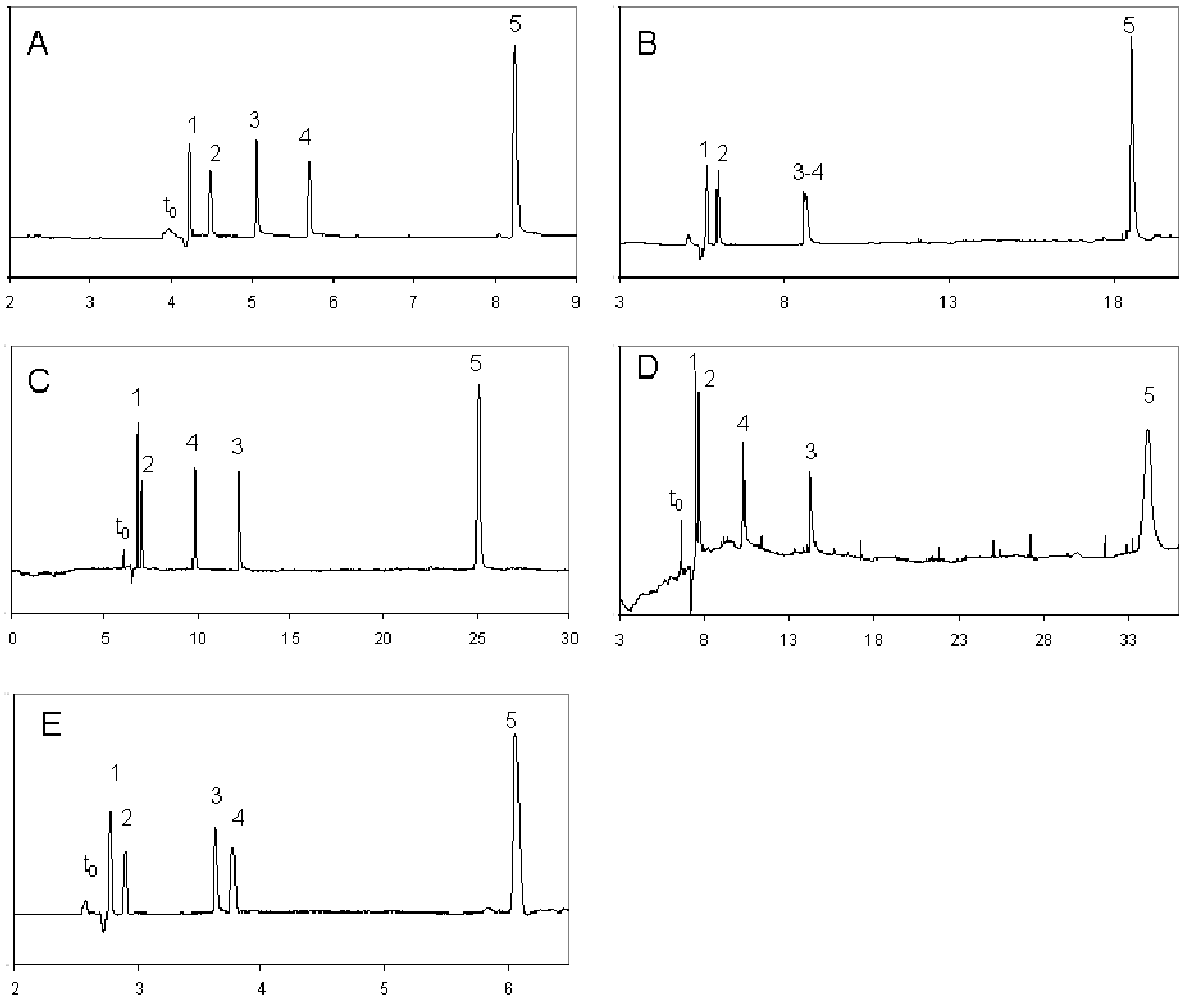


**Figure 6.3:** Electropherograms of amine containing solutes detection at 223nm. A: $C_{16}$TMAB 45mM, B, $C_{16}$TEAB 45mM, C: $C_{16}$TPAB 45mM, D: $C_{16}$TBAB 45mM, E: $C_{16}$MPDB 45mM. 1: Quinine, 2: Caffeine, 3: Acetaminophen, 4: Guaifensin, 5: Nictoamide.

Guaifenesin and acetaminophen are well resolved with the smallest headgroup $C_{16}$TMAB having a selectivity value of 1.97. The selectivity is reduced to 1.03 with $C_{16}$TEAB. When the headgroup size is further increased the two solutes switch migration order and the reversed selectivity increases as seen in $C_{16}$TPAB and $C_{16}$TBAB giving selectivity values of 1.55 and 2.31 respectively. The differences in migration times and retention factors of quinine and caffeine decrease as the headgroup size of the surfactant is increased as reflected in the selectivity values going from 4.26, to 1.76 with the $C_{16}$TMAB, and $C_{16}$TBAB surfactants respectively.

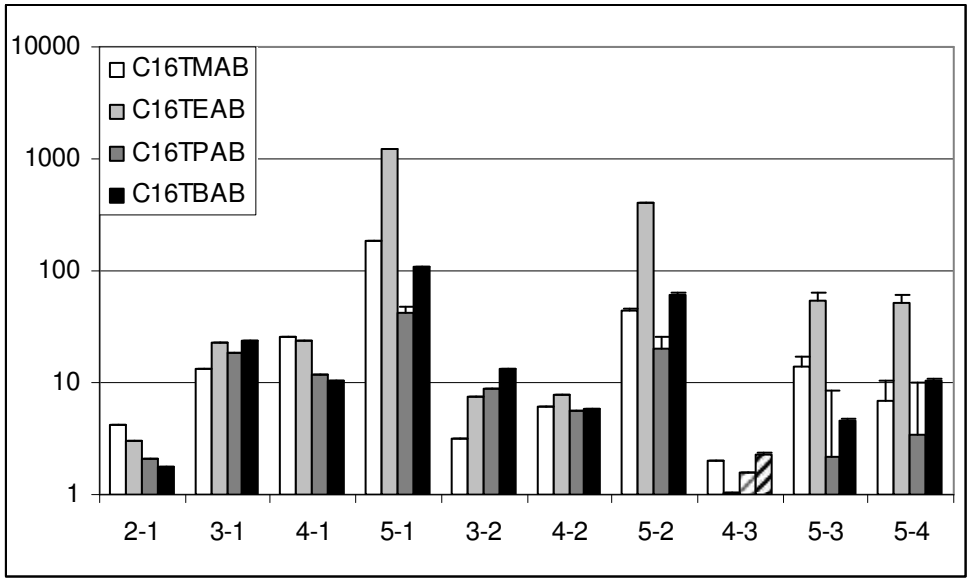


**Figure 6.4:** The selectivity(α) values of peak pairs for the amine containing solutes with the $C_{16}$TMAB, $C_{16}$TPAB and $C_{16}$MPDB surfactants. Hashed bars represent a switch in migration order relative to $C_{16}$TMAB. The solutes are 1: Quinine, 2: Caffeine, 3: Guaifenesin, 4: Acetaminophen, and 5: Nicotinamide

The peak shapes and resolution for these amine containing analyte separations were acceptable under our conditions. The differences in selectivity between the

surfactants and the similar high efficiencies makes these a suitable and powerful family of PSPs for the analysis of basic compounds.

### 6.2.3 Separation of Hydrophobic Solutes

To determine the efficacy of the surfactants for the separation of hydrophobic compounds we examined the separation of six corticosteroids. The separation of corticosteroids is important due their prevalent use for replacement therapy of adrenocortical insufficiency and nonspecific treatment of inflammatory and allergic conditions. These steroids are traditionally difficult to separate by MEKC requiring the use of a mixed micellar system consisting of SDS and a bile salt or the use of an organic modifier [2, 94, 106-109]. Currently the most successful micellar phase to separate steroids is the bile salt sodium cholate; bile salts are better able to separate steroids because of their greater interaction with polar compounds and relatively high cohesivity [94]. An LSER analysis of sodium cholate showed that the v and s values, which pertain to the phase's cohesiveness and ability to interact with polar compounds, are 2.27 and -0.60 [30]. These values are similar to phase descriptors for some of the surfactants reported here.

Total resolution of all six steroids could be achieved with all surfactants under the conditions of 20mM surfactant, 20% acetonitrile in 30mM Tris buffer at pH 7. However, we purposely avoided the use of organic modifiers for the separations shown in Figure 6.5 in order to maintain generic conditions where the headgroup of the surfactant is the dominating factor controlling the separation and in order to be able to make better correlations with LSER results obtained in aqueous buffers. Under purely aqueous conditions, low concentrations of surfactant (5mM) were required to resolve the

hydrophobic compounds. Under these conditions, total resolution of all six steroids was achieved only with the $C_{16}$TPAB and $C_{16}$TBAB. We believe that this is due to the increased resistance of cavity formation and the increased interaction with polar compounds as seen in the LSER results.

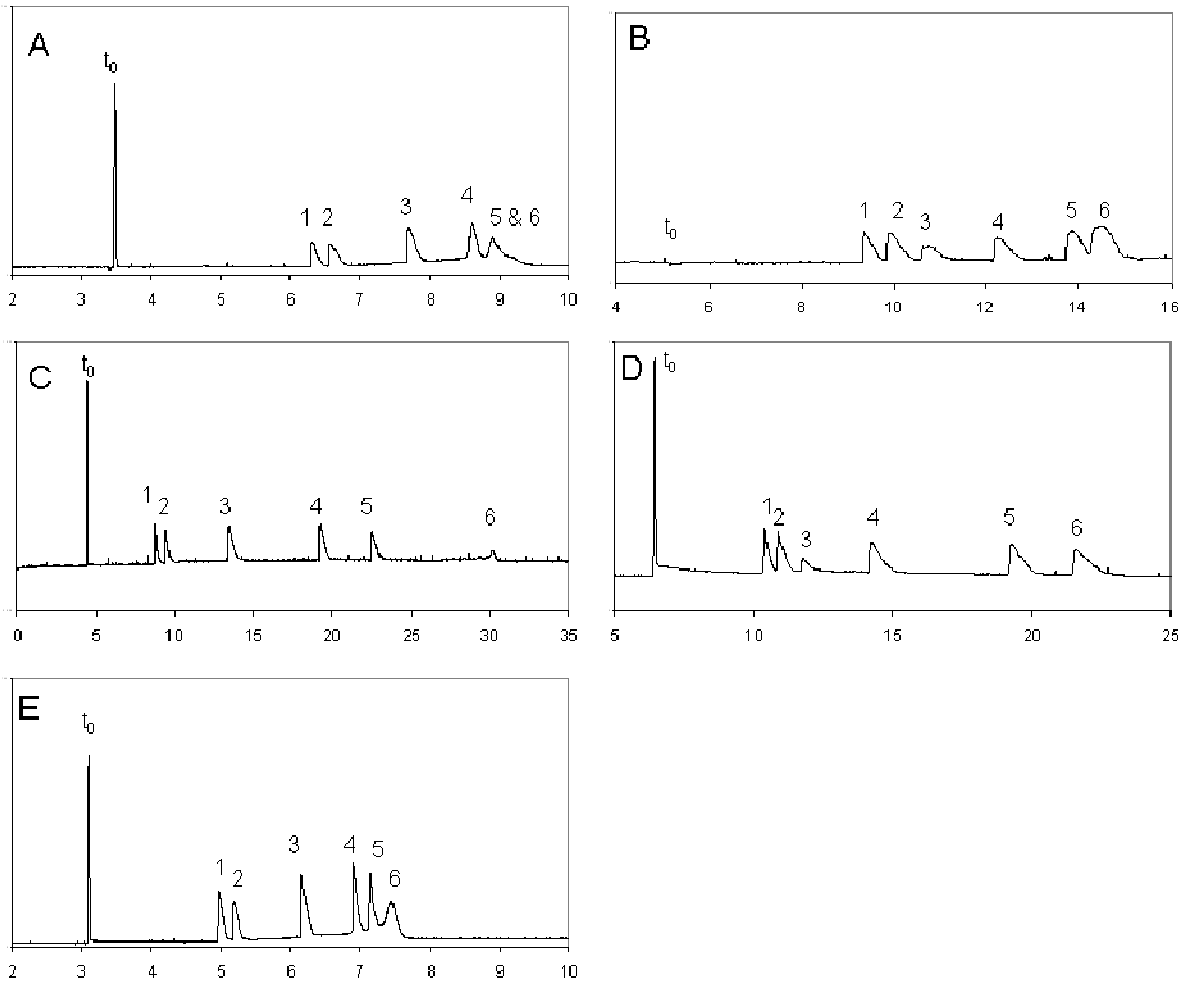


**Figure 6.5:** Electropherograms of hydrophobic analytes detection at 254nm. A: $C_{16}$TMAB 5mM, B:$C_{16}$TEAB 45mM, C: $C_{16}$TPAB 5 M, D:$C_{16}$TBAB 45mM, E: $C_{16}$MPDB 5mM. 1: Prednisolone, 2: Cortisone, 3: Betamethasone, 4: Prednisone, 5: Methylpredinisolone, and 6: Triamcinolone.

These two factors would both limit the interaction between the large and non-polar steroids and the pseudo-phase thus preventing the solutes being poorly resolved with migration times near $t_{mc}$, the migration time of the micelle. This was especially significant for $C_{16}$TPAB and $C_{16}$TBAB, which were able to resolve even the most highly retained solutes methylpredinisolone and triamcinolone. With the exception of these two solutes, however, no significant differences or trends in selectivity were observed as the headgroup size was increased (results not shown). Due to sample overloading, the peak shapes of the steroid analytes were poor, especially for $C_{16}$TEAB and $C_{16}$TBAB. Low absorbtivity of the analytes necessitated high sample concentrations (500 ppm) to allow detection while optimization of the separations required low surfactant concentrations. To the author's knowledge, $C_{16}$TPAB and $C_{16}$TBAB are the only MEKC systems not to contain a bile salt or mixed micelle aggregate to resolve these analytes without an organic additive.

**6.3 Concluding remarks**

Five cationic surfactants were applied to three different classes of analytes to determine the applicability of the surfactants and the effects of headgroup on separation selectivity. In the first system consisting of methoxyphenol solutes remarkable changes in resolution and selectivity were seen. Dramatic changes in selectivity were also observed when the three surfactants were applied to the separation of amine containing solutes.

Systematic changes in the surfactant headgroup structure, which resulted in trends in the LSER parameters, also resulted in trends in the migration of some of the solutes studied.

$C_{16}$TPAB and $C_{16}$TBAB are the first reported cationic surfactants suitable for the separation of hydrophobic corticosteroids, due to their cohesive nature and strong ability to interact with polar compounds. With these surfactants, the corticosteroids were separated without the addition of organic solvent or cosurfactant.

The new surfactants were shown to offer good chromatographic performance and unique chromatographic selectivity for the separation of a wide range of analytes. At least part of the performance of the large headgroup surfactants can be attributed to the wide migration range observed with these surfactants. The wide migration range, however, results primarily from reduced electroosmotic flow, which also results in longer analysis times.

**6.4 Reagents and Materials**

Separations were conducted in 30 mM Tris (Aldrich, St. Louis, MO) buffer adjusted to pH 7 ± 0.05 using dilute phosphoric acid (Fisher Scientific). $C_{16}$TMAB was obtained from Acros (Geel, Belgium), the synthesis of the $C_{16}$TEAB, $C_{16}$TPAB, $C_{16}$TBAB, and $C_{16}$MPDB surfactants was described previously in Chapter 5. The surfactants were dissolved at concentrations of between 5mM and 45mM which exceed their critical micelle concentrations (CMC) as determined in Chapter 4. All aqueous solutions were passed through 0.45 μm nylon syringe filters prior to MEKC separations. The methoxyphenol analytes (Figure 6.6) consisted of guaiacol, acetovanillone, syringaldehyde, vanillin, and 4-ethyl-2-methoxyphenol, all from Acros Organic. The amine containing analytes (Figure 6.7) consisted of nicotinamide, acetaminophen, quinine, guaifenesin, and caffeine, all from Sigma-Aldrich. The hydrophobic analytes (Figure 6.8) consisted of betamethasone (BMS), cortisone (CTS), triamcinolone (TCL),

prednisone (PNS), prednisolone (PNL), and methylpredinisolone (MPL), also from Sigma-Aldrich. All analytes were used as received with out further purification. The analyte stock solutions were prepared at 2000 ppm in 50% acetone and 50% water and diluted to 100-200 ppm in run buffer (including surfactant) for analysis. For each surfactant, a fused-silica capillary with dimensions 50 μm id and 360 μm od was obtained from Polymicro Technologies (Phoenix, AZ). The capillaries had total lengths 49.6 to 50.4 cm and effective lengths of 42.2 to 43.1 cm. The capillaries were first conditioned with a 30 min flush with 0.10 M NaOH (Aldrich) followed by a 30 min flush with buffer. The migration time of acetone was use as an electroosmotic flow marker and the time of acetone in each run was used to calculate $\mu_{eo}$. To obtain $\mu_{mc}$, we used the iterative method presented by Bushey and Jorgenson [88] which was discussed in detail in Chapter 5. The solvation parameter results are present in Chapter 5, and are shown in Table 5.3. The selectivity (α) values reported are the ratio of the two solutes retention factors given by $\alpha = k_2/k_1$.

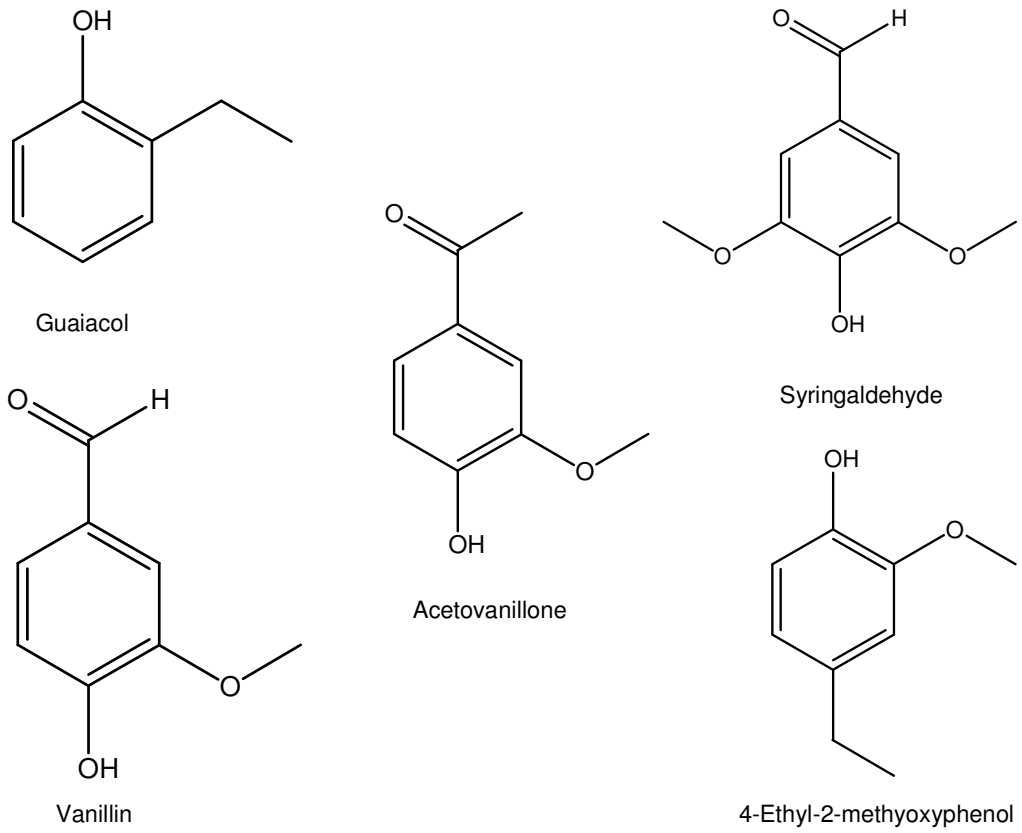


**Figure 6.6:** Structures of the methoxyphenol analytes.

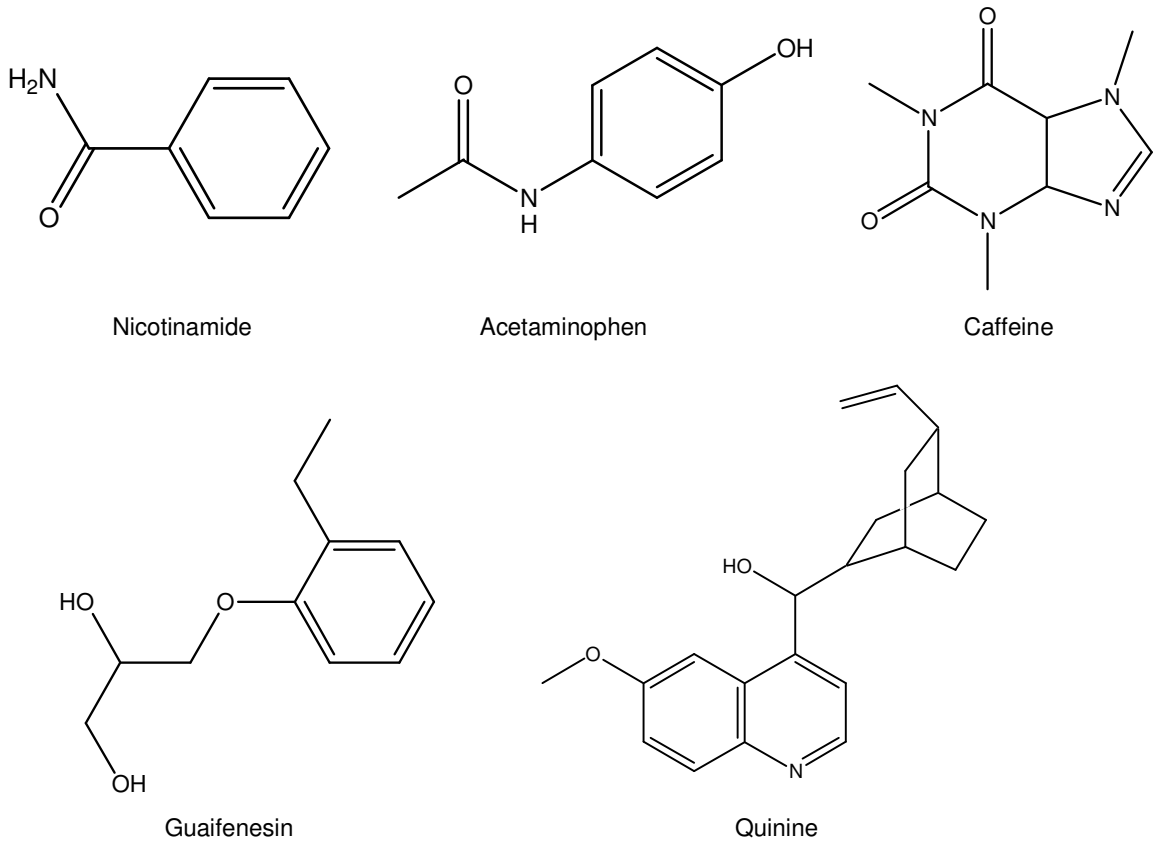


**Figure 6.7:** Structures of the amine analytes.

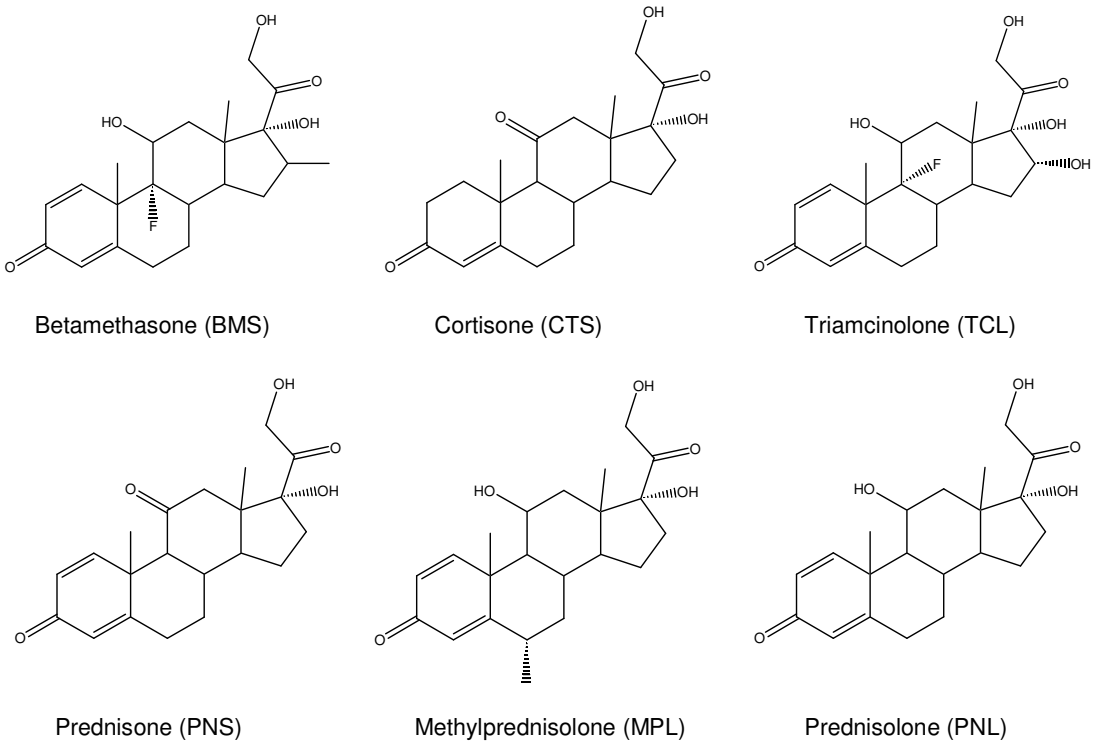


**Figure 6.8:** Structures of the Steroid analytes.

# Chapter 7
# Characterization of a Phosphonium Surfactant for MEKC

## 7.1 Introduction

EKC has emerged as a powerful tool for the separation of neutral and charged solutes [8]. The selectivity of EKC is principally determined by the pseudostationary phase used [28, 29]. Thus, it is important to seek out and characterize new pseudostationary phases with unique selectivity, as well as to perform systematic fundamental studies of the effects of pseudostationary phase chemistry and structure on EKC performance and selectivity.

Many different aspects of pseudostationary phase structure and chemistry have been examined in efforts to determine how such factors control selectivity. Studies have been performed that examine the effects of tail length [31, 49, 51], counter ion [33], and headgroup [32]. The majority of these studies have focused on anionic surfactants, for which a variety of functional groups can constitute the charged headgroup [32]; sulfate [$SO_4^-$], sulfonate [$SO_3^-$], carboxylate [$CO_2^-$], phosphate [$P(OH)O_3^-$], carbonyl valine [$OC(O)CH_2SO_3^-$], and sulfoacetate [$OC(O)CH_2SO_3^-$]. Although this represents a wide variety of chemical structures, it is difficult to compare the results with these materials in a systematic manner.

Cationic surfactants are particularly amenable to systematic fundamental studies of headgroup structure since series of homologous structures can be synthesized and compared. All of the cationic surfactants studied as pseudostationary phases to date have a quaternary ammonium ion [$R_4N^+$] as the headgroup. This work is the first report of a cationic EKC pseudostationary phase where the charge is generated by a phosphonium

ion [$R_4P^+$]. The effects of this change in the headgroup chemistry are studied by comparing the performance and selectivity of the phosphonium surfactant to an ammonium surfactant with otherwise analogous structure.

The significant differences in the size and chemistry of nitrogen and phosphorus atoms represent potential sources of changes in the performance, solvation characteristics and selectivity between these two surfactants. The size of nitrogen and phosphorus differs by one atomic shell with their valance shells consisting of [He] $2s^2$ $2p^4$ and [Ne] $3s^2$ $3p^4$ respectively. This leads to atomic radius differences of 1.2 Å and 0.92 Å respectively for the two atoms [110]. Nitrogen and phosphorous in the quaternary cationic form as seen in these two surfactants have a tetrahedral geometry with four $sp^3$ hybrid orbitals. The bond lengths of the carbon-phosphorus bonds are also significantly different from a carbon-nitrogen length of 1.48 Å to a carbon-phosphorous length of 1.84 Å. Other differences are seen in the ionization potential of the two atoms, which are 14.55 V and 10.98 V for nitrogen and phosphorus respectively. Additionally, the electron affinity differs between these two atoms with nitrogen having a value of 3.07 and phosphorus having a value of 2.06. The electron affinity of nitrogen is higher than that of carbon (2.50), while the electron affinity of phosphorus is lower. Modeling studies of ammonium and phosphonium surfactants using Mulliken and natural population atomic (NPA) charges have shown that the differences in electron affinity result in significant differences in charge distribution around the headgroup. The results of the modeling show that the positive charge of an ammonium headgroup is distributed over the substituent groups, giving the nitrogen atom a negative charge. In contrast, the model of a quaternary phosphonium headgroup surfactant shows that the phosphorus center is positively

charged, giving slightly negative substituents [111]. The change in charge distribution between ammonium and phosphonium is also believed to enhance the rate of $S_N2$ type reactions in micellar catalysis systems using the phosphonium surfactants [111]. Despite these chemical differences between nitrogen and phosphorus, ammonium and phosphonium hexadecyltributyl surfactants have similar critical micelle concentrations of 0.27 mM and 0.26 mM for the ammonium[91] and phosphonium[112] surfactants respectively.

**7.2 Results and Discussion**

In our study the charge center of the cationic headgroup of the surfactants (Figure 7.1) is generated by one of two nonmetal pnictogens, nitrogen and phosphorus. The surfactants are identical in other respects, having the same tail length, counter ion, and three butyl groups off of the charge center. This leads us to believe that any change in the separation system is due the change in charge center. This study also reveals the relative importance of the charge center compared to other structural factors that can be changed in the pseudostationary phase.

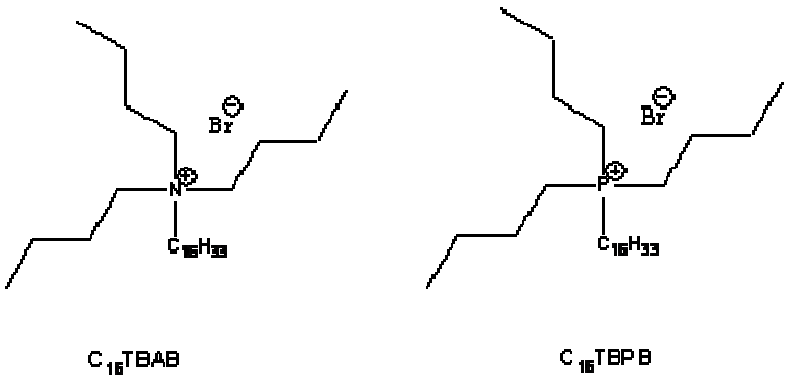


**Figure 7.1:** Structures of the cationic surfactants; Hexadecyltributyl ammonium bromide ($C_{16}$TBAB), Hexadecyltributyl phosphonium bromide ($C_{16}$TBPB)

The mean electroosmotic mobilities ($\mu_{eo}$) provided by each surfactant are presented in Table 7.1. In the absence of significant differences in viscosity, these are a measure of

the amount surfactant that is adsorbed to the capillary wall. The change in charge center from ammonium to phosphonium had no effect on the amount of surfactant that adsorbed to the capillary wall. The electroosmotic flow provided by both surfactants is statistically equivalent, with a flow rate of -3.04 x $10^{-4}$ $cm^2V^{-1}s^{-1}$. The EOF for the commonly used trimethyl headgroup surfactant $C_{16}$TMAB under the same conditions used in Chapter 5 is –4.76 x $10^{-4}$ $cm^2V^{-1}s^{-1}$, which is significantly faster than that observed with these tributyl-surfactants. This result indicates that the charge center has essentially no effect on EOF, and certainly much less of an effect than the size of the headgroup.

The electrophoretic mobilities ($\mu_{mc}$) of the micelles presented in Table 7.1 were determined by an iterative method using the migration behavior of a series of six alky phenyl ketone homologs. The change in the charge center had no effect on electrophoretic mobility of the surfactant aggregate, $C_{16}$TBAB and $C_{16}$TBPB having equal mobilities of 2.27 x $10^{-4}$ $cm^2V^{-1}s^{-1}$.

**Table 7.1.**
Electrophoretic mobilities and chromatographic properties of surfactant micelles

| Surfactant | $\mu_{mc}$ x $10^4$ ($cm^2V^{-1}s^{-1}$) | $\mu_{eo}$ x $10^4$ ($cm^2V^{-1}s^{-1}$) | $t_{mc}/t_0$ | $\alpha_{(CH2)}$ | Theoretical plates |
|---|---|---|---|---|---|
| $C_{16}$TBAB | 2.27(0.07) | -3.05 (0.19) | 2.84 (0.12) | 2.66 (0.03) | 143000 (5000) |
| $C_{16}$TBPB | 2.27 (0.01) | -3.04 (0.17) | 2.80 (0.07) | 2.55 (0.02) | 152000 (6000) |

a) The numbers reported in parentheses are the standard errors

Since the change in charge center did not affect $\mu_{eo}$ or $\mu_{mc}$, there was no change in the migration range, as defined by $t_{mc}/t_0$. The migration range is a significant factor in EKC separations, because it affects the resolution attainable for solutes with a given selectivity and separation efficiency [14]. These tributyl surfactants provide a significantly wider migration range $t_{mc}/t_o$ = 2.80 than the commercially-available and

commonly-employed $C_{16}$TMAB, $t_{mc}/t_o$ = 1.97-2.08 presented in Chapter 5. While this should result in better attainable resolution with these surfactants, the result is primarily due to reduced $\mu_{eo}$, meaning that any improvement in resolution would come at the expense of longer analysis times.

The influence of the charge center on solute-micelle interactions was investigated using the LSER model. The LSER model was discussed in detail in Chapter 2. Additionally, the use of "generic" experimental conditions has been argued by Poole et. al. [29] as to limit selectivity effects of other factors than the phase being studied. The resulting coefficients from the solvation parameter model are presented in Table 7.2.

The first significant difference between the two surfactants is in the cohesivity (v) term in the solvation parameter model. The values are 2.37 and 3.29 for $C_{16}$TBAB and $C_{16}$TBPB respectively and are different at an 88% level of confidence. The value of 2.37 for $C_{16}$TBAB makes it one of the most cohesive micelles with only the perfluorinated LPFOS v =1.97 [30] and the bile salt sodium cholate v = 2.27 [30] being more cohesive. The $C_{16}$TBPB surfactant, on the other hand, is one of the least cohesive phases reported with only cationic vesicles DHAB v = 4.01 [39] and polymeric phases [47] ranging from v = 3.56-3.78 being less cohesive.

The strength of interaction with polar compounds is also affected by the change in charge center. The s term of the solvation parameter model gives the values of -0.06 and 0.11 for $C_{16}$TBAB and $C_{16}$TBPB respectively and are different at an 65% level of confidence. These are both very high values for the ability to interact with polar compounds. They comprise the highest s values for any micellar phase reported, with previous values ranging from -0.24 to -1.03 [50]. The only other reported EKC phases

that also have positive s values like $C_{16}$TBPB are poly(sodium 11-acrylamidoundecanoate) [42] and poly(sodium 7-octenyl sulfate [43], 0.45 and 0.26 respectively.

**Table 7.2:** Solvation parameter results

| Surfactant | e | s | a | b | v | $R^2$ |
|---|---|---|---|---|---|---|
| $C_{16}$TBAB | 0.64 (0.18) | -0.06 (0.16) | 0.98 (0.12) | -2.61 (0.25) | 2.37 (0.30) | 0.90 |
| $C_{16}$TBPB | 0.40 (0.15) | 0.11 (0.14) | 1.14 (0.10) | -3.35 (0.21) | 3.29 (0.26) | 0.94 |

a) The numbers reported in parentheses are the standard errors

Khaledi and Trone [32] showed that the charge center of anionic surfactants plays a role in the ability of the pseudo-phase interact with acidic and basic compounds. The change from ammonium to phosphonium cationic surfactants shows similar results. The hydrogen-bond donating ability of the micellar phases (b-term) changes from -2.61 to -3.35 for the $C_{16}$TBAB and $C_{16}$TBPB surfactants respectively. It has been suggested that differences in hydrogen-bond donor strength relates to the attachment, penetration, content, and orientation of water at the interphase micellar regions (Stern and palisade layers) [28, 95-97]. These results indicate that the atom generating the charge has an effect on the orientation of water in interphase micellar regions.

The difference between an ammonium and phosphonium charge center does not cause a significant effect on the phases' ability to interact with π and n-type electrons represented by the e term in the solvation parameter model. The e values for $C_{16}$TBAB and $C_{16}$TBPB, 0.64 and 0.40 are smaller in magnitude than other reported cationic surfactants, which range from 0.75 to 1.11[30, 38].

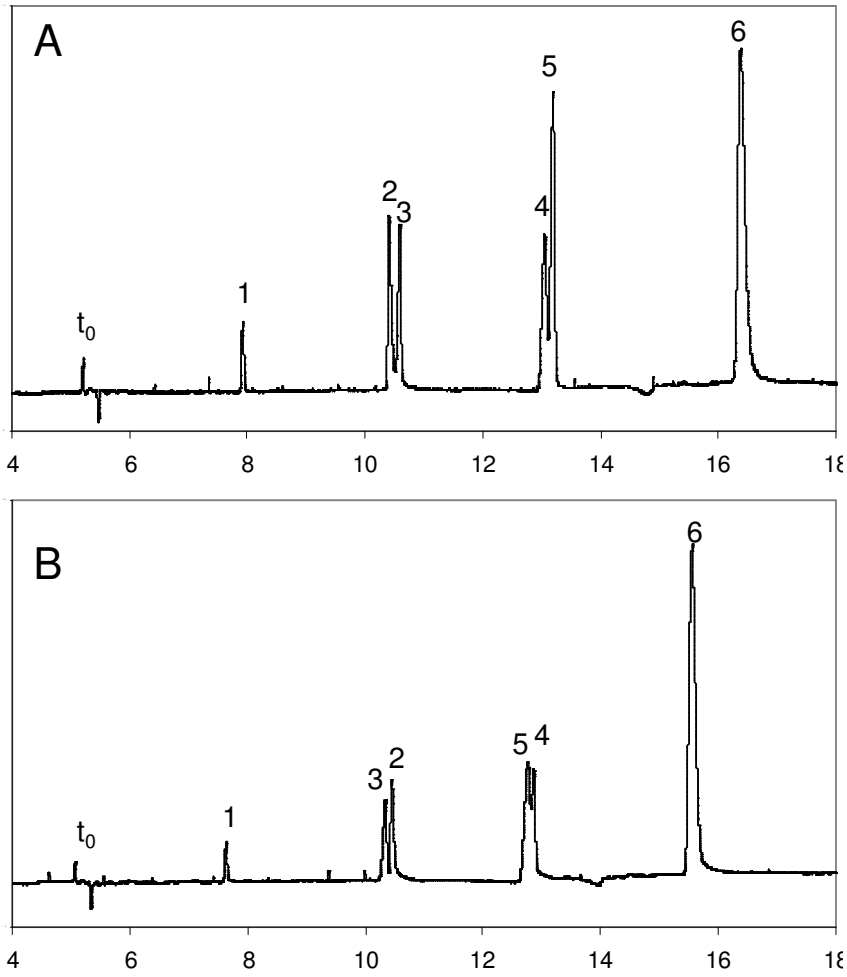


**Figure 7.2**: Representative MEKC electropherograms of $C_{16}$TBAB (A) and $C_{16}$TBPB (B). The solutes are 1: Phenyl Acetate, 2: Propiopheone, 3: Nitrobenzene, 4: Methyl-o-toluate, 5: 4-Nitrotoluene, 6: Indole. Conditions: 30 mM Tris buffer, pH 7, 25°C; 50mbar injection; applied voltage -20kV, anodic detection at 223 nm. Acetone was used as the EOF marker.

The effect of the chemical selectivity differences is seen in representative electropherograms shown in Figure 7.2. The electropherograms are runs consisting of six of the LSER analytes. In theses runs the migration order of the analytes is not consistent, with propiophenone/nitrobenzene and methyl-o-toluate/4-nitrotoluene switching migration order with the two surfactants.

### 7.3 Concluding remarks

Because the structures of the two surfactants studied are identical except for the charge center, changes in the solvation parameter results and selectivities must be primarily due to the switch from ammonium to phosphonium charge center. These results clearly show that ammonium ion makes the pseudostationary phase more cohesive and increases the hydrogen-bond donating ability of the micelles. Other minor changes are seen in the ability to interact with polar compounds and π or n-type electrons. The source of these changes could be related to the differences in electro negativity, atomic radius and bond length between nitrogen and phosphorus. These differences, or the change in the charge distribution reported in modeling studies [111], may result in differences in the amount, orientation, and penetration of water at the interfacial regions of the micelle, leading to the observed differences in chemical selectively and changes in the LSER results.

Despite these changes seen in the solvation parameter results the two phase have remarkably similar electrophoretic properties, with the anodic EOF produced by the dynamic coating and the electrophoretic mobility of the two surfactants being statistically equal. These findings show that chemical selectivity of a phase can be changed while maintaining the same basic chromatographic properties and performance.

#### 7.4.1 Reagents and Materials

Separations were conducted in 30 mM Tris (Aldrich, St. Louis, MO) buffer adjusted to pH 7 ± 0.05 using dilute phosphoric acid (Fisher Scientific). Hexadecyltributyl phosphonium; bromide ($C_{16}$TBPB) was obtained from Sigma-Aldrich (St. Louis, MO). The synthesis of the hexadecyltributyl ammonium; bromide ($C_{16}$TBAB)

surfactant was reported in Chapter 3. The surfactants were dissolved at a concentration of 15 mM, which exceeds their CMC. All aqueous solutions were passed through 0.45 μm nylon syringe filters prior to MEKC separations. Analytes were obtained in the highest purity available form Sigma-Aldrich or Acros Organics and were not further purified.

### 7.4.2 MEKC Separations

All the separations were carried out on an Agilent 3DCE system using ChemStation software. Fused-silica capillary with dimensions 50 μm id and 360 μm od obtained from Polymicro Technologies (Phoenix, AZ) was used for all studies. A single fresh capillary was prepared for each surfactant. The dimensions of the capillaries were total lengths from 50.8 and 50.4 cm and effective lengths of 42.3 and 42.2 cm for the $C_{16}$TBAB and $C_{16}$TBPB surfactants, respectively. . The capillaries were first conditioned with a 30 min flush with 0.10 M NaOH (Aldrich) followed by a 30 min flush with buffer. Between injections, the capillaries were flushed for 2 min with 0.10 M NaOH then 2 min with the surfactant buffer. Analyte solutions containing from one to six solutes at 100-200 ppm in separation buffer were introduced by 150 mbar· s injection, and a separation potential of –20 kV was applied. The solutes and their solvation parameter descriptors are listed in Appendix A. All studies were conducted with a capillary temperature of 25 $^0$C, and the diode array detector signal was monitored at 200, 223, and 254 nm, each at a bandwidth of 20 nm. Solutes were identified by matching spectra with a library generated using solutions containing single solutes, or by spiking of the sample with particular solutes.

The migration time of acetone was used as an electroosmotic flow marker in each run and was used to calculate $\mu_{eo}$. To obtain electrophoretic mobility of the micelle $\mu_{mc}$,

we used the iterative method presented by Bushey and Jorgenson [88] discussed in Chapter 5.

# Chapter 8
# Characterization of Chemical Interaction of Glucocationic Surfactants for MEKC

## 8.1 Introduction

In the previous chapters I have by examining the selectivity and performance of a series of cationic surfactants as pseudostationary phases using the LSER model. My results indicated that minor changes in the structure and chemistry of the cationic headgroup lead to significant changes in the solvation environment. It is thought that these changes result in large part from changes in the organization and chemistry of water at the micelle-buffer interface. In the current study, we evaluate the solvation environment and performance for the first time of two cationic carbohydrate based surfactants. These so-called glucocationic surfactants have a vastly different headgroup structure than other cationic surfactants which incorporates a carbohydrate group adjacent to the charge center. To determine whether this substantial change in headgroup structure would lead to more significant differences in the selectivity of the pseudostationary phase I evaluated two glucocationic surfactants using the LSER model.

Several varieties of carbohydrates or carbohydrate derivatives have been used for separation science applications, including cyclodextrins [113, 114], and polysaccharide stationary phases [114, 115], In most cases, the interest in these carbohydrate-based phases is as chiral selectors for the analysis of pharmaceutical enantiomers.

Neutral and anionic carbohydrate based surfactants have also been widely studied. These include nonionic glycosidic surfactants which have been used as chiral additives for the enantioseparation of charges chiral solutes by CZE [116]. Additionally, these nonionic glycosidic surfactants can undergo an in situ complexation with borate or boronate ions to from a charged complex which functions as chiral selector [117].

Anionic carbohydrate surfactants which have their charge generated by the incorporation of a sulfate or a phosphate group in sugar structure have also been reported. These anionic carbohydrate surfactants have been used as pseudostarionary phases for the separation of dansylated amino acids [118,119].

With cationic surfactants offering a unique selectivity compared to other surfactants in MEKC [50] we anticipate that these glucocationic surfactants will provide different achiral selectivity then other reported surfactants. Additionally, Rizvi and Shamsi reported the used of chiral ionic liquid surfactants and polymers made of these surfactants for chiral resolution in EKC [76]. These cationic pseudostationary phases were more successful in resolving anionic compounds than anionic pseudostationary phases. They believe that anionic solute are repelled from anionic pseudostationary phases and the cationic phases have favorable electrostatic interactions with anionic solute facilitating better chiral resolution.

**8.2 Results and discussion**

The influence of a carbohydrate headgroup and differing chemical functionality on the chemistry and EKC selectivity of micellar PSPs of glucocationic surfactants was investigated. The two surfactants consisted of a 16-carbon linear hydrocarbon tail, a bromide counter ion, and a quaternary ammonium headgroup linked to glucose or a peracetylated glucose molecule and are shown in Figure 8.1.

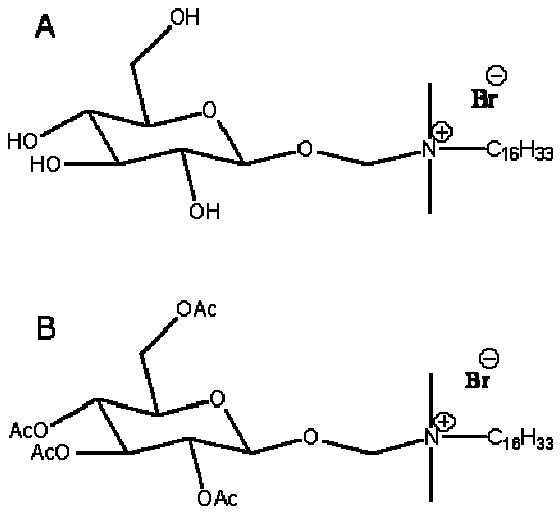


**Figure 8.1:** The structure of the (A) hydroxyl glucocationic surfactant $C_{16}$-Gluco-OH, and (B) the acetylated glucocationic surfactant $C_{16}$-Gluco-Ac

The critical micelle concentration (CMC) and micelle properties of the surfactants were determined previously [120].

The cationic surfactants adsorb to the capillary wall under the reported conditions and provide a dynamic coating on the fused-silica capillary surface. This changes the sign of the zeta potential and results in EOF in the direction of the anode. Absent a change in viscosity, the magnitude of the electroosmotic flow is a measure of the amount or concentration of surfactant adsorbed to the surface. The EOF generated by these two surfactants, $\mu_{eo}$ is presented in Table 8.1. The values of EOF generated by these two surfactants are within random error of each other, indicating that the two surfactants adsorb in similar amounts to the fused silica surface. The mean EOF generated by the two glucocationic surfactants (-2.02 x $10^{-4}$ $cm^2V^{-1}s^{-1}$) is substantially lower than the commonly employed hexadecyltrimethyl ammonium; bromide cationic surfactant CTAB which under identical buffer conditions produces a flow of -4.76 x $10^{-4}$ $cm^2V^{-1}s^{-1}$(Chapter 5). In chapter 5 it was seen that EOF decreased with an increase in headgroup size from

trimethyl to tributyl. We believe that steric effects from the increased size from the carbohydrate at the headgroup hinder the adsorption of these cationic surfactants to the silica surface.

The electrophoretic mobilities of the two glucocationic surfactants are presented in Table 8.1, with the C16-Gluco-Ac having a greater electrophoretic mobility than the C16-Gluoc-OH surfactant. This seems counter intuitive with the larger acetylated glucocationic surfactant having a faster electrophoretic mobility. This is probably due to the acetylated surfactant forming more compact micelles with greater aggregation number. Due to the limited amount of the two surfactants I was unable to measure the aggregation number of the micelles.

**Table 8.1:**
Electrophoretic mobilities and chromatographic properties of surfactant micelles

| Surfactant | $\mu_{ep}$ x $10^4$ ($cm^2V^{-1}s^{-1}$) | $\mu_{eo}$ x $10^4$ ($cm^2V^{-1}s^{-1}$) | $t_{mc}/t_0$ | $\alpha_{(CH2)}$ | CMC (mM) |
|---|---|---|---|---|---|
| $C_{16}$-Gluco-OH | 1.13 (0.29) | -1.95 (0.13) | 3.73 (0.44) | 2.08 (0.66) | 1.42 |
| $C_{16}$-Gluco-AC | 1.45 (0.01) | -2.08 (0.03) | 3.30 (0.17) | 2.17 (0.68) | 1.25 |

The LSER coefficients for the glucocationic surfactants and other relevant PSPs are represented in Table 8.2. The most significant differences seen in the LSER results between the $C_{16}$-Gluco-OH and $C_{16}$-Gluco-Ac surfactants are their effective polarities represented by the *s* and *e* terms. The *s* term represents the polarity and polarizablity of the pseudostationary phase. The values are -0.19 and -0.48 for the $C_{16}$-Gluco-OH and $C_{16}$-Gluco-Ac surfactants respectively. The hydroxyl form of the glucocationic surfactant not surprisingly shows stronger interactions with polar compounds than the acetylated surfactant. Even more significant changes are seen in the ability of the pseudostationary phases to interact with non-bonding and π electrons. The *e* values for the glucocationic

surfactants are 0.17 and 0.91 for the hydroxyl and acetylated surfactants respectively. The value of 0.17 is the lowest *e* value for any cationic surfactant reported [32, 50, 51]. On the other hand the 0.91 value for the acetylated glucocationic surfactant is more like other reported cationic surfactants. These two values span the values for the most commonly used anionic and cationic MEKC phases SDS [30] and CTAB (Chapter 4), with the $C_{16}$-Gluco-OH having weaker interactions with non-bonding electrons and the $C_{16}$-Gluco-Ac have stronger interactions.

The acid and base properties which are thought to be controlled by the penetration, amount, and orientation of water in the interfacial regions of surfactants [32] differs slightly when comparing the glucocationic surfactants to CTAB and SDS. The H-bond accepting ability of the glucocationic surfactants is slightly less than that of CTAB and considerably higher than that of SDS. The H-bond donating ability of the glucocationic surfactants is less than that of CTAB and larger than that of SDS.

**Table 8.2:**
LSER Phase Descriptors for the Glucocationic, and Common MEKC Systems.

| System | e | s | a | b | v | $R^2$ or Ref. |
|---|---|---|---|---|---|---|
| *Glucocationic Surfactants* | | | | | | |
| $C_{16}$-Gluco-OH | 0.17 (0.18) | -0.19 (0.13) | 0.77 (0.12) | -2.14 (0.25) | 2.61 (0.31) | 0.93 |
| $C_{16}$-Gluco-AC | 0.91 (0.24) | -0.48 (0.17) | 0.50 (0.16) | -1.97 (0.34) | 2.41 (0.41) | 0.91 |
| *Common Surfactants* | | | | | | |
| CTAB ($C_{16}$TMAB) | 0.65 | -0.58 | 1.06 | -2.77 | 3.28 | 0.96 |
| SDS | 0.56 | -0.60 | -0.27 | -1.67 | 2.72 | [30] |
| *Cationic Surfactants* | | | | | | |
| $C_{16}$TEAB | 0.63 | -0.33 | 1.06 | -2.83 | 3.23 | 0.97 |
| $C_{16}$TPAB | 0.39 | -0.04 | 0.89 | -3.04 | 2.62 | 0.89 |
| $C_{16}$TBAB | 0.64 | -0.06 | 0.98 | -2.61 | 2.37 | 0.90 |

The number in parentheses is the standard error.

The ability of a solute to partition into the micellar phase represented by the v term of the LSER model is relatively unchanged between the two glucocationic surfactants. The two glucocationic surfactants are relatively cohesive compared to SDS and significantly more cohesive than CTAB.

Compared to other cationic surfactants triethyl-hexadecyl-ammonium; bromide ($C_{16}$TEAB), Tripropyl-hexadecyl-ammonium; bromide ($C_{16}$TPAB), and tributyl-hexadecyl-ammonium; bromide ($C_{16}$TBAB) the glucocationic surfactant show similar solvation properties. The glucocationic surfactants have cohesivity values similar to the larger cationic headgroup tripropyl and tributyl and also give a stronger interaction when donating a H-bond. The polarity of the two glucocationic surfactants is similar to the trimethyl and triethyl surfactants.

I attempted to resolve the chiral analytes 1-1'bi-2-naphthaol, and the two enantiomers of dibenzoyl-tartaric acid with out any success. Due to limited amount of the glucocationic surfactants I was unable to attempt the resolution of any anionic analytes.

**8.3 Concluding remarks**

The solute-solvent interactions of two carbohydrate based surfactants have been investigated using MEKC and the LSER model for the first time. These glucocationic surfactants were found to differ from the commonly employed MEKC phases SDS and CTAB. The glucocationic surfactants differed from SDS in their ability to accept a H-bond. The glucocationic surfactants differ from CTAB in that they are more cohesive and have less of an ability to donate a H-bond. Additionally, the C16-Gluoc-OH surfactant

was found to be more polar and have a grater interaction with non-bonding electrons than CTAB.

The glucocationic surfactants have similar solvation properties to many of the cationic surfactants described and characterized in Chapters 4-7. These properties are different from other commonly used surfactants, and could be expected to lead to differences in separation selectivity when these pseudostationary phases are used.

## 8.4. Materials and methods

### 8.4.1. Reagents and materials

Separations were conducted in 30 mM Tris (Aldrich, St. Louis, MO) buffer adjusted to pH 7 ± 0.05 using dilute phosphoric acid (Fisher Scientific). The synthesis of the two glucocationic surfactants, *N*-[2-(*β*-D-Glucopyranosyl)ethyl]-*N*,*N*-dimethyl-*N*-hexadecylammonium Bromide (C16-Gluco-OH) and *N*-[2-(2,3,4,6-Tetra-*O*-acetyl-*β*-D-glucopyranosyl)ethyl]-*N*,*N*-dimethyl-*N*-hexadecylammonium Bromide (C16-Gluco-Ac) was reported earlier [120]. The surfactants were dissolved at a concentration of 10mM which is in excess of their previously reported CMC [120]. All aqueous solutions were passed through 0.45 μm nylon syringe filters prior to MEKC separations. Analytes were obtained in the highest purity available form Sigma-Aldrich or Acros Organics and were not further purified.

### 8.4.2 MEKC separations

All the separations were carried out on an Agilent 3DCE system using ChemStation software. Fused-silica capillary with dimensions 50 μm id and 360 μm od obtained from Polymicro Technologies (Phoenix, AZ) was used for all studies. Fresh capillaries with total lengths from 33.5 and 31.3 cm and effective lengths of 25.4 and

22.7 cm were prepared for each surfactant. The capillaries were first conditioned with a 30 min flush with 0.10 M NaOH (Aldrich) followed by a 30 min flush with buffer. Between injections, the capillaries were flushed for 2 min with 0.10 M NaOH then 2min with the surfactant buffer. Analyte solutions containing from one to six solutes at 100-200 ppm in separation buffer were introduced by 37.5 mbar· s injection, and a separation potential of -10kV was applied. All studies were conducted with a capillary temperature of $25^0$C, and the diode array detector signal was monitored at 200, 223, and 254nm, each at a bandwidth of 20 nm. Solutes were identified by matching spectra with a library generated using solutions containing single solutes, or by spiking of the sample with particular solutes. The retention factors were calculated in the same manner as the other work presented here in. The solutes and their descriptor are listed in Appendix A.

# Chapter 9
# Concluding Remarks and Future Work

## 9.1 Conclusions

The LSER model was applied to 13 new surfactant systems for MEKC. The surfactants were introduced to expand the selectivity space available of EKC separation, and gain a greater understanding for how structure of a pseudostationary phase controls selectivity.

The $C_n$MPYB surfactants were the first examples of ionic liquid pseudostationary phases and were found to provide highly efficient MEKC separations. The magnitudes of the solvation parameter coefficients showed that lipophilicity ($v$) and hydrogen-bond acidity ($b$) still play the most important roles in MEKC retention. Using $C_{16}$TMAB as a point of reference, however, $C_n$MPYB micellar pseudo-phases provide unique solvent characteristics and are: (i) less "hydrophobic", i.e., better able to interact with polar compounds; (ii) more cohesive; and (iii) less polarizable. No trends were found with alkyl tail length, showing the primary influence exerted by the nature of the headgroup on the chemical selectivity.

Eight cationic surfactants with systematic variations in head group structure were characterized with respect to their micellization behavior and selectivity and performance as pseudostationary phases for EKC. The results suggest that significant increases in the size and hydrophobicity of the cationic headgroup result in more stable, compact and cohesive micelles.

The micellization behavior of the surfactants is affected by the structure of headgroup, particularly for headgroups consisting of linear hydrocarbon chains of increasing length attached to an ammonium center. Among this series, the CMC and

aggregation numbers of the surfactants decreased with increasing headgroup size and hydrophobicity. The LSER analysis of these two series of surfactants showed that the solvation milieu of these micelles is influenced by the structure of the surfactant headgroup. The solvation properties of the linear headgroup series vary in a systematic fashion, with the micelles becoming more cohesive and having greater ability to interact with polar compounds as the size and hydrophobic character of the headgroup increases. The surfactants with the largest, most hydrophobic headgroups provided a very cohesive environment and strongest interactions with polar compounds of any surfactants reported to date. Polar compounds are not as easily solvated within the interior of these more cohesive structures, or are sterically restricted from entering the micelle, and are thus solvated in a more polar environment at the exterior of the micellar structure. Somewhat surprisingly, alterations in the structure of the headgroup did not affect the strength of acid/base interactions, indicating that it had little effect on the chemistry of water in the palisade layer.

Five of the eight cationic surfactants were applied to three different classes of analytes to determine the applicability of the surfactants and the effects of headgroup on separation selectivity. In the first system consisting of methoxyphenol solutes remarkable changes in resolution and selectivity were seen. Dramatic changes in selectivity were also observed when the three surfactants were applied to the separation of amine containing analytes.

Systematic changes in the surfactant headgroup structure, which resulted in trends in the LSER parameters, also resulted in trends in the migration of some of the solutes studied.

$C_{16}$TPAB and $C_{16}$TBAB are the first reported cationic surfactants suitable for the separation of hydrophobic corticosteroids, due to their cohesive nature and strong ability to interact with polar compounds. With these surfactants, the corticosteroids were separated without the addition of organic solvent or cosurfactant.

The new surfactants were shown to offer good chromatographic performance and unique chromatographic selectivity for the separation of a wide range of analytes. At least part of the performance of the large headgroup surfactants can be attributed to the wide migration range observed with these surfactants. The wide migration range, however, results primarily from reduced electroosmotic flow, which also results in longer analysis times.

Additionally, two surfactants that are identical except for the charge center were examined by the LSER model. Given the otherwise homologous structures of these surfactants, any resulting change in the selectivity must be primarily due to the switch from ammonium to phosphonium charge center. These results clearly show that ammonium ion makes the pseudostationary phase more cohesive and increases the hydrogen-bond donating ability of the micelles. Other minor changes are seen in the ability to interact with polar compounds and $\pi$ or n-type electrons. The source of these changes could be related to the differences in electro negativity, atomic radius and bond length between nitrogen and phosphorus. These differences, or the change in the charge distribution reported in modeling studies [111], may result in differences in the amount, orientation, and penetration of water at the interfacial regions of the micelle, leading to the observed differences in chemical selectively and changes in the LSER results.

Finally, the solute-solvent interactions of two carbohydrate based surfactants were investigated using the LSER model for the first time. These glucocationic surfactants were found to differ from the commonly employed MEKC phases SDS and CTAB. The glucocationic surfactants differed from SDS in their ability to accept a hydrogen-bond, and they differ from CTAB in that they are more cohesive and have less of an ability to donate a hydrogen-bond. Additionally, the $C_{16}$-Gluoc-OH surfactant was found to be more polar and have a greater interaction with non-bonding electrons than CTAB.

The glucocationic surfactants have similar solvation properties to many of the cationic surfactants that are characterized. These properties are different from other commonly used surfactants, and could be expected to lead to differences in separation selectivity when these pseudostationary phases are used particularly for the analysis of anionic enantiomers.

This work will make a significant contribution to MEKC separations by introduction of new characterized pseudostationary phases, and greater understanding of how selectivity is controlled structure.

**9.2 Future Work**

The further development of new cationic surfactants should utilize the information gathered in this work and others. I believe the most interesting avenue that should be explored in further pseudostationary phase development would be a partially fluorinated cationic surfactants. The fluorinated anionic surfactant LPFOS provides selectivity unlike any other EKC system. I believe that a fluorinated cationic surfactant would additionally provide unique selectivity. From what was learned in this work and

previous work the greatest impact of fluorination would be at the headgroup of this type of surfactant.

Most importantly the gained knowledge for EKC system should be applied to difficult and relevant separation systems. These could include one dimensional assays for environmental, pharmaceutical analysis, or multidimensional separation systems to analyze complex biological matrixes.

# Appendix A

| Solute | V | E | A | B | R | Used in System |
|---|---|---|---|---|---|---|
| 1-Methylnapthalene | 1.226 | 0.9 | 0 | 0.2 | 1.344 | 1, 3-14 |
| 1-Naphthol | 1.144 | 1.12 | 0.22 | 0.44 | 1.2 | 1-2 |
| 2-Napthol | 1.1441 | 1.08 | 0.61 | 0.4 | 1.52 | 5-14 |
| 3,5-Dimethylphenol | 1.057 | 0.84 | 0.57 | 0.36 | 0.82 | 5-12 |
| 3-Bromophenol | 0.95 | 1.15 | 0.7 | 0.16 | 1.06 | 1-14 |
| 3-Chlorophenol | 0.898 | 1.06 | 0.69 | 0.15 | 0.909 | 1-14 |
| 3-Methyl Benzyl Alcohol | 1.057 | 0.9 | 0.33 | 0.59 | 0.815 | 1-14 |
| 4-Bromophenol | 0.95 | 1.17 | 0.67 | 0.2 | 1.08 | 1-14 |
| 4-Chloroacetophenone | 1.136 | 1.09 | 0 | 0.44 | 0.955 | 1-3, 5-15 |
| 4-Chloroaniline | 0.939 | 1.13 | 0.3 | 0.31 | 1.06 | 1-12 |
| 4-Chloroanisole | 1.038 | 0.86 | 0 | 0.24 | 0.838 | 1, 2, 4-12 |
| 4-Chlorophenol | 0.898 | 1.08 | 0.67 | 0.2 | 0.915 | 3-14 |
| 4-Chlorotoluene | 0.98 | 0.67 | 0 | 0.07 | 0.705 | 1-14 |
| 4-Ethylphenol | 1.057 | 0.9 | 0.55 | 0.36 | 0.8 | 1-12 |
| 4-Fluorophenol | 0.793 | 0.97 | 0.63 | 0.23 | 0.67 | 1-14 |
| 4-Nitroaniline | 0.9904 | 1.91 | 0.42 | 0.38 | 1.22 | 5-14 |
| 4-Nitrotoluene | 1.032 | 1.11 | 0 | 0.28 | 0.87 | 1-12 |
| Acetotphenone | 1.014 | 1.01 | 0 | 0.48 | 0.818 | 1-14 |
| Benzene | 0.716 | 0.52 | 0 | 0.14 | 0.61 | 1-14 |
| Benzonitrile | 0.871 | 1.11 | 0 | 0.33 | 0.742 | 1-14 |
| Benzyl Alcohol | 0.916 | 0.87 | 0.33 | 0.56 | 0.803 | 3-14 |
| Biphenyl | 1.324 | 0.99 | 0 | 0.22 | 1.36 | 5-12 |
| Bromobenzene | 0.891 | 0.73 | 0 | 0.09 | 0.882 | 1-12 |
| Chlorobenzene | 0.839 | 0.65 | 0 | 0.07 | 0.718 | 1-14 |
| Ethylbenzene | 0.998 | 0.51 | 0 | 0.15 | 0.613 | 1-14 |
| Ethylbenzoate | 1.214 | 0.85 | 0 | 0.46 | 0.689 | 1, 2, 4-12 |
| Indole | 0.946 | 1.12 | 0.44 | 0.22 | 1.2 | 1-14 |
| Iodebenzene | 0.975 | 0.82 | 0 | 0.12 | 1.188 | 1-14 |
| M-Cresol | 0.916 | 0.88 | 0.57 | 0.34 | 0.822 | 1-14 |
| Methyl benzoate | 1.073 | 0.85 | 0 | 0.46 | 0.733 | 1-14 |
| Methyl-o-toluate | 1.214 | 0.87 | 0 | 0.43 | 0.772 | 1-14 |
| Napthalene | 1.085 | 0.92 | 0 | 0.2 | 1.36 | 1-12 |
| Nitrobenzene | 0.891 | 1.11 | 0 | 0.28 | 0.871 | 1-14 |
| p-Cresol | 0.916 | 0.87 | 0.57 | 0.31 | 0.82 | 1-12 |
| Phenol | 0.775 | 0.89 | 0.6 | 0.3 | 0.805 | 1, 3-12 |
| Phenyl acetate | 1.073 | 1.13 | 0 | 0.54 | 0.661 | 5-12 |
| Propiophenone | 1.155 | 0.95 | 0 | 0.51 | 0.804 | 1-12 |
| Propylbenzene | 1.139 | 0.5 | 0 | 0.15 | 0.604 | 5-12 |
| p-Xylene | 0.998 | 0.52 | 0 | 0.16 | 0.613 | 1-12 |
| Resorcinol | 0.834 | 1 | 1.1 | 0.58 | 0.98 | 3, 5-12 |
| Toluene | 0.857 | 0.52 | 0 | 0.14 | 0.601 | 1-14 |

| Systems | # |
|---|---|
| $C_{12}$MPY | 1 |
| $C_{14}$MPY | 2 |
| $C_{16}$MPY | 3 |
| $C_{18}$MPY | 4 |
| $C_{16}$TMAB (CTAB) | 5 |
| $C_{16}$TEAB | 6 |
| $C_{16}$TPAB | 7 |

| Systems | # |
|---|---|
| $C_{16}$TBAB | 8 |
| $C_{16}$MPD | 9 |
| $C_{16}$MAP | 10 |
| $C_{16}$MAC | 11 |
| $C_{16}$TBPB | 12 |
| $C_{16}$-Gluco-OH | 13 |
| $C_{16}$-Gluco-Ac | 14 |

## Reference List


1. H. M. McNair and M. Miller James, *Basic Gas Chromatography*, John Wiley and Sons Inc., New York, NY , 1998.

2. L. R. Snyder, J. J. Krirkland and J. L. Glanjch, *Practical HPLC Method Development*, John Wiley and Sons, Inc., New York, 1997.

3. J. C. Giddings, *Unified Separation Science*, John Wiley and Sons, Inc., New York, 1991.

4. S. Ehlert and U. Tallarek, *Analytical and Bioanalytical Chemistry*, 388 (2007) 517.

5. R. P. Manginell, P. R. Lewis, D. R. Adkins, R. J. Kottenstette, D. Wheeler, S. Sokolowski, D. Trudell, J. Byrnes, M. Okandan, J. M. Bauer and R. G. Manley, *Proceedings of SPIE-The International Society for Optical Engineering*, 5591 (2004) 44.

6. Y. Du and E. Wang, *Journal of Separation Science*, 30 (2007) 875.

7. S. Eeltink and F. Svec, *Electrophoresis*, 28 (2007) 137.

8. U. Pyell, *Electrokinetic Chromatography Theory, Instrumentation and Applications*, John Wiley and Sons, West Sussex, 2006.

9. S. Terabe, K. Otsuka, K. Ichikawa, A. Tsuchiya and T. Ando, *Analytical Chemistry*, 56 (1984) 111.

10. S. Terabe, K. Otsuka and T. Ando, *Analytical Chemistry*, 57 (1985) 834.

11. M.-L. Riekkola, J. A. Joensson, R. M. Smith, D. Moore, F. Ingman, K. J. Powell, R. Lobinski, G. G. Gauglitz, V. P. Kolotov, K. Matsumoto, R. M. Smith, Y. Umezawa, Y. Vlasov, A. Fajgelj, H. Gamsjaeger, D. B. Hibbert, W. Kutner, K. Wang, E. A. G. Zagatto, M.-L. Riekkola, H. Kim, A. Sanz-Medel and T. Ast, *Pure and Applied Chemistry*, 76 (2004) 443.

12. E. P. E. Parmauro, *Comprehensive Analytical Chemistry Surfactants in Analytical Chemistry Applications of Organized Amphiphilic Media*, Elservier, Amsterdam, 1996.

13. S. Terabe, *Micellar Electrokinetic Chromatography*, Beckman, Fullerton, 1993.

14. J. P. Foley, *Analytical Chemistry*, 62 (1990) 1302.

15. U. D. Neue, *Journal of Separation Science*, 30 (2007) 1611.

16. Carr P W, Doherty R M, Kamlet M J, Taft R W, Melander W and Horvath C, *Anal Chem*, 58 2674.

17. Kamlet M J, Doherty R M, Abboud J L, Abraham M H and Taft R W, *J Pharm Sci*, 75 (1986) 338.

18. Abraham M H, Kamlet M J, Taft R W, Doherty R M and Weathersby P K, *J Med Chem*, 28 865.

19. M. H. Abraham, G. S. Whiting, R. M. Doherty and W. J. Shuely, *Journal of the Chemical Society, Perkin Transactions 2: Physical Organic Chemistry (1972-1999)* (1990) 1451.

20. M. H. Abraham, *Chemical Society Reviews*, 22 (1993) 73.

21. M. H. Abraham, C. Treiner, M. Roses, C. Rafols and Y. Ishihama, *Journal of Chromatography, A* , 752 (1996) 243.

22. M. H. Abraham, H. S. Chadha, G. S. Whiting and R. C. Mitchell, *Journal of Pharmaceutical Sciences*, 83 (1994) 1085.

23. M. H. Abraham and McGown J. C. *Chromatographia*, 23 (1987) 243.

24. M. H. Abraham, C. F. Poole and S. K. Poole, *Journal of Chromatography, A*, 842 (1999) 79.

25. M. H. Abraham, A. Ibrahim and A. M. Zissimos, *Journal of Chromatography, A*, 1037 (2004) 29.

26. A. M. Zissimos, M. H. Abraham, C. M. Du, K. Valko, C. Bevan, D. Reynolds, J. Wood and K. Y. Tam, *Journal of the Chemical Society, Perkin Transactions 2* (2002) 2001.

27. J. A. Platts, D. Butina, M. H. Abraham and A. Hersey, *Journal of Chemical Information and Computer Sciences*, 39 (1999) 835.

28. C. F. Poole and S. K. Poole, *Journal of Chromatography, A*, 792 (1997) 89.

29. C. F. Poole, S. K. Poole and M. H. Abraham, *Journal of Chromatography, A*, 798 (1998) 207.

30. E. Fuguet, C. Rafols, E. Bosch, M. H. Abraham and M. Roses, *Journal of Chromatography, A*, 942 (2002) 237.

31. M. F. Vitha and P. W. Carr, *Separation Science and Technology*, 33 (1998) 2075.

32. M. D. Trone and M. G. Khaledi, *Analytical Chemistry*, 71 (1999) 1270.

33. M. D. Trone, J. P. Mack, H. P. Goodell and M. G. Khaledi, *Journal of*

*Chromatography, A*, 888 (2000) 229.

34. M. D. Trone and M. G. Khaledi, *Electrophoresis*, 21 (2000) 2390.

35. M. D. Trone and M. G. Khaledi, *Journal of Chromatography, A*, 886 (2000) 245.

36. W. L. Klotz, M. R. Schure and J. P. Foley, *Journal of Chromatography, A*, 962 (2002) 207.

37. M. Adlard, G. Okafo, E. Meenan and P. Camilleri, *Journal of the Chemical Society, Chemical Communications* (1995) 2241.

38. Y. Ishihama and N. Asakawa, *Journal of Pharmaceutical Sciences*, 88 (1999) 1305.

39. A. A. Agbodjan and M. G. Khaledi, *Journal of Chromatography, A*, 1004 (2003) 145.

40. S. T. Burns, A. A. Agbodjan and M. G. Khaledi, *Journal of Chromatography, A*, 973 (2002) 167.

41. A. A. Agbodjan, H. Bui and M. G. Khaledi, *Langmuir*, 17 (2001) 2893.

42. C. Fujimoto, *Electrophoresis*, 22 (2001) 1322.

43. C. Akbay and S. A. Shamsi, *Electrophoresis*, 25 (2004) 635.

44. D. S. Peterson and C. P. Palmer, *Electrophoresis*, 22 (2001) 3562.

45. S. Schulte and C. P. Palmer, *Electrophoresis*, 24 (2003) 978.

46. M. D. Trone, M. S. Leonard and M. G. Khaledi, *Analytical Chemistry*, 72 (2000) 1228.

47. W. Shi, D. S. Peterson and C. P. Palmer, *Journal of Chromatography, A*, 924 (2001) 123.

48. W. Shi and C. P. Palmer, *Electrophoresis*, 23 (2002) 1285.

49. M. D. Trone and M. G. Khaledi, *Journal of Microcolumn Separations*, 12 (2000) 433.

50. E. Fuguet, C. Rafols, E. Bosch, M. H. Abraham and M. Roses, *Electrophoresis*, 27 (2006) 1900.

51. V. P. Schnee, G. A. Baker, E. Rauk and C. P. Palmer, *Electrophoresis*, 27 (2006) 4141.

52. C. P. Palmer, *Electrophoresis*, 28 (2007) 164.

53. S. A. Shamsi, C. P. Palmer and I. M. Warner, *Analytical Chemistry*, 73 (2001) 140A.

54. C. P. Palmer, *Electrophoresis*, 23 (2002) 3993.

55. C. P. Palmer and J. P. McCarney, *Journal of Chromatography, A*, 1044 (2004) 159.

56. C. Akbay, N. L. Gill and I. M. Warner, *Electrophoresis*, 28 (2007) 1752.

57. R. J. Pascoe and J. P. Foley, *Electrophoresis*, 24 (2003) 4227.

58. S. K. Wiedmer, J. M. Holopainen, P. Mustakangas, P. K. Kinnunen and M. L. Riekkola. *Electrophoresis*, 21 (2000) 3191.

59. S. K. Wiedmer, M. S. Jussila, J. M. Holopainen, J.-M. Alakoskela, P. K. J. Kinnunen and M.-L. Riekkola, *Journal of Separation Science*, 25 (2002) 427.

60. G. A. Baker, S. Pandey, S. Pandey and S. N. Baker, *Analyst (Cambridge, United Kingdom)*, 129 (2004) 890.

61. A. M. Dattelbaum, S. N. Baker and G. A. Baker, *Chemical Communications (Cambridge, United Kingdom)* (2005) 939.

62. A. M. Stalcup and B. Cabovska, *Journal of Liquid Chromatography & Related Technologies*, 27 (2004) 1443.

63. F. Pacholec and C. F. Poole, *Chromatographia*, 17 (1983) 370.

64. F. Pacholec, H. T. Butler and C. F. Poole, *Analytical Chemistry*, 54 (1982) 1938.

65. E. Fuguet, C. Rafols, E. Bosch and M. Roses, *Electrophoresis*, 23 (2002) 56.

66. M. Vaher, M. Koel and M. Kaljurand, *Chromatographia*, 53 (2001) S302-S306.

67. M. Vaher, M. Koel and M. Kaljurand, *Electrophoresis*, 23 426.

68. W. Qin and S. F. Y. Li, *Analyst (Cambridge, United Kingdom)*, 128 (2003) 37.

69. S. M. Mwongela, A. Numan, N. L. Gill, R. A. Agbaria and I. M. Warner, *Analytical Chemistry*, 75 (2003) 6089.

70. T.-F. Jiang, Y.-L. Gu, B. Liang, J.-B. Li, Y.-P. Shi and Q.-Y. Ou, *Analytica Chimica Acta*, 479 (2003) 249.

71. E. G. Yanes, S. R. Gratz, M. J. Baldwin, S. E. Robison and A. M. Stalcup, *Analytical Chemistry*, 73 (2001) 3838.

72. K. A. Fletcher, I. A. Storey, A. E. Hendricks, S. Pandey and S. Pandey, *Green*

*Chemistry*, 3 (2001) 210.

73. G. Suxuan, L. Fujia, L. Wei, G. Fei, G. Chunjin, L. Yiping and L. Huwei, *J Chromatogr A*, 1121 274.

74. H.-J. Shen and C.-H. Lin, *Electrophoresis*, 27 (2006) 1255.

75. J. L. Anderson, J. Ding, T. Welton and D. W. Armstrong, *Journal of the American Chemical Society*, 124 (2002) 14247.

76. S. A. A. Rizvi and S. A. Shamsi, *Analytical Chemistry*, 78 (2006) 7061.

77. K. Tian, S. Qi, Y. Cheng, X. Chen and Z. Hu, *Journal of Chromatography, A*, 1078 (2005) 181.

78. M. L. Dietz, J. A. Dzielawa, M. P. Jensen and M. A. Firestone, *ACS Symposium Series*, 856 (2003) 526.

79. G. A. Baker and S. Pandey, *ACS Symposium Series*, 901 (2005) 234.

80. J. Bowers, C. P. Butts, P. J. Martin, M. C. Vergara-Gutierrez and R. K. Heenan, *Langmuir*, 20 (2004) 2191.

81. Z. Miskolczy, K. Sebok-Nagy, L. Biczok and S. Goektuerk, *Chemical Physics Letters*, 400 (2004) 296.

82. T. Kaneta, S. Tanaka and M. Taga, *Journal of Chromatography*, 653 (1993) 313.

83. H. Nishi, T. Fukuyama, M. Matsuo and S. Terabe, *Journal of Chromatography*, 513 (1990) 279.

84. S. Yang and M. G. Khaledi, *Analytical Chemistry*, 67 (1995) 499.

85. Y. Yang, M. C. Breadmore and W. Thormann, *Journal of Separation Science*, 28 (2005) 2381.

86. K. A. Fletcher, S. N. Baker, G. A. Baker and S. Pandey, *New Journal of Chemistry*, 27 (2003) 1706.

87. S. N. Baker, G. A. Baker, M. A. Kane and F. V. Bright, *Journal of Physical Chemistry B*, 105 (2001) 9663.

88. M. M. Bushey and J. W. Jorgenson, *Analytical Chemistry*, 61 (1989) 491.

89. S. A. A. Rizvi and S. A. Shamsi, *Electrophoresis*, 24 (2003) 2514.

90. M. H. Abraham, A. M. Zissimos, J. G. Huddleston, H. D. Willauer, R. D. Rogers and W. E. J. Acree, *Industrial & Engineering Chemistry Research*, 42 (2003) 413.

91. S. A. Buckingham, C. J. Garvey and G. G. Warr, *Journal of Physical Chemistry*, 97 (1993) 10236.

92. R. F. Borch and A. I. Hassid, *Journal of Organic Chemistry*, 37 (1972) 1673.

93. K. Kalyanasundaram and J. K. Thomas, *Journal of the American Chemical Society*, 99 (1977) 2039.

94. C.-Y. Kuo and S.-M. Wu, *Journal of Separation Science*, 28 (2005) 144.

95. P. Mukerjee and J. S. Ko, *Journal of Physical Chemistry*, 96 (1992) 6090.

96. P. Mukerjee and J. R. Cardinal, *Journal of Physical Chemistry*, 82 (1978) 1620.

97. C. Ramachandran, R. A. Pyter and P. Mukerjee, *Journal of Physical Chemistry*, 86 (1982) 3198.

98. S. Pandey, R. A. Redden, A. E. Hendricks, K. A. Fletcher and C. P. Palmer, *Journal of Colloid and Interface Science*, 262 (2003) 579.

99. N. J. Turro and A. Yekta, *Journal of the American Chemical Society*, 100 (1978) 5951.

100. M. Molina and M. Silva, *Electrophoresis*, 23 (2002) 3907.

101. M. Silva, *Electrophoresis*, 28 (2007) 174.

102. A. Dobashi, M. Hamada and J. Yamaguchi, *Electrophoresis*, 22 (2001) 88.

103. S.-P. Wang and T.-H. Huang, *Analytica Chimica Acta*, 534 (2005) 207.

104. Beckers Jozef L and Bocek Petr, *Electrophoresis*, 23 (2002) 1947.

105. D. Friedecky, J. Tomkova, V. Maier, A. Janost'akova, M. Prochazka and T. Adam, *Electrophoresis*, 28 (2007) 373.

106. S. Noe, J. Bohler, E. Keller and A. W. Frahm, *Journal of Pharmaceutical and Biomedical Analysis*, 18 (1998) 911.

107. J. G. Bumgarner and M. G. Khaledi, *Journal of Chromatography, A*, 738 (1996) 275.

108. J. G. Bumgarner and M. G. Khaledi, *Electrophoresis*, 15 (1994) 1260.

109. J. Palmer, D. S. Burgi and J. P. Landers, *Analytical Chemistry*, 74 (2002) 632.

110. A. J. Grodon and R. A. Ford, *The Chemist's Companion A Handbook of Practical Data, Techniques, and References*, John Wiley and Sons, New York, 1972.

111. M. M. Mohareb, K. K. Ghosh, G. Orlova and R. M. Palepu, *Journal of Physical Organic Chemistry*, 19 (2006) 281.

112. M. S. Bakshi and I. Kaur, *Colloids and Surfaces, A: Physicochemical and Engineering Aspects* , 227 (2003) 9.

113. P. T. T. Ha, J. Hoogmartens and A. Van Schepdael, *Journal of Pharmaceutical and Biomedical Analysis*, 41 (2006) 1.

114. R. Vespalec and P. Bocek, *Chemical Reviews (Washington, D. C.)*, 100 (2000) 3715.

115. H. Nishi, K. Nakamura, H. Nakai and T. Sato, *Analytical Chemistry*, 67 (1995) 2334.

116. M. Ju and Z. El Rassi, *Electrophoresis*, 20 (1999) 2766.

117. Z. El Rassi, *Journal of Chromatography, A*, 875 (2000) 207.

118. D. C. Tickle, G. N. Okafo, P. Camilleri, R. F. D. Jones and A. J. Kirby, *Analytical Chemistry*, 66 (1994) 4121.

119. D. Tickle, A. George, K. Jennings, P. Camilleri and A. J. Kirby, *Journal of the Chemical Society, Perkin Transactions 2: Physical Organic Chemistry* (1998) 467.

120. P. Quagliotto, G. Viscardi, C. Barolo, D. D'Angelo, E. Barni, C. Compari, E. Duce and E. Fisicaro, *Journal of Organic Chemistry*, 70 (2005) 9857.